COMPARISON OF MEASURED AND CALCULATED FLOW PROPERTIES AFTER THE ROTATING CASCADES OF A THREE-STAGE AXIAL-FLOW COMPRESSOR

by

Salvatore Frank Gallo

UNITED STATES
NAVAL POSTGRADUATE SCHOOL

THESIS

COMPARISON OF MEASURED AND CALCULATED

FLOW PROPERTIES AFTER THE ROTATING CASCADES OF A

THREE-STAGE AXIAL-FLOW COMPRESSOR

by

Salvatore Frank Gallo

June 1968

COMPARISON OF MEASURED AND CALCULATED FLOW PROPERTIES AFTER THE ROTATING CASCADES OF A THREE-STAGE AXIAL-FLOW COMPRESSOR

by

Salvatore Frank Gallo
Lieutenant Commander, United States Navy
B. S., State University Maritime College, New York, 1957

Submitted in partial fulfillment of the
requirements for the degree of

AERONAUTICAL ENGINEER

from the

NAVAL POSTGRADUATE SCHOOL
June 1968

ABSTRACT

This work was undertaken to check the feasibility of obtaining the velocity profiles downstream of the rotors of turbomachines by measuring only the radial distributions of total temperature, total pressure, and absolute flow angle and using these data to calculate the flow velocities by the non-isentropic radial equilibrium equation such that the measured flow rate is matched. Curvature effects are ignored in this analysis.

The velocities calculated by this method are compared with those obtained by measurements with flow probes and hot-wire anemometers.

The tests were conducted on a 3-stage axial flow compressor of the Turbo-Propulsion Laboratory at the Naval Postgraduate School. Measurements were made over the entire operating range of the compressor at a fixed rotor speed of about 1200 rpm.

TABLE OF CONTENTS

LIST OF TABLES

LIST OF ILLUSTRATIONS

TABLE OF SYMBOLS

Symbols

B_k	Gross weight flow blockage factor
c_p	Specific heat at constant pressure for air (0.24 Btu/lbm-°R)
g	Gravitational constant (32.17 lbm-ft/lbf-sec^2)
H	Stagnation enthalpy (Btu/lbm)
J	Conversion factor (778 ft-lbf/Btu)
M_v	Mach number of absolute velocity
M_w	Mach number of relative velocity
P	Static pressure (psfa)
P_t	Total pressure (psfa)
q	Velocity head - $\frac{1}{2} \rho V^2$ (psf)
r	Radius (ft)
R	Radius (in.)(symbol used in figures only)
R	Gas constant for air (53.35 ft-lbf/lbm-°R)
S	Stagnation entropy (Btu/lbm-°R)
T	Static temperature (°R)
T_t	Total temperature (°R)
U	Peripheral velocity (ft/sec)
V	Absolute velocity (ft/sec)
W	Relative velocity (ft/sec)
W	Mass flow rate (lbm/sec)
z	Axial direction

Greek Letters

α	Absolute flow angle (degrees)
β	Relative flow angle (degrees)
γ	Ratio of specific heats (1.4 for air)
ρ	Mass density (slugs/ft^3)
φ	Axial velocity ratio
$\overline{\Phi}$	Average axial velocity ratio
ψ	Pressure coefficient

Subscripts

a	Axial direction
0	Outer (used in conjunction with radius)
r	Radial direction
T	Tip (used in conjunction with peripheral velocity)
u	Peripheral direction
0	Inlet screen position
1	Inlet survey plane
2	Inlet guide vane

SECTION 1

INTRODUCTION

The experimental analysis of performance of turbomachinery requires detailed and accurate measurement of the flow properties within the passages of the machine under investigation.

Even at the present state of the art it is necessary to make a number of simplifying assumptions for the design of turbomachines. A limited amount of basic design data is available which may not apply directly to a particular type of machine. It is necessary, therefore, to check the accuracy of the design method by testing actual machines. For axial type turbomachines it is of great interest to know the flow profiles after the different stages since this information indicates whether the flow deflections, losses, and velocity distributions on which the design was based have been realized. Comparison of assumed and actual flow properties will make it possible to correct or improve the design procedure with the result that the performance of later machines can be predicted with greater accuracy.

The measuring of the flow properties between the rows of blades of axial turbomachines is connected with considerable difficulties. It is necessary to use small probes to avoid disturbing the flow; and some of the more accurate probes, such as Pitot-static probes, cannot be arranged because of small axial blade clearances. Flow angles, total pressures, and total temperatures can be measured with relative ease and sufficiently small probes. To establish the velocity profiles, however, it is necessary to know the static pressure and the static temperature. The measuring of these quantities between the rows of turbomachines can usually be carried out only with probes that have been calibrated for different

Mach number, Reynolds number, proximity of walls, and flow angles. For these reasons the accuracy of such measurements is low, and the experimental procedure is quite difficult.

The purpose of this study is to determine whether it is possible to use the first-mentioned measurements together with certain theoretical flow relations to obtain the flow profiles with a sufficient degree of accuracy. These conditions are checked on a three-stage axial compressor of large size where the axial clearances between the rows of blades make it possible to measure the velocities directly with calibrated flow probes and hot-wire instruments. This compressor will henceforth be called the O.N.R. compressor since the Naval Postgraduate School received this machine from the Office of Naval Research, Department of the Navy.

The author greatfully acknowledges the guidance and counsel of Professor M. H. Vavra of the Department of Aeronautics of the Naval Postgraduate School. Professor Vavra not only guided this research project but also gave the author an appreciation of what it means to be an engineer.

The author also wishes to express his appreciation to the Office of Naval Research which made the compressor used in this study available to the Naval Postgraduate School.

Thanks are due also to Mr. J. E. Hammer and Mr. R. W. Savage of the technical staff of the Turbo-Propulsion Laboratory as well as to Mr. T. B. Dunton and the staff of the Instrument Shop of the Department of Aeronautics.

SECTION 2

BASIS FOR THE ANALYSIS

For any flow condition there are two principal equations of conservation which must be satisfied, namely, the equation of motion and the equation of continuity.

The following simplifying assumptions are made for the present treatment:

1. The fluid is assumed to be a perfect gas.

2. The general flow equations are applied to compute fluid properties between blade rows where blade forces are nonexistent.

3. The flow is assumed to be steady.

4. The flow is assumed to be axisymmetric. By this assumption, all partial derivatives with respect to the peripheral coordinate are taken to be equal to zero. Basically, this is the equivalent of saying that the three dimensional flow through a blade row can be represented by the circumferential average of the flow conditions at each radial position.

5. The flow is assumed to be adiabatic.

6. The shearing stresses at the annulus boundaries are ignored in the equation of motion, but their effects are reflected by the use of measured data.

7. The specific heat of the gas is assumed to be constant.

With these simplifying assumptions, the equation of motion as defined by Vavra (1) and the equation of continuity, respectively, are

$$\nabla H = T\nabla S + \vec{V} \times (\nabla \times \vec{V}) \qquad (1)$$

$$\nabla \cdot (\rho \vec{V}) = 0 \qquad (2)$$

Since this study deals with the radial variations of fluid properties, it suffices to use the radial components of Eq. 1. In consistent engineering units,

$$J_g C_P \frac{\partial T_t}{\partial r} = J_g T \frac{\partial S}{\partial r} + V_u \frac{\partial V_u}{\partial r} + \frac{V_u^2}{r} + V_a \frac{\partial V_a}{\partial r} - V_a \frac{\partial V_r}{\partial z} \qquad (3)$$

A further simplifying assumption is made inasmuch as the radial accelerations due to streamline curvature are ignored, thus eliminating the last term in Eq. 3. This assumption is valid for lightly loaded machines where the curvatures of the meridional flow path are small as described by Harrison (2) and Giamati and Finger (3). Since both conditions are met by the O.N.R. compressor, the error introduced by this assumption will be small.

In consistent engineering units the equation of continuity can be expressed by

$$\dot{W} = 2\pi g \int_{r_{hub}}^{r_{tip}} \rho V_a r \, dr \qquad (\text{lbm/sec}) \qquad (4)$$

The integration of Eq. 4 within the boundary layer of the annulus walls requires extensive data in the boundary layer. These data were not available in this study due to the physical dimensions of the probes which were used to obtain the surveys. The introduction of a gross weight flow blockage factor in the equation simulates the effect of the boundary layer by increasing slightly the axial velocity components to meet the required continuity condition. With the weight flow blockage factor B_k, Eq. 4 becomes

$$\dot{W} = 2\pi g B_K \int_{r_{hub}}^{r_{tip}} \rho V_a r \, dr \qquad (\text{lbm/sec}) \qquad (5)$$

Equations 3 and 5 require iterative solutions to satisfy both equations. In addition, the non-linearities in Eq. 3 require numerical solutions; hence, the use of a high speed computer is almost a necessity to carry out the procedure.

Equation 3 was multiplied by dr, and integration yields

$$\int_{\pi_i}^{\pi} J_g C_p \frac{\partial T_t}{\partial \pi} d\pi = \int_{\pi_i}^{\pi} J_g T \frac{\partial S}{\partial \pi} d\pi + \int_{\pi_i}^{\pi} V_u \frac{\partial V_u}{\partial \pi} d\pi + \int_{\pi_i}^{\pi} \frac{V_u^2}{\pi} d\pi + \int_{\pi_i}^{\pi} V_a \frac{\partial V_a}{\partial \pi} d\pi \qquad (6)$$

Stations r and r_i are two closely adjoining radial stations.

Some of the terms in Eq. 6 may be integrated directly, but the integrals containing entropy changes and the one involving V_u^2/r must be determined numerically.

Across any blade row the difference in entropy at a given streamline may be expressed by

$$J\left(\frac{S}{R}\right)_2 - J\left(\frac{S}{R}\right)_1 = \ln\left[\frac{(T_{t_2}/T_{t_1})^{\frac{\gamma}{\gamma-1}}}{(P_{t_2}/P_{t_1})}\right] \qquad (7)$$

The symbol S represents the stagnation entropy. Subscript 2 refers to the downstream position and subscript 1 to the upstream position. The entropy gradient across the blade row on two closely adjoining streamlines may now be calculated. For descriptive purposes two such streamlines will be subscripted by i and j.

Subtracting the axial entropy change across the blade row on streamline i from that on j yields

$$J\left(\frac{S}{R}\right)_{2j} - J\left(\frac{S}{R}\right)_{1j} - J\left(\frac{S}{R}\right)_{2i} + J\left(\frac{S}{R}\right)_{1i} = \qquad (8)$$

$$\ln\left[\frac{(T_{t_{2j}}/T_{t_{1j}})^{\frac{\gamma}{\gamma-1}}}{(P_{t_{2j}}/P_{t_{1j}})}\right] \qquad \ln\left[\frac{(T_{t_{2i}}/T_{t_{1i}})^{\frac{\gamma}{\gamma-1}}}{(P_{t_{2i}}/P_{t_{1i}})}\right]$$

The numerical value of the entropy gradient in the radial direction may now be simplified by assuming that position 1 is far upstream where no radial entropy gradient exists and where radial gradients of total temperature and total pressure are zero. Therefore, $T_{t_{1i}}$ equals $T_{t_{1j}}$, and $P_{t_{1i}}$ equals $P_{t_{1j}}$. Then Eq. 8 simplifies to

$$S_{2j} - S_{2i} = \frac{R}{J} \ln \left[\frac{(T_{t_{2j}} / T_{t_{2i}})^{\frac{\gamma}{\gamma-1}}}{(P_{t_{2j}} / P_{t_{2i}})} \right] \tag{9}$$

The integration of the term in Eq. 6 that contains the entropy gradient $\partial S / \partial r$ is then

$$\int_{\pi_i}^{\pi} J_g T \frac{\partial S}{\partial \pi} d\pi = \frac{1}{2} \frac{R}{J} \ln \left[\frac{(T_t / T_{t_i})^{\frac{\gamma}{\gamma-1}}}{(P_t / P_{t_i})} \right] J_g (T + T_i) \tag{10}$$

The static temperature appearing in Eq. 10 may be expressed by the stagnation temperature T_t and the absolute velocity V, or by

$$T = T_t - \frac{\gamma - 1}{2} \frac{V^2}{\gamma g R} \tag{11}$$

With Eq. 11, Eq. 10 becomes

$$\int_{\pi_i}^{\pi} J_g T \frac{\partial S}{\partial \pi} d\pi = \frac{1}{2} \ln \left[\frac{(T_t / T_{t_i})^{\frac{\gamma}{\gamma-1}}}{(P_t / P_{t_i})} \right] \left[g R (T_t + T_{t_i}) - \frac{\gamma - 1}{2\gamma} (V^2 + V_i^2) \right] \tag{12}$$

The non-linear term in Eq. 6 containing V_u^2/r can be evaluated numerically by

$$\int_{\pi_i}^{\pi} \frac{V_u^2}{\pi} d\pi = \frac{\left(\frac{V_u^2}{\pi} + \frac{V_{u_i}^2}{\pi_i} \right)}{2} (\pi - \pi_i) \tag{13}$$

For simplification, let

$$F = \ln\left[\frac{(T_t/T_{t_i})^{\frac{\gamma}{\gamma-1}}}{(P_t/P_{t_i})}\right] \tag{14}$$

Since V_a at an arbitrary radius is to be determined, V and V_u in Eq. 6 are expressed by V_a and α, or

$$\begin{aligned} V_u^2 &= V_a^2 \tan^2\alpha \\ V^2 &= V_a^2(1+\tan^2\alpha) \end{aligned} \tag{15}$$

Equation 6 may now be solved for V_a at an arbitrary radius r,

$$\begin{aligned} V_a^2 = &\left[\frac{1}{1 - F\frac{\gamma-1}{2\gamma} + \tan^2\alpha\left(2 - \frac{r_i}{r} - F\frac{\gamma-1}{2\gamma}\right)}\right] \\ &\left[2gR\frac{\gamma}{\gamma-1}(T_t - T_{t_i}) - FgR(T+T_{t_i}) + \right. \\ &\left. V_{a_i}^2\left(F\frac{\gamma-1}{2\gamma}+1\right) + V_{a_i}^2\tan^2\alpha_i\left(F\frac{\gamma-1}{2\gamma}+2-\frac{r_i}{r}\right)\right] \end{aligned} \tag{16}$$

With measured values of total temperature, total pressure and flow angle as a function of radius, Eq. 16 could be solved at all radial positions if the reference axial velocity V_{a_i} were known.

In Eq. 5 the density is a function of velocity. For a perfect gas

$$g\rho = \frac{P}{RT} \tag{17}$$

From isentropic relationships

$$\left(\frac{P_t}{P}\right) = \left(\frac{T_t}{T}\right)^{\frac{\gamma}{\gamma-1}} \tag{18}$$

Combining eqs. 17 and 18 with the static temperature of Eq. 11

$$g\rho = \frac{P_t}{RT_t}\left(1 - \frac{\gamma-1}{2\gamma}\frac{V^2}{Rg\,T_t}\right)^{\frac{1}{\gamma-1}} \tag{19}$$

This quantity introduced into Eq. 5 establishes the flow rate for the assumed velocity V_{a_i}. If it does not agree with the measured flow rate, a new reference axial velocity V_{a_i} is assumed to obtain an improved solution of Eq. 16; and the process is repeated until agreement between the measured and calculated mass flow rates is reached.

Since Eq. 16 contains differences instead of differentials, it is evident that small increments in radius are necessary to insure accuracy in the final results.

The described method of velocity determination is similar to that presented in Ref. 3 for the design and off-design analysis of axial flow compressors.

SECTION 3

COMPUTER TECHNIQUE FOR SOLUTION

A computer program for the calculation of the radial flow properties downstream of a rotor row was prepared for the IBM-360-67 computer in Fortran IV language.

The program is specifically set up for the O.N.R. three-stage axial compressor of the Naval Postgraduate School described in Section 4, but slight modifications make it applicable to radial surveys downstream of arbitrary axial rotor rows of either turbines or compressors for the assumptions stated in Section 2.

3.1 Non-Isentropic Radial Equilibrium Equation

The computer program has been set up for data from a maximum of fifty radial stations, not necessarily extending to the hub and to the tip radii, although accuracy would be reduced if data were not measured close to the hub and the tip of the blading. Values of total pressure, total temperature, and absolute flow angle are introduced as a function of radius. Other input values are measured flow rate, initial reference value of axial velocity, assumed blockage factor, desired accuracy in flow rate matching, and rotor speed.

The introduced data which are measured at discrete radii are first expressed with fourth order polynomials as a function of radius. The polynomial fit for the data was obtained by the method of least squares. Due to the smooth change of the data, the polynomial fit was extremely accurate throughout the radial span for all the parameters. An example of the accuracy of the curve fit is given in Table B-2 where the symbol X signifies radius; F2, the input data for different radii; Y, the values

of the parameter obtained from the polynomial; and DELY, the difference between the measured data and those from the polynomial. The subprogram used for the polynomial curve fitting is available in the Naval Postgraduate School subroutine library and is presented in Appendix B.

A maximum of one hundred points may be specified at which the equilibrium equation is to be solved. For brevity, the non-isentropic radial equilibrium equation shall be referred to as the NISRE equation in the remainder of this presentation. The radial positions of the points are obtained by dividing the radius from hub to tip into equal increments. Values of total pressure, total temperature and absolute angle of flow are then obtained from the polynomials at these specified radial positions. The measured mass flow rate is calculated from measured conditions in the inlet to the compressor.

The subprogram dealing with the NISRE equation then solves for the axial velocity and density profile from blade hub to blade tip. The profiles thus obtained are used in the continuity equation which is integrated by the trapezoidal method. The initial axial velocity at the reference position is then changed arbitrarily, and a second solution is generated. The third and subsequent values of the reference axial velocity are calculated with the Newton-Raphson iteration technique. This process continues until the desired accuracy in mass flow rate is obtained.

With the axial velocity profile thus determined, all remaining fluid properties may be calculated. These properties are printed out in dimensional and non-dimensional form. Examples of the print out of the solutions are presented in Tables B-3 and B-4.

3.2 Determination of Velocity Profiles with Flow Probes

The measured values of total pressure, static pressure, absolute flow angle, total temperature and rotor speed are used to obtain the axial velocity profile. The fluid properties at different radial stations are calculated and printed out in a format similar to that of the NISRE equation (See Tables B-5 and B-6.).

3.3 Determination of Velocity Profiles with the Hot-Wire Anemometer

The hot-wire anemometer survey was made at the same positions as the flow probe and total temperature surveys. To place the hot-wire as nearly perpendicular as possible to the flow, the absolute flow angle at each radial position was obtained from a five-hole probe. The hot-wire output was set to a reference value at the mean square radius of the annulus, and all values were measured with respect to this setting. The velocity determined by the flow probe at the mean square radius was used as the reference velocity for the hot-wire anemometer. The root mean square radius was used as reference radius since the wall interference effects on the flow probe are small at this location.

Tables B-7 and B-8 give sample outputs of the flow properties at different radii calculated from the measured data. It should be noted that the static pressures and static temperatures are the values obtained from the analysis. The measured static pressures are not used in these calculations.

SECTION 4

O.N.R. THREE-STAGE AXIAL-FLOW COMPRESSOR

The compressor installation is shown in Fig. 1. A detailed description of the test installation is given by Bowen et al. (4). Marshall (5) describes the test set up at the Naval Postgraduate School.

The compressor is suitable for a large variety of research experiments. Each one of the rotor and stator blade rows may be removed. Although stagger angles are adjustable, they were not varied during the present experiments. All three rotor blade cascades were set at a stagger angle of 43.8 degrees, with all stator blade stagger angles at 39.8 degrees.

The casing of the compressor was designed to give maximum accessibility for measuring instruments. Six rectangular instrument ports are located in the upper half of the casing. These ports accommodate a special instrument carriage permitting detailed surveys in radial and peripheral directions (Fig. 2). Three of the instrument ports are suitable for stator outlet surveys over a peripheral arc of 15 degrees, and the other three are suitable for rotor outlet surveys over the same arc. Only rotor outlet surveys were made during this study.

The casing has numerous radial survey ports. Several of these were used downstream of each rotor.

The compressor is electrically driven and operates at two fixed speeds of either about 900 rpm or 1200 rpm.

The inlet duct (Fig. 3) consists of a screen, an entrance bellmouth and a length of straight pipe with a honeycomb flow straightener ahead of the inlet guide vanes.

The compressor discharge (upper foreground of Fig. 1) is fitted with an electrically operated throttle valve whose positions are indicated by a counter.

SECTION 5

INSTRUMENTATION

The compressor inlet duct allows vertical and horizontal surveys to be made across the inlet as well as at 60 degrees from the vertical direction by unbolting and rotating the inlet duct. A 3/32 inch diameter Prandtl-type Pitot-static probe was mounted for vertical survey (Fig. 4) with readout on a Meriam Instrument Company Model-750 Micromanometer (Fig. 5). A 1/4 inch diameter hot-wire anemometer probe was mounted for horizontal survey. The hot-wire probe was constructed at the Naval Postgraduate School and provides for quick changing of tips in the event of wire breakage (Fig. 6). A supply of tips was kept readily available during the inlet surveys, and tip replacement was effected on several occasions while the compressor was in operation. Hot-wire data were read on a Security Associates Applied Sciences Model 200 Constant Temperature Anemometer. Details of the flow rate measurement are given in Section 6.

Wet and dry bulb Mercury glass thermometers were mounted on the inlet screen.

A 1/4 inch diameter Prandtl-type Pitot-static probe was installed between two of the inlet supports ahead of the guide vanes (foreground of Fig. 7) with readout on the same micromanometer as the inlet duct Pitot-static probe. This was made possible by the use of two scanner valves (Fig. 8). In addition, a 1/8 inch diameter Kiel probe with a total type thermocouple was mounted in the same meridional plane through one of the radial access ports. This total temperature probe is shown in the foreground of Fig. 7. The reference junction of the thermocouple

was placed in an ice bath. The output of the thermocouple was read on a Leeds and Northrup Potentiometer (Fig. 9).

Radial surveys were conducted downstream of each of the three rotor blade rows. Total and static pressure measurements were obtained with a United Sensor Corporation DA120 five hole probe (serial number 535) although the pitch angle was assumed to be zero. The five hole probe was mounted in the special carriage mentioned in Section 4 with readout on a water manometer board (Fig. 10). Flow direction was obtained by balancing pressure on the static ports. Total pressure and the difference between total pressure and static pressure were measured with the same manometer board. Total temperature measurements at different radii were obtained by use of a thermocouple mounted in a 1/4 inch diameter Kiel probe which was placed in one of the radial access holes. The reference junction for this thermocouple was also placed in an ice bath, and the aforementioned potentiometer was used for the readout by the use of the double-pole double-throw knife switch shown in the background of Fig. 9. Hot-wire anemometer data at different radii were measured after each of the three rotor blade rows by means of a 1/4 inch diameter hot-wire probe. Figure 11 shows the installation of the total temperature probe and the hot-wire anemometer probe used for the radial surveys. The hot-wire anemometer readout instrument is shown in Fig. 9.

Compressor speed was measured with a flux cutter mounted on the compressor drive shaft whose impulses were read on a Monsanto Model 100A Counter-timer.

SECTION 6

FLOW RATE CALIBRATION

The purpose of the flow calibrations was to obtain a factor which, when multiplied by the velocity ahead of the inlet guide vanes, gives the volume flow rate through the compressor.

Marshall (5) found a flow rate calibration factor for the O.N.R. compressor by means of horizontal and vertical surveys of the inlet with the existing Pitot-static probe. This calibration factor was to be checked by a more accurate survey with a hot-wire anemometer.

Since Marshall showed that the velocity profiles in the vertical and horizontal planes were similar, it was decided to conduct a survey in the horizontal plane only.

Since hot-wire instruments give only the ratio of the actual velocity to some reference velocity, initial hot-wire instrument setting was made at the inlet duct centerline where the velocity obtained from readings of the Prandtl type Pitot-static probe was used as the reference velocity. At the inlet duct centerline the Pitot-static probe is 18 inches from the duct wall; hence, wall effects are minimized. The hot-wire instrument was set at 90 per cent of full readout range at the centerline, and surveys were made at radial increments of 3 inches to a radius of 15 inches and of 0.2 inches to a point 0.2 inches from the duct wall. The design of the hot-wire probe prevented measurements closer to the wall. Frequent checks were made at the duct centerline to ascertain that the centerline setting of 90 per cent had not drifted. Such instrument drifts were noticed only on rare occasions. If drift occurred, it was always less than 2 per cent of full scale, and the hot-wire instrument

was then reset to 90 per cent. Surveys of this type were conducted on both sides of the centerline. Total pressure and velocity head readings were also taken at the duct centerline and ahead of the inlet guide vanes with the fixed Pitot-static pressure probe connected to a water micromanometer. Wet and dry bulb temperatures were recorded from the Mercury thermometers on the inlet screen. The temperature in the test cell was recorded also for the purpose of correcting water column heights.

The following symbols are used for the recorded data:

q_{1r} -velocity head at the centerline of the inlet duct (in.H_2O)

$P_{t_{1r}}$ -total pressure at the centerline of the inlet duct (in.H_2O)

q_{2r} -velocity head ahead of the inlet guide vanes (in. H_2O)

$P_{t_{2r}}$ -total pressure ahead of the inlet guide vanes (in. H_2O)

TOR -temperature at the inlet screen (°F)

BAR -barometric pressure (in.Hg.)

TBAR -temperature of the Mercury column (°F)

TW -temperature of the water column (°F)

VRR -hot-wire anemometer readings, right of centerline looking downstream (dimensionless)

VRL -hot-wire anemometer reading, left of centerline looking downstream (dimensionless)

The specific gravity of the Mercury in the barometer was corrected for temperature by

$$GHGRM = 13.63905 - 0.00136303\,TBAR \quad (20)$$

The specific gravity of the water column was corrected for temperature by

$$GWRM = 0.99837633 + 1.0605756\,TW \times 10^{-4} - 1.593186\,TW^{2} \times 10^{-6} \quad (21)$$

These specific gravity relations were obtained from tabulated data of Ref. 6.

With these corrections, pressures were converted to absolute values, or

$$PAMB = BAR\,(0.4891585)\,GHGRM\,\frac{144}{13.54} \quad (psfa) \quad (22)$$

where the constant 0.4891585 is the conversion factor from inches of Hg. to pounds per square inch for a specific gravity of Mercury of 13.54. Then

$$P_{t_1} = P_{t_{1R}}(GWRM)\,\frac{62.42732}{12} + PAMB \quad (psfa) \quad (23)$$

The constant 62.42732 is the conversion factor from feet of water to pounds per square foot for a specific gravity of water of 1.0.

$$q_1 = q_{1R}(GWRM)\,\frac{62.42732}{12} \quad (psf) \quad (24)$$

The static pressure P_1 was then calculated by

$$P_1 = P_{t_1} - q_1 \quad (psfa) \quad (25)$$

Because of the low velocities of about 70 feet per second in the inlet duct, and ahead of the compressor inlet guide vanes, compressibility effects were ignored, and the temperature TOR at the inlet screen was used as the static temperature.

$$T_o = TOR + 459.7 \quad (^\circ R) \quad (26)$$

Considering the air entering the compressor as a perfect gas having a gas constant R of 53.35 (ft-lb)/(lbm-°R), the mass density is

$$\rho_1 = \frac{P_1}{gRT_0} \qquad (slug/ft^3) \tag{27}$$

For each run the density was taken as the average obtained from all readings.

The velocity at the inlet duct centerline was then calculated by

$$V_1 = \sqrt{\frac{2g_1}{\rho_1}} \qquad (ft/sec) \tag{28}$$

This velocity was used as the reference velocity for the hot-wire anemometer setting. Then, the average velocity V at an arbitrary radius is taken as

$$V = \left(\frac{VRL \quad VRR}{2}\right) \frac{V_1}{0.9} \quad (ft/sec) \tag{29}$$

The constant 0.9 must be introduced since the hot-wire anemometer was set at 90 per cent of full scale readout of the instrument at the centerline in case velocities higher than those at the centerline would occur.

The volume flow rate was calculated by

$$VOLFL = 3.1416\, V_1 \left(\frac{\pi_2}{2}\right)^2 + 3.1416 \sum_{i=2}^{n-1} \left\{ V_i \left[\left(\frac{\pi_i + \pi_{i+1}}{2}\right)^2 - \left(\frac{\pi_i + \pi_{i-1}}{2}\right)^2 \right] \right\} + 3.1416\, V_n \left[(\pi_{n+1})^2 - \left(\frac{\pi_n + \pi_{n-1}}{2}\right)^2 \right] \quad (ft^3/sec) \tag{30}$$

The subscript 1 in the summation refers to the inlet duct centerline. The subscript n pertains to the reading 0.2 inches from the duct wall, and the subscript n+1 is for the conditions at the duct wall.

The velocity V_2 ahead of the inlet guide vanes was obtained in a similar manner, using the temperature measured at the inlet screen as the static temperature since the difference between total and static temperature is less than 0.4°F at the highest velocity of 70 feet per second.

The calibration constant for each run was obtained from

$$CCC = \frac{VOLFL}{V_2} \quad (ft^3/sec \text{ per } ft/sec) \tag{31}$$

This constant was found to be 4.4050 ft^3/sec per ft/sec velocity obtained ahead of the inlet guide vanes. The maximum relative deviation of CCC for all surveys was 0.3 per cent.

This data reduction was carried out on the IBM-360-67 computer. The program is explained in Appendix A which also gives a sample of the computer output.

SECTION 7

RADIAL SURVEYS

Radial surveys were conducted downstream of each row of rotor blades of the O.N.R. compressor. Radial distributions of total pressure, velocity head, total temperature, absolute flow angle, and hot-wire velocity ratio were obtained at various flow rates.

Flow rate was varied by means of the discharge throttle valve. After setting the throttle valve to a new position, data were taken only after waiting for about 20 minutes to stabilize the temperature in the test cell. The test cell has a front door through which air is normally admitted to the compressor from the atmosphere. The air is discharged back into the atmosphere through a door located opposite to the front door and aft of the compressor. However, experience showed that gusts in the atmosphere produced erratic measurements particularly with the hot-wire instrumentation. By closing the front door it was found that the flow oscillations could be minimized, but the above-mentioned waiting period was necessary for the air to reach a new equilibrium temperature in the test cell. Steady temperature conditions were checked by the mercury thermometer at the inlet screen and the total temperature Kiel probe ahead of the inlet guide vanes.

Periodic readings of the total pressure, velocity head and total temperature ahead of the inlet guide vanes were recorded during each run for the determination of the flow rates. Conditions at the inlet screen and ahead of the inlet guide vanes were found to be very stable for all flow rates irrespective of throttle settings and atmospheric conditions.

The previously described traversing instruments for the radial

surveys were mounted downstream of each one of the rotors. Initially, a peripheral survey was made with the flow probe at various radii to check whether the flow conditions were uniform in the peripheral direction. Generally, this was found to be true downstream of each row of rotor blades at flow rates above full stall.

For most of the radial survey runs a hot-wire instrument setting of 90 per cent was used at a reference radius of 14.5 inches, or very close to the root mean square radius of the annulus. To properly position the hot-wire with respect to flow direction, initial angle setting of the probe was made with the flow angles obtained from the flow probe. This setting was then refined by turning the hot-wire into the direction which gave maximum output. Almost without exception, the hot-wire angle position thus found was identical with the angle measured by the flow probe. The instrument setting of 90 per cent at the radius of 14.5 inches was periodically checked for drift. Drift was encountered only occasionally and was always less than 2 per cent. If drift was noticed, the hot-wire instrument was reset to 90 per cent of full scale at the reference radius.

The total temperature Kiel probe was set at the angle which was obtained from the flow probe at the particular radius.

For each run, radial survey readings of total temperature, total pressure, velocity head, absolute flow angle, and hot-wire anemometer velocity ratio were taken from the blade tip radius of 18 inches to a distance of 0.2 inches from the hub which has a radius of 10.8 inches. Although readings closer to the hub would have been desirable, the design of the flow probe prevented readings at distances less than 0.2 inches from the hub.

Data were taken at radial increments of 0.5 inches for the majority of the runs. Initially, the increment in radius was chosen as 0.2 inches. However, because of the smooth variation of the flow conditions in the annulus, this increment could be increased to 0.5 inches without loss of accuracy.

Various flow rates were set by means of the discharge throttle valve. The throttle valve position is indicated by means of a digital counter. The counter is calibrated from 0 to 1360 (closed to open). Radial surveys downstream of each rotor row were taken at counter readings of 1000, 900, 800, 700, 600, 500, and 435. Below a counter reading of 435, low rumbling noises and vibrations were observed as well as significant read-out fluctuations, indicating that major portions of the blading were stalled. Peripheral surveys with the flow probe at a counter setting below 435 showed significant flow variations with respect to the peripheral direction. These conditions existed between the hub and approximately mid-blade height. In addition, extreme variation in the hot-wire anemometer reading was noticed also in this region. In some cases, the hot-wire oscillations approached 30 per cent of the instrument read-out. Because of this condition no surveys were made at throttle settings below 435 counts. At a throttle setting of 435 counts, slight fluctuations in the hot-wire anemometer readings were noticed between the hub radius of 10.8 inches and a radius of 12 inches, whereas the flow probe readings were steady in this portion of the annulus.

No flow profiles are presented for readings of the throttle valve counter above 1000, although four such surveys were undertaken. They do not show appreciable differences since the flow rate increases only by about 2 per cent for counter readings between 1000 and 1360.

SECTION 8

DISCUSSION OF RESULTS

8.1 General

For the present study the O.N.R. compressor was run for 68 hours, of which 28 hours were required for the flow rate calibrations.

The tests were conducted with the so-called free-vortex blading of the compressor installed. The rotor blades of all three rotor rows were set at the design stagger angles of 43.8 degrees with respect to the axial direction. All stator blades had stagger angles of 39.8 degrees. The runs were made at the high rotor speed of about 1190 rpm.

8.2 Flow Rate Calibration

The flow rate calibrations were undertaken to verify the calibration factor found by Marshall (5). The fluctuating readings due to atmospheric conditions experienced by Marshall were eliminated by closing the door in front of the compressor inlet duct. It is interesting to note that during the radial surveys downstream of the third rotor, the door to the atmosphere was opened. Even though the atmospheric conditions were calm, fluctuations of up to 10 per cent were noticed in the hot-wire readings. The fluctuations stopped when the door was closed.

Velocity measurements in the inlet duct were made from the centerline to a radius of 17.8 inches. It was not possible to measure the velocities closer than 0.2 inches from the wall. Since the inlet pipe has a diameter of 36 inches, the hot-wire probe had to be supported from both walls to eliminate vibration. Therefore, the probe had to be attached at right angles to the support structure (Fig. 6). The

probe thickness of 1/4 inch and the fillet at the attachment point prevented measurements closer than 0.2 inches from the wall. Velocity measurements to the wall would have been desirable for a more accurate calculation of volume flow rate. In the calculation of volume flow rate, the velocity measured at a radius of 17.8 inches was assumed to be that at the wall also.

8.3 Presentation of Data

The axial velocity profiles obtained from the NISRE solution and from the flow probe and hot-wire measurements are presented in Figs. 12 through 32 in dimensionless form. These quantities were made dimensionless by dividing the velocities by the rotor tip speed. The parameter φ thus obtained is convenient for two reasons. First, assuming that a mean axial velocity $\overline{V}_a$ exists in the flow annulus, the volume flow rate can be expressed by

$$VF = \overline{V}_a \frac{651.4}{144} \qquad (ft^3/sec) \tag{32}$$

and the rotor tip speed is

$$U_T = \omega \frac{18}{12} \qquad (ft/sec) \tag{33}$$

where ω is the angular velocity of the rotor in radians per second. Thus

$$\overline{\Phi} = \frac{VF}{\omega}\left(\frac{12}{18}\right)\left(\frac{144}{651.4}\right) = \frac{VF}{\omega}(0.1474) \tag{34}$$

Therefore, $\overline{\Phi}$ is a flow coefficient relating volume flow rate to rotor speed. A numerical average of the values of Φ obtained from the radial distribution of axial velocities at a given flow rate gives an average value of $\overline{\Phi}$ which is a measure of the volume flow rate at

a particular throttle setting and rotor speed. Second, the flow coefficient is a convenient parameter for comparing the velocities obtained by the NISRE solution and those measured with the flow probe and the hot-wire anemometer because changes in rotor speed have no influence on Φ.

The total pressures measured with the flow probe downstream of each of the rotors at various flow rates are presented in Figs 33 through 35. These pressures are shown in dimensionless form by the parameter

$$\psi = \frac{P_t - P_a}{\rho_a U_T^2} \tag{35}$$

where the subscript "a" refers to the atmospheric conditions.

The work input of a blading element in an axial-flow compressor can be expressed by the so-called Euler turbine equation. The rise in total temperature from station (1) ahead of to station (2) after the blading is

$$\Delta T_t = \frac{\omega}{C_p g J}(r_2 V_{u_2} - r_1 V_{u_1}) \quad (^\circ R) \tag{36}$$

For a frictionless process of an incompressible fluid, the theoretical rise in total pressure $(\Delta P_t)^*$ then becomes

$$(\Delta P_t)^* = \rho \omega (r_2 V_{u_2} - r_1 V_{u_1}) \quad (psf) \tag{37}$$

With losses, the pressure rise ΔP_t is

$$\Delta P_t = \eta (\Delta P_t)^* = \rho \omega \eta (r_2 V_{u_2} - r_1 V_{u_1}) \quad (psf) \tag{38}$$

where η is the stage efficiency. Rewritten

$$\Delta P_t = \rho U_T^2 \eta \left(\frac{U_2}{U_T} \frac{V_{u_2}}{U_T} - \frac{U_1}{U_T} \frac{V_{u_1}}{U_T} \right) \equiv \rho U_T^2 \Psi$$

The so-called pressure coefficient Ψ is therefore a function of the flow angles and the losses only and is independent of the density of the flow and the rotor speed, as long as the influences of Reynolds number and Mach number can be ignored. The aforementioned parameter ψ is suitable for comparing the radial distributions of the total and static pressures measured after the rotors because the influences of varying densities and rotor speeds are eliminated.

Since the present study was not concerned with determining blade losses, no measurements of total pressure were made upstream of the rotors while the radial surveys were conducted downstream of them. Since the surveys after the rotors were conducted on different days, it was not possible to maintain exactly the same value of the average flow coefficient $\overline{\Phi}$; hence, the values of ψ presented for the total pressure cannot be used to establish the quantity Ψ defined earlier.

The static pressures calculated by the NISRE method, those measured by the flow probe, and the ones calculated by using the velocity measured by the hot-wire anemometer were made dimensionless by the same method. The dimensionless parameter thus obtained is convenient for comparing the static pressures determined by these different methods because changes of atmospheric pressure, density, and tip speed do not influence the data.

Figures 36 through 56 show the measured values of the absolute flow angles α obtained for all runs.

8.4 Accuracy of the NISRE Method

Figures 12 through 32 show very good agreement between the velocity profiles calculated by the NISRE method and those measured by the flow probe and hot-wire anemometer. The agreement is good downstream of all rotors through the range of flow rates, with the possible exception of

Fig. 24. This figure shows axial velocity profiles obtained after the second stage rotor at a flow rate of 22.85 lbm/sec corresponding to a discharge throttle valve counter setting of 500. This run was repeated to check the results; but for both runs they were almost identical. The calculated velocities differ from the measured ones by as much as 7.5 per cent at radius ratios R/R_0 of 0.67 and 0.9. No obvious explanation could be found for this deviation from the otherwise close agreement between the calculated and measured data.

Figures 57 through 77 show the comparison of the static pressures obtained from the three methods. This is not an independent comparison since these pressures are dependent on the velocities also. With the flow probe, the static pressures were measured directly, but for the NISRE calculation and hot-wire measurement, the static pressures were calculated by using Eqs. 11, 17, and 19. However, good agreement has been obtained with the three methods.

8.5 Blockage Factor

The value of the gross weight flow blockage factor to be used with the NISRE method has a large influence on the results. Reference 2 suggests a blockage factor of 0.98 for the first stage and 0.96 for all subsequent stages.

Blockage factors of 0.96 for the second and third stage rotors gave the results of Figs. 19 through 32. Blockage factors of 0.98 were first tried for the calculations of the velocity profiles for the first stage rotor but gave velocities well below those measured by the flow probe and the hot-wire anemometer. The effect of the area blockage by the wall boundary layers was then increased by changing the blockage factor to 0.97

and finally to 0.96. This increase in area blockage did not materially change the shape of the calculated profiles but increased the magnitudes of the velocities. Blockage factors of 0.96 for the first rotor gave the best correlation between the axial velocities calculated by the NISRE method and those measured. Figures 12 through 18 show the axial velocity profiles after the first rotor for this value. It is believed that the requirement for a smaller blockage factor after the first rotor is caused by the boundary layer build-up along the walls of the inlet duct which has a length of six feet.

8.6 Compressor Design Point

As stated in subsection 8.1, the tests were conducted with the so-called free-vortex blading of the compressor. At their design point, such bladings are supposed to produce flow patterns where the product of the radius r and the peripheral component V_u of the absolute velocity remain constant in the radial direction after each row of blades. If entropy gradients are ignored, free-vortex flows have constant total pressure P_t, constant total temperature T_t, and constant axial velocity components V_a between the rows of blades. However, if entropy gradients occur even though total temperatures do not change in the radial direction, the axial velocity components of the absolute velocity are not constant. Equation 3, without the term involving meridional streamline curvature, can be expressed also by

$$J g C_p \frac{\partial T_t}{\partial r} = J g T \frac{\partial S}{\partial r} + \frac{V}{r} \frac{\partial (r V_u)}{\partial r} + V_u \frac{\partial V_a}{\partial r}$$

Hence, if the product rV_u were constant in the radial direction, the term containing V_u would be zero. If the total temperature were also constant in the radial direction, the only terms remaining are those involving entropy and axial velocity component. This indicates that with the aforementioned assumptions, the variations of the axial velocity components are a function of the entropy gradients and the static temperatures.

From the presented data it can be noticed that neither constant velocities V_a nor constant total pressures P_t were reached with the installed blading, irrespective of flow rate. In Ref. 3, the design stagger angle of the stator blades is given as 29.8 degrees. Hence, since a value of 39.8 degrees was used for the present tests, it is likely that radial changes in V_a and P_t were due to this condition.

All the axial velocity profiles calculated by the NISRE method show regions of increased axial velocities at radius ratios R/R_0 of about 0.67 and 0.90. At which of these two stations the maximum velocity occurs depends on the flow rate. As flow rate decreases, the region of highest velocity moves from the inner to the outer part of the annulus. The measured velocity profiles show the same trend but are generally flatter. The crossover point, where the maximum velocity at both regions has about the same magnitude, occurs at a flow rate of about 26.5 lbm/sec, as shown in Figs. 12, 14, 15, 22, and 29. To this flow rate corresponds a flow coefficient $\overline{\Phi}$ of about 0.44, which is the average of the flow coefficients obtained from the calculated and measured axial velocity profiles presented in the abovementioned figures. Except for the regions near the hub and the tip, the axial velocity is nearly constant at this flow rate. Further evidence that the design criteria of a free-vortex

flow were most nearly met at a $\overline{\Phi}$ of 0.44 is given in Figs. 33 through 35, where it is shown that total pressure is nearly constant except for the hub and tip regions. However, this uniformity is not so well realized after the second and third stage rotor. For this discussion it is of interest to note that Ref. 4 gives a design value of $\overline{\Phi}$ of 0.45 for the free-vortex blading at rotor and stator stagger angles of 43.8 and 29.8 degrees respectively.

Reduced total pressures and low axial velocities occur in the regions near the hub and near the outer casing downstream of all rotor rows. They are caused by end and tip clearance losses, by the wall boundary layers, and by the effect of the rotating hub. These conditions produce large entropy gradients at the inner and outer radii of the annulus for the reason shown in the explanation of Eq. 3 in this subsection. Their effect near the hub extends from radius ratios of 0.6 at the hub to about 0.64 for the first rotor, 0.66 for the second rotor, and 0.69 for the third rotor. Near the outer casing, they influence the velocity distributions at radius ratios of about 0.91 after the first rotor and about 0.94 after the second and third rotor. The regions which are affected by the hub and tip losses become larger as the fluid proceeds downstream since the losses accumulate from stage to stage and further deteriorate the flow profiles.

The velocities at the outer casing are difficult to measure. Since the probes extended into the flow annulus from the outer casing, radial position changes of the probes of the order of 0.01 inches at the outer radius caused changes in the measured data of up to 40 per cent. It is believed that these discrepancies were caused by small errors in the probe

position indication. The probes retract into the radial access holes, and small changes in radial position cause the access holes to block the measuring holes of the probes.

SECTION 9

CONCLUSIONS AND RECOMMENDATIONS

The accurate determination of the radial distribution of absolute velocity in magnitude and direction is important for the evaluation of the performance of turbomachines. If these distributions were known, the velocity triangles would be completely determined. Knowledge of the velocity triangles allows direct comparison between the applied design criteria and the actual results for a turbomachine.

The accurate predictions of these velocity triangles is of particular importance in the design of multi-stage axial-flow machines. With the exception of the first stage, the inlet conditions of a given stage are the discharge conditions of the preceding stage. If a stage has inlet conditions different from those for which it was designed, its performance is likely to be marginal and could produce discharge conditions that deviate even more from the design values. The result is that the machine will not be able to handle the desired enthalpy change at the expected level of efficiency. The radial distributions of losses and flow deflections in a row of blades are a function of inlet conditions as well as the design of the blades. A blade element designed for a certain range of flow incidence angles, but operating outside of this range, may either stall or not develop the required blade forces, depending on whether the incidence angle is too large or too small. Optimum design of multi-stage axial-flow machines therefore requires that the discharge conditions of any stage match the design inlet conditions of the following stage.

Since designs of turbomachines are based on the results of experimental

work and the experience of the designer, checking the results of new designs is important for two reasons: first, to evaluate the performance of a new design, and second, to improve the design procedures for future machines.

The NISRE method represents a fairly accurate and simple method for determining the velocity profile downstream of an axial-flow rotor. The data which are required can be obtained by small and accurate probes in the vaneless space between blade rows with small axial clearance. The method as presented in this study is limited by the fact that the effect of meridional streamline curvature is ignored. For designs where the curvatures of the meridional streamlines are appreciable, the computing process could be improved in the manner carried out by Harrison (2).

Further experimentation seems necessary to accurately predict the gross weight flow blockage factors, particularly with machines having many stages. The blockage factors used for the velocity profiles after the first rotor were determined by arbitrary variation until accurate matching with the measured profiles were obtained. By changing the length of the inlet duct of the O.N.R. compressor the effect of boundary layer growth on blockage factors could be investigated.

The hot-wire anemometer was not used for an analysis of the unsteady flow in the passages downstream of the rotors. The presented average velocities were read on an instrument which heavily damps the signal and cannot follow the high frequency response of the hot-wire anemometer which is up to 50 kilohertz. However, some oscilloscope traces were photographed downstream of the second rotor. Sample pictures of these oscillograms, with the hot-wire probe at a radius of 13 inches, are presented in Fig. 78. The oscillogram marked (a) was made with the throttle

valve open, and the oscillogram marked (g) was made at a throttle valve counter setting of 425. The measured flow rates are indicated in the figures. The time for successive blades to pass by the hot-wire is 1.675 milliseconds, corresponding to a frequency of about 0.6 kilohertz which is well within the frequency response of the hot-wire anemometer. Therefore, the hot-wire probe will be able to measure the flow conditions in the wakes between neighboring blades.

The low signal amplitudes in Fig. 78, which are marked by arrows, were found to have the time interval of 1.675 milliseconds. Hence, they are caused by blade wakes. The trace of the hot-wire output moves from left to right on the oscillograms. Hence, the wakes start on the concave side of the blade profiles and end on the convex side of the profiles. Therefore, the flow profiles from left to right between the indicated wakes start from the pressure side of one blade and extend to the suction side of the neighboring blade.

An interesting phenomenon occurs in the oscilloscope traces at a flow rate of 19.26 lbm/sec which is evident from the oscillogram marked (g). An additional trace of lesser intensity but greater amplitude is superimposed on the aforementioned wake pattern. This pattern is periodic in nature and seems to be an indication of the propagating stall discussed by Iura and Rannie (7).

If the resolution of the oscilloscope traces could be improved or if the hot-wire signal were recorded on magnetic tape and transferred to a strip chart recorder, the wake pattern of the flow profiles could be analyzed in greater detail to detect incipient stall conditions. Using instrumentation of this type, it seems feasible to apply the momentum theorem to determine the losses associated with either different blade

shapes or various stagger angles of a given set of blades. The O.N.R. compressor is suitable for such studies since it is possible to vary rotor stagger angles and to install different types of blades. Such a study would require accurate calibrations of the hot-wire probes to enable measurements of velocity in absolute values rather than as ratios with a known velocity. A test rig is now being designed at the Naval Postgraduate School for such calibrations.

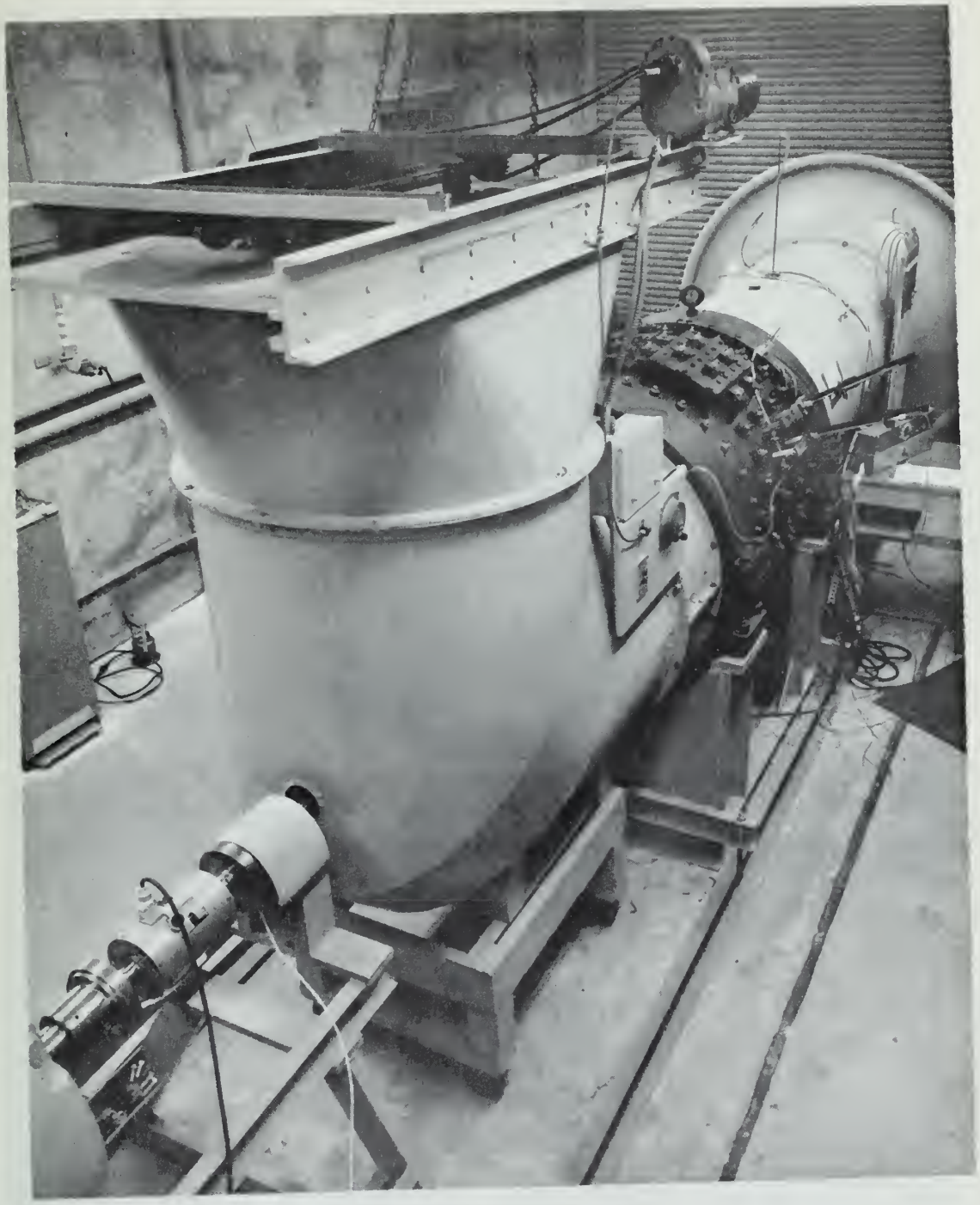

FIGURE 1
COMPRESSOR INSTALLATION

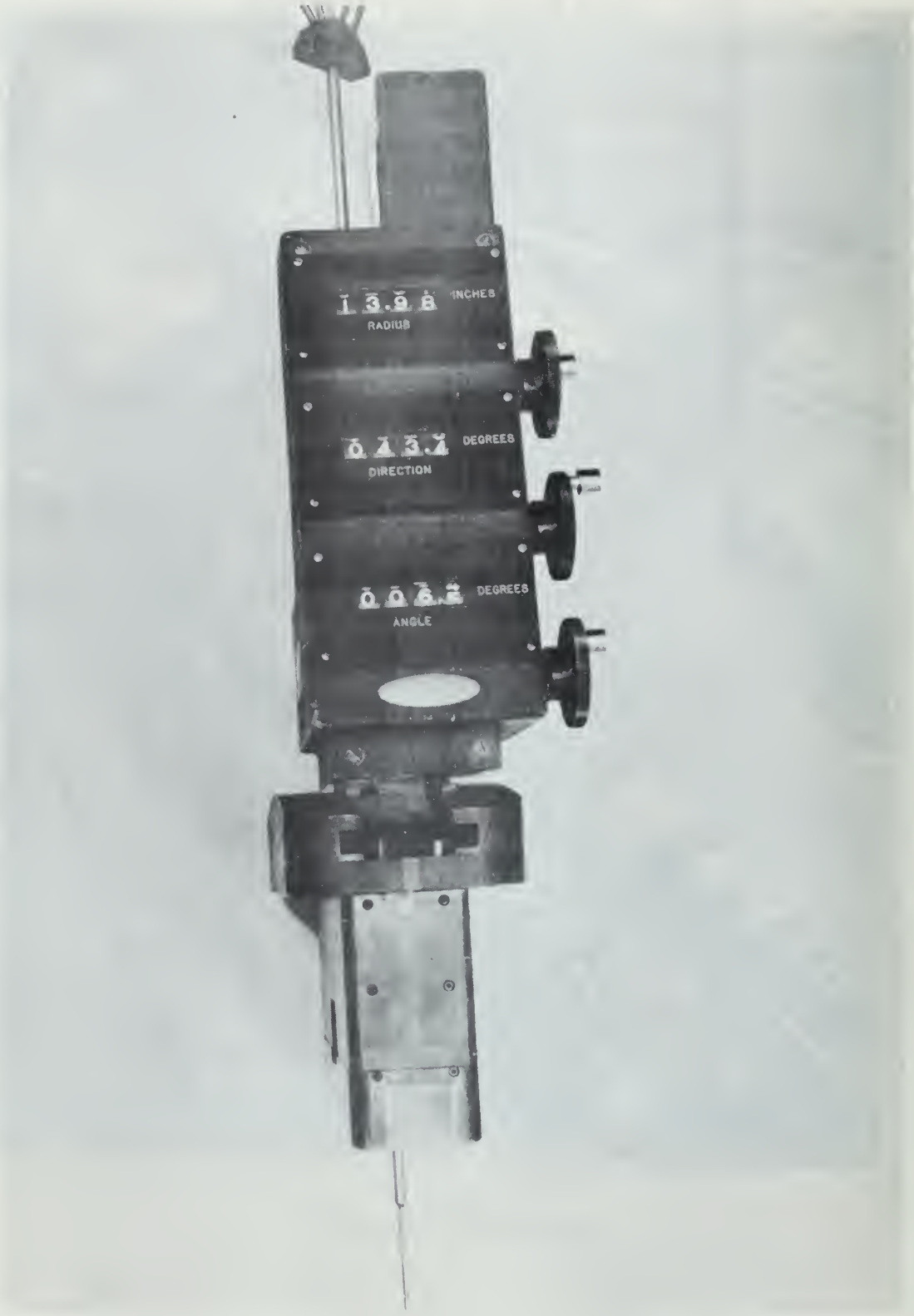

FIGURE 2
DETAIL OF FLOW PROBE CARRIAGE

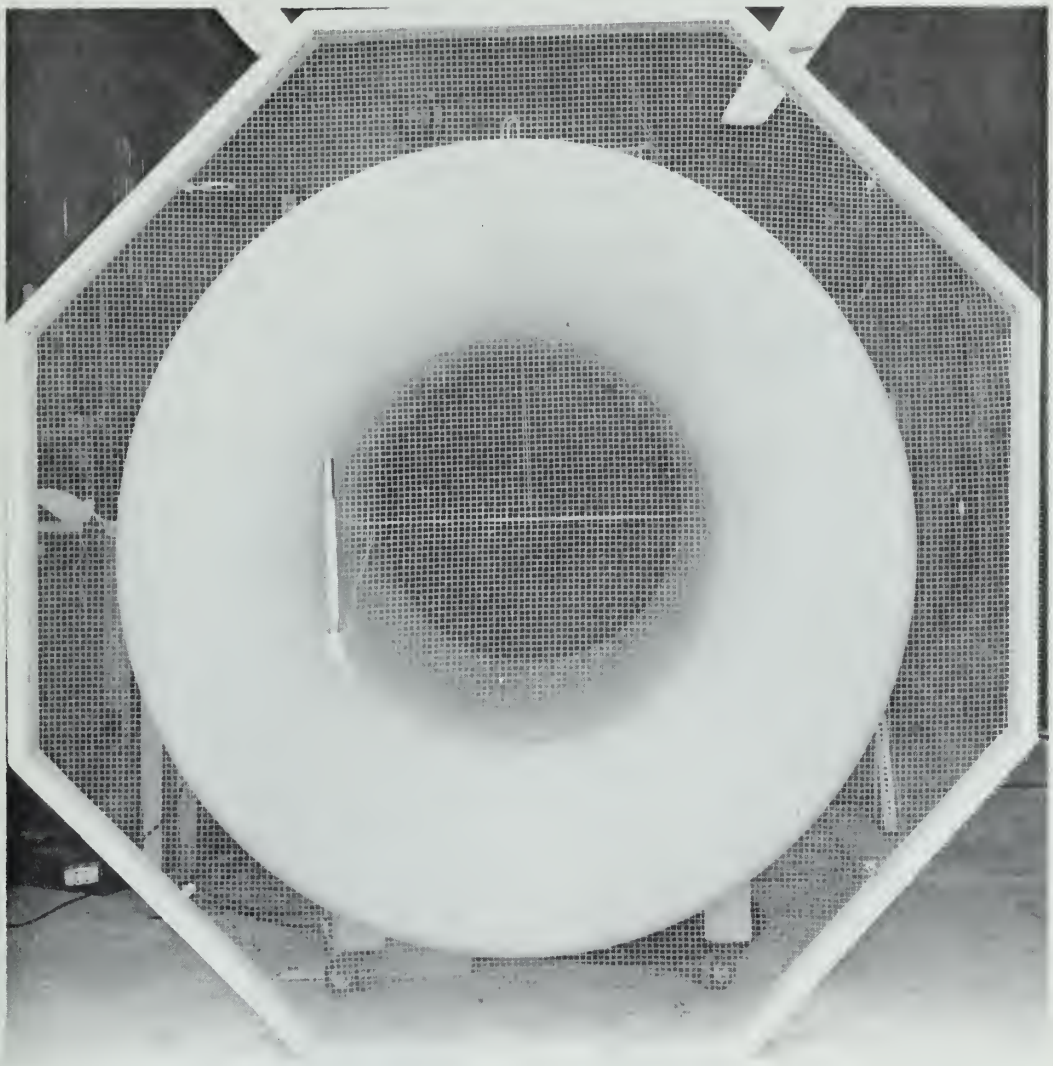

FIGURE 3
COMPRESSOR INLET DUCT

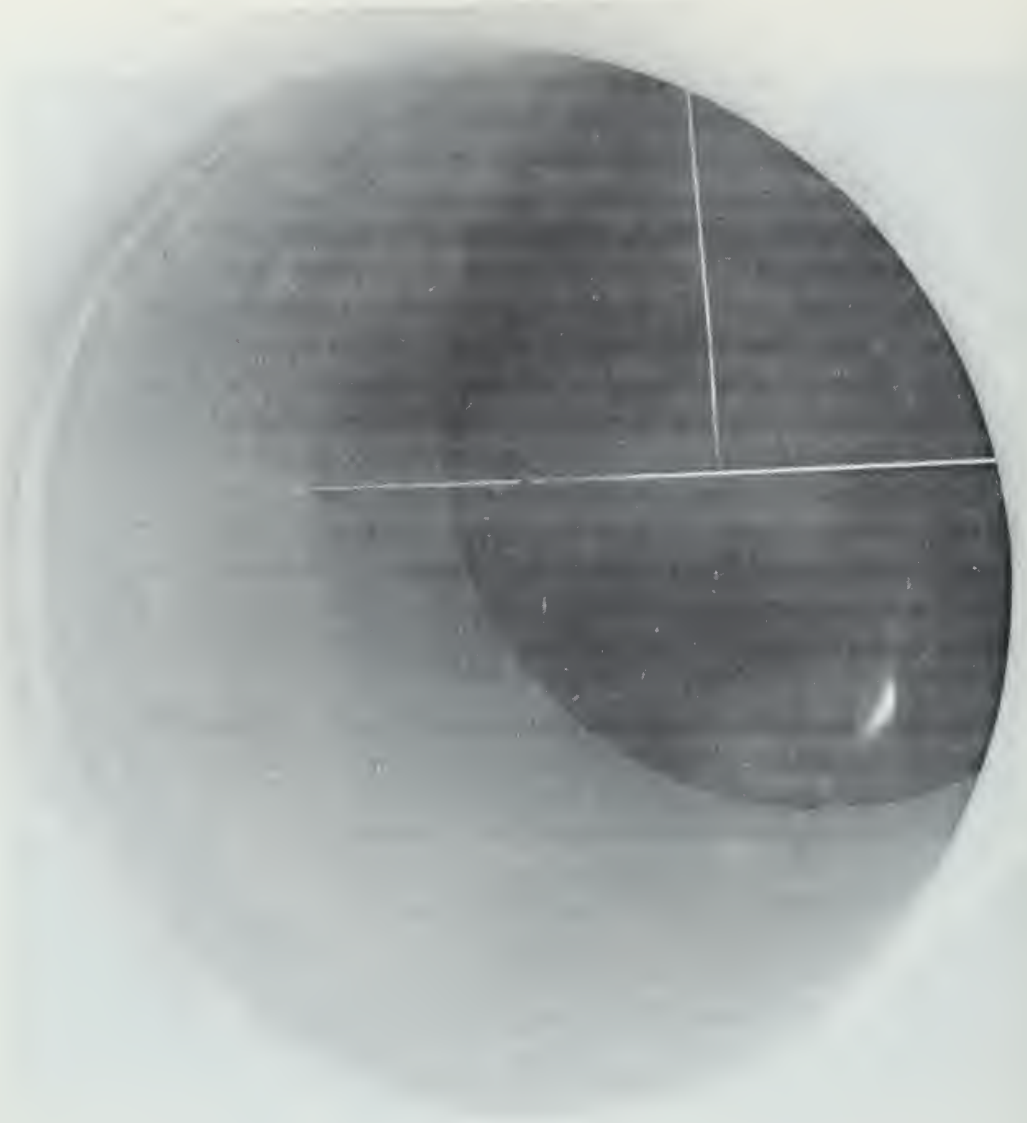

FIGURE 4
COMPRESSOR INLET WITH INSTALLED FLOW RATE SURVEY INSTRUMENTS

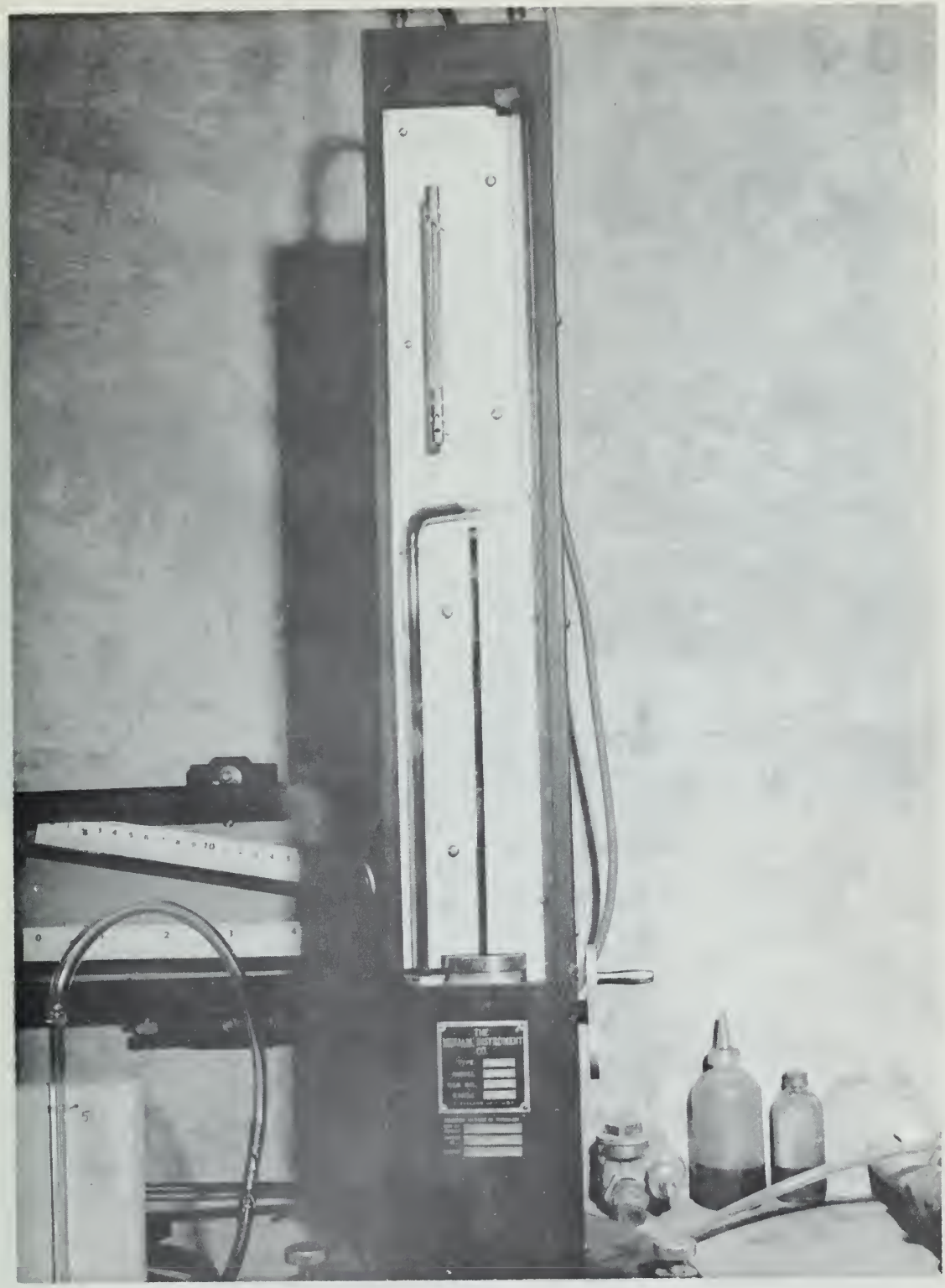

FIGURE 5
MICROMANOMETER

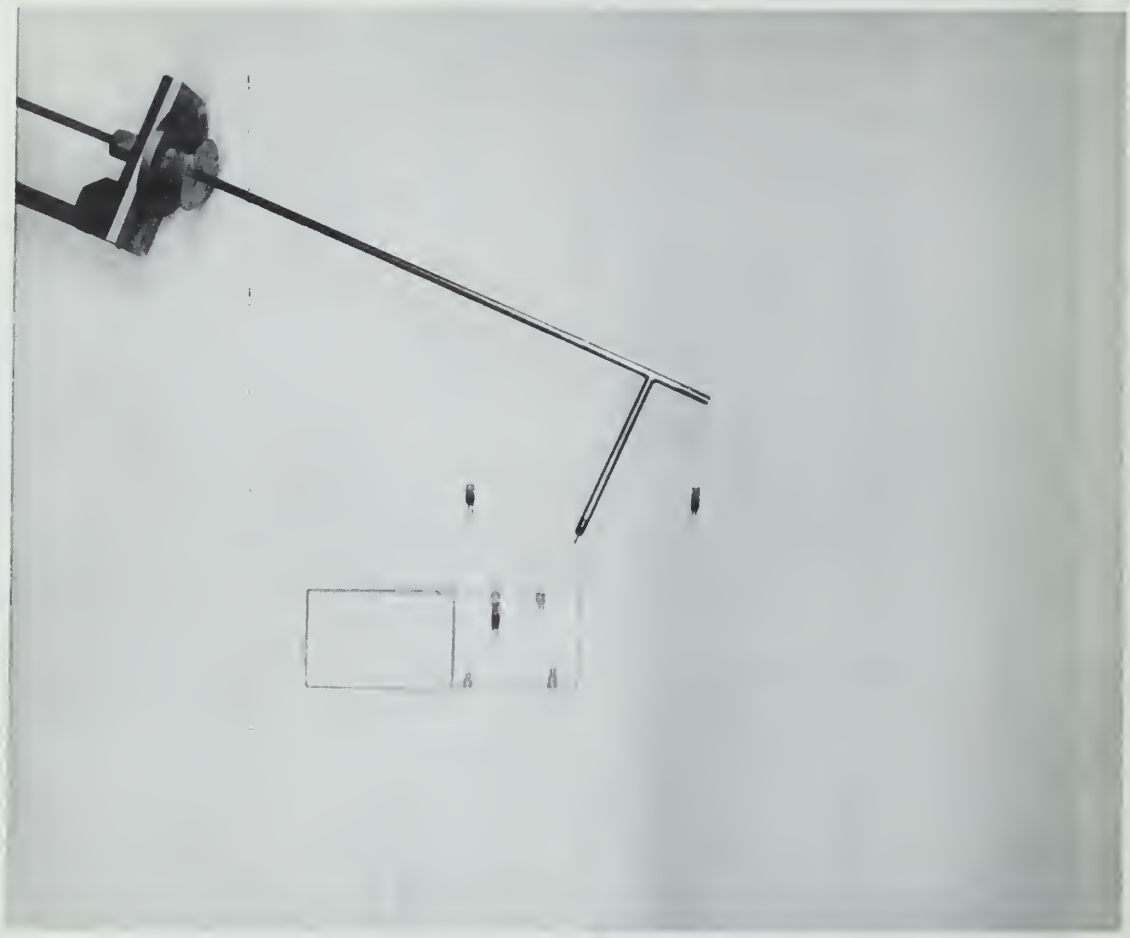

FIGURE 6
DETAIL OF INLET HOT-WIRE ANEMOMETER PROBE

FIGURE 8
PRESSURE SCANNER VALVES AND CONTROLLERS

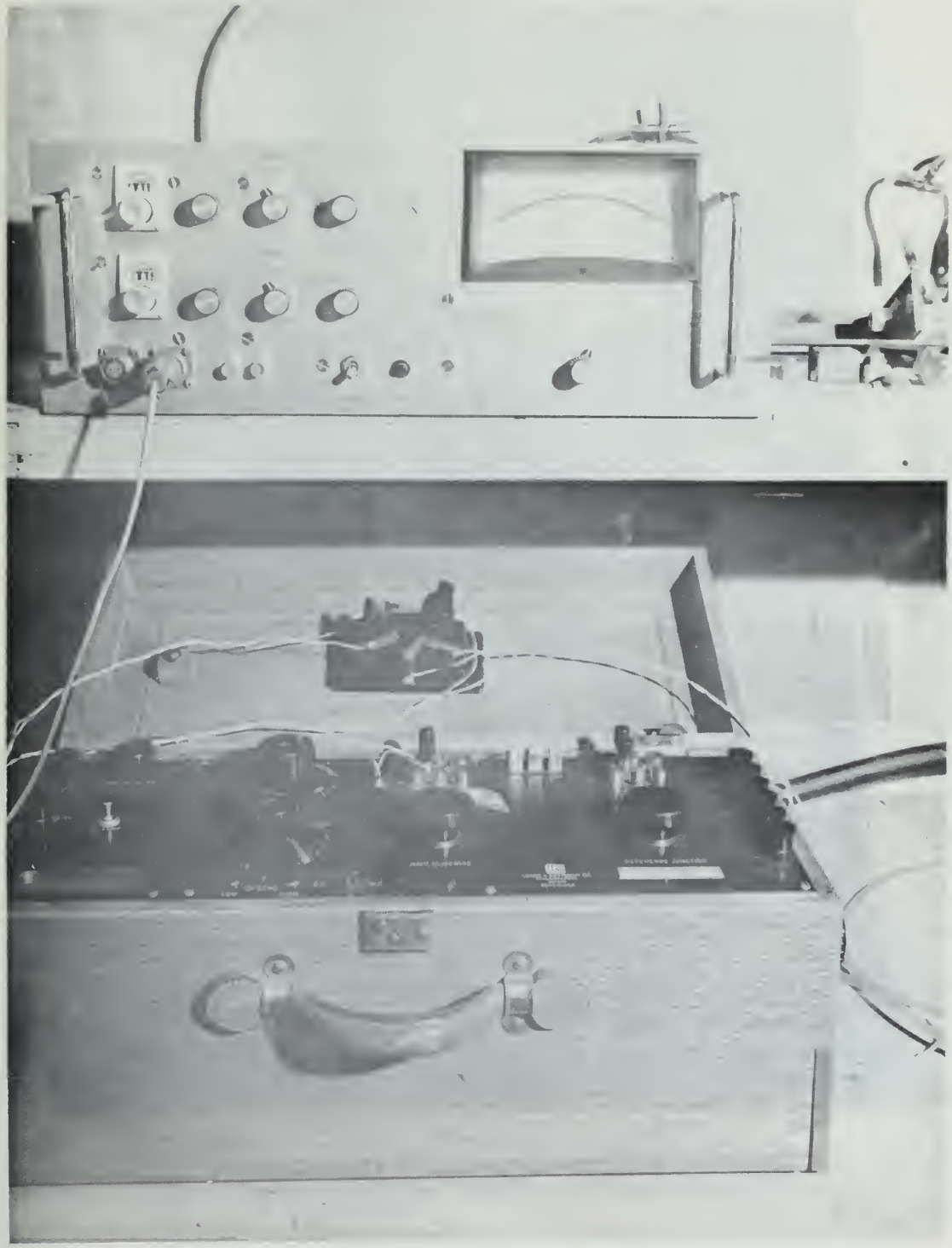

FIGURE 9
HOT-WIRE ANEMOMETER INSTRUMENT READOUT
AND THERMOCOUPLE READOUT

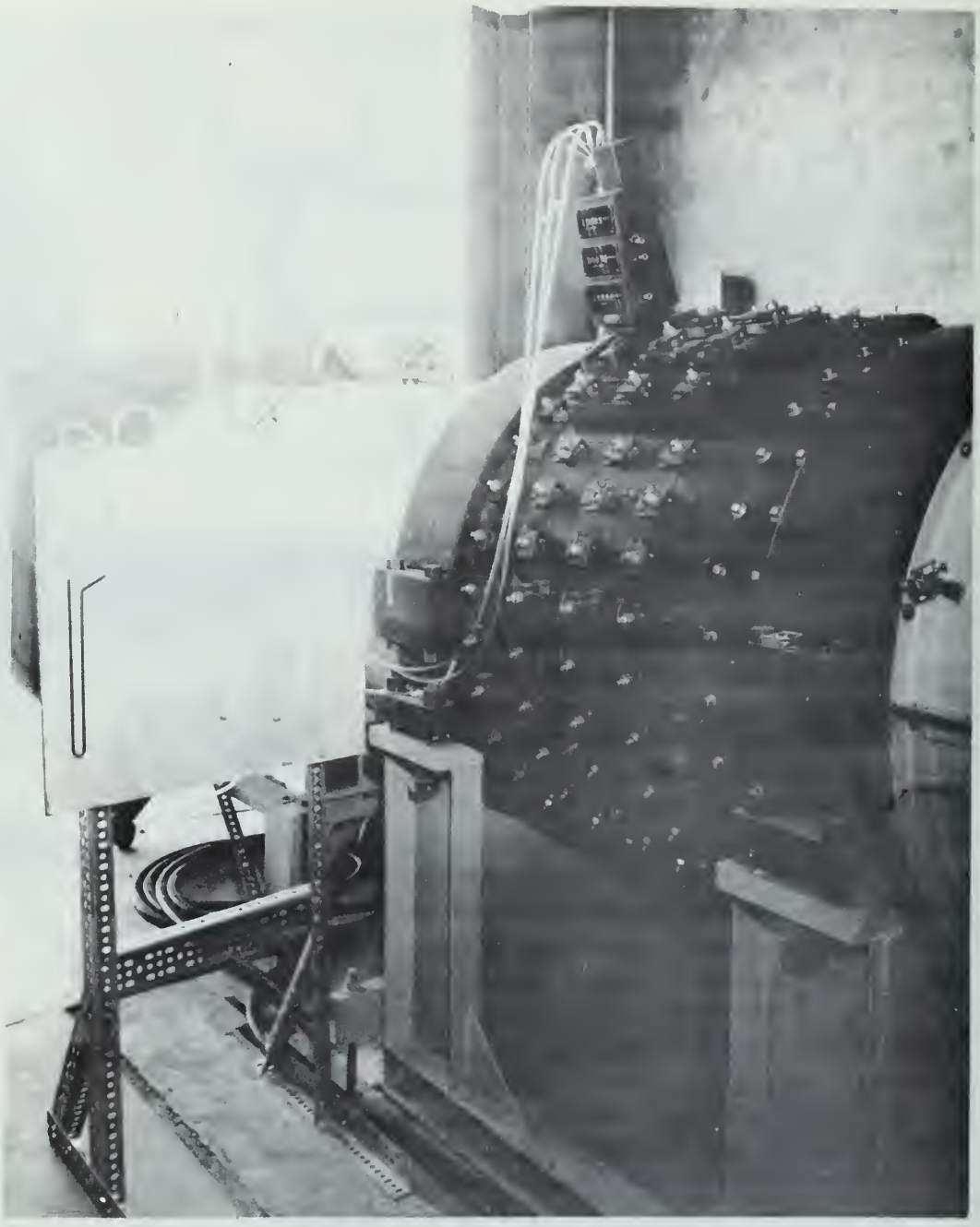

FIGURE 10
VIEW OF COMPRESSOR SHOWING FLOW PROBE CARRIAGE
INSTALLED AND ASSOCIATED MANOMETER BOARD

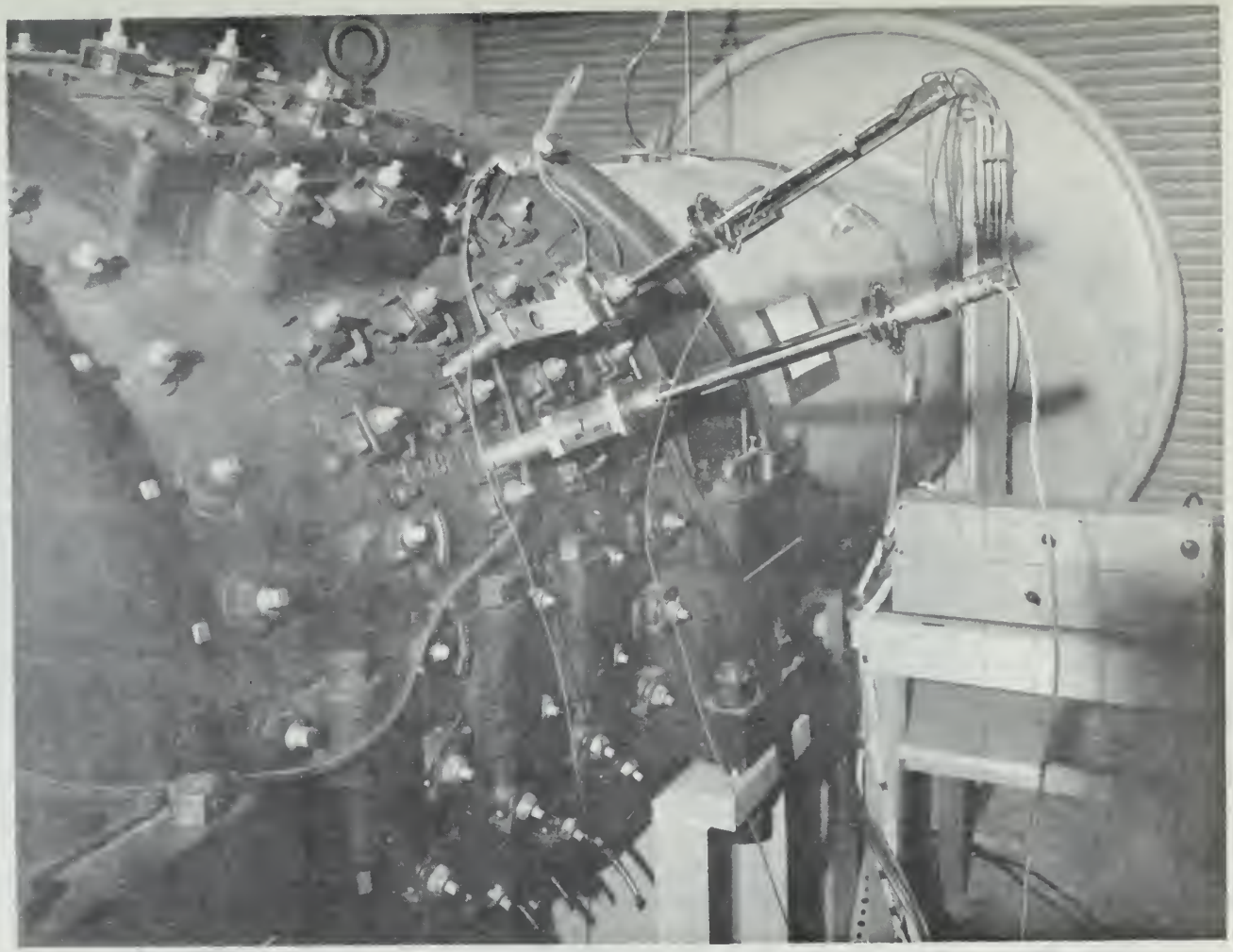

FIGURE 11
VIEW OF COMPRESSOR SHOWING HOT-WIRE ANEMOMETER
AND TOTAL TEMPERATURE PROBES INSTALLED

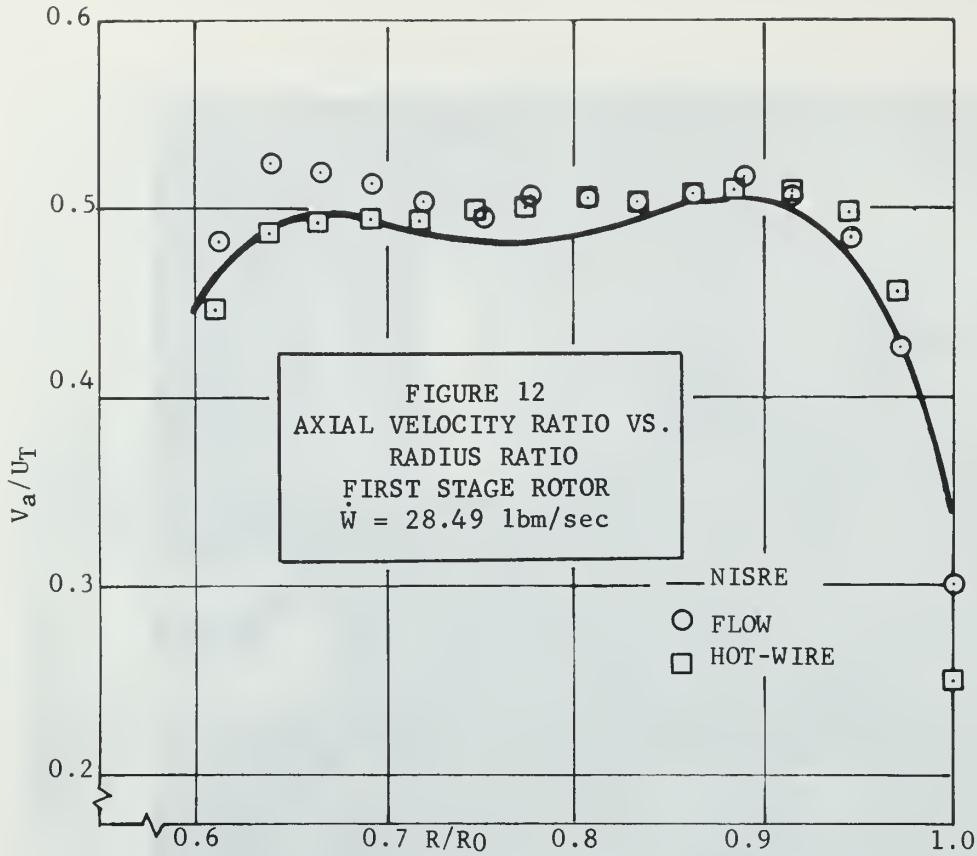

FIGURE 12
AXIAL VELOCITY RATIO VS.
RADIUS RATIO
FIRST STAGE ROTOR
$\dot{W}$ = 28.49 lbm/sec

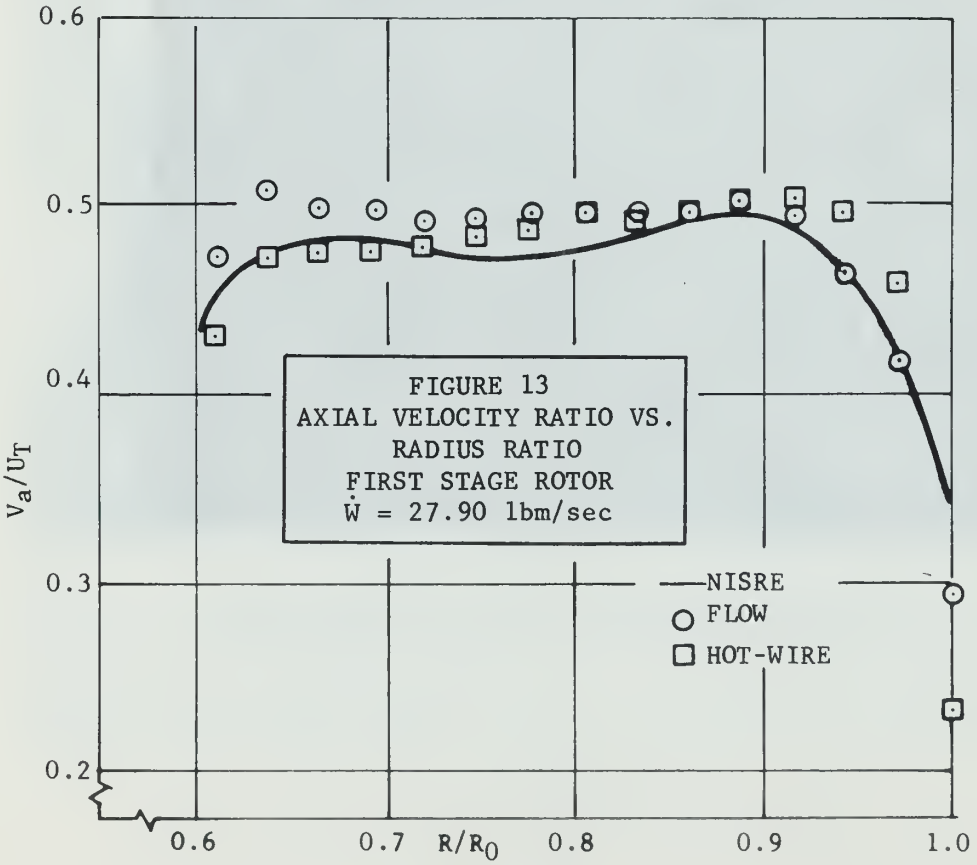

FIGURE 13
AXIAL VELOCITY RATIO VS.
RADIUS RATIO
FIRST STAGE ROTOR
$\dot{W}$ = 27.90 lbm/sec

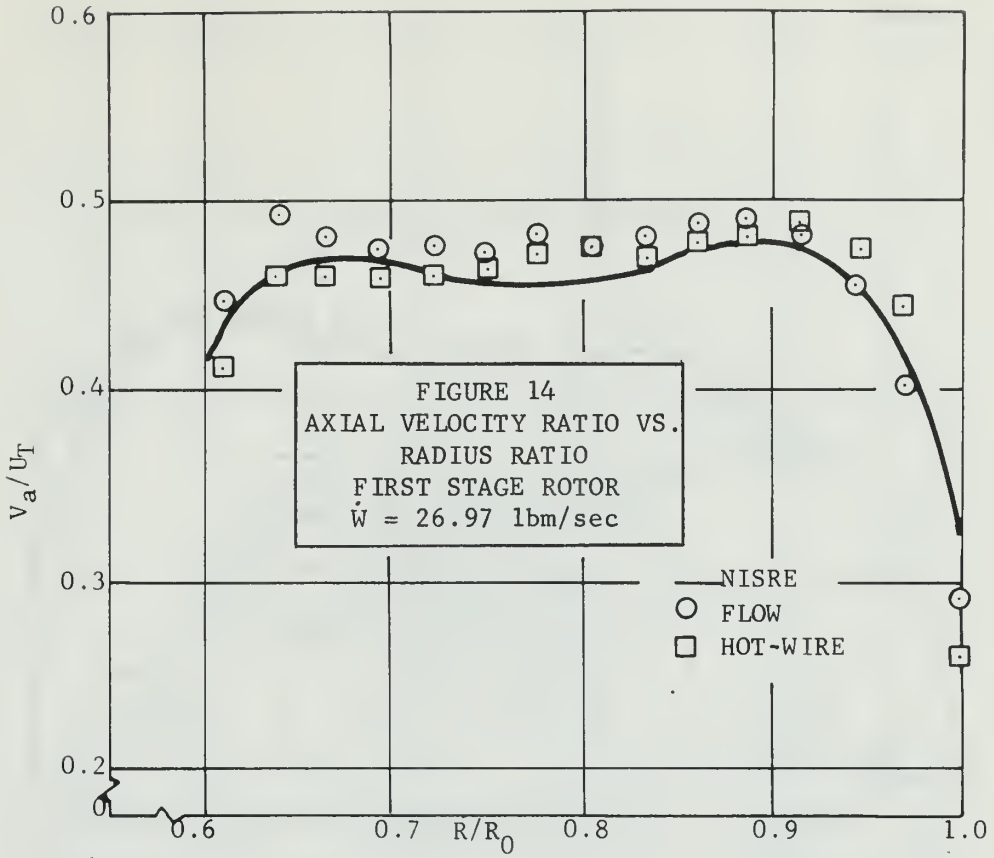

FIGURE 14
AXIAL VELOCITY RATIO VS.
RADIUS RATIO
FIRST STAGE ROTOR
$\dot{W}$ = 26.97 lbm/sec

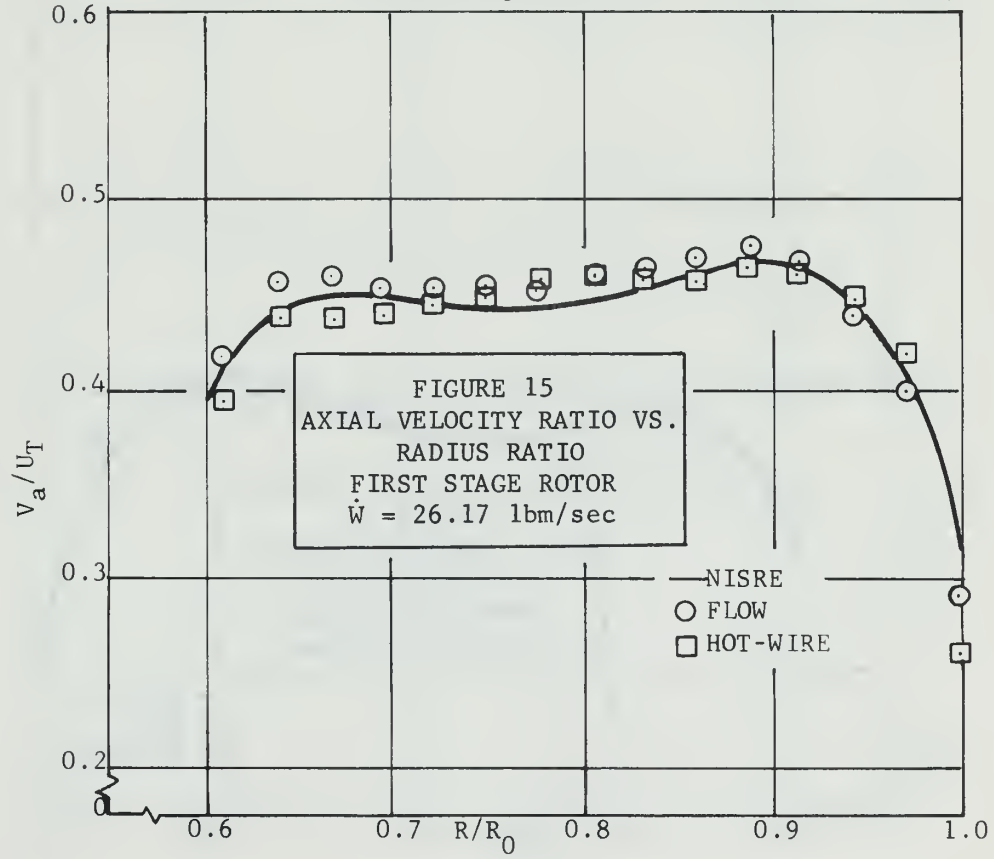

FIGURE 15
AXIAL VELOCITY RATIO VS.
RADIUS RATIO
FIRST STAGE ROTOR
$\dot{W}$ = 26.17 lbm/sec

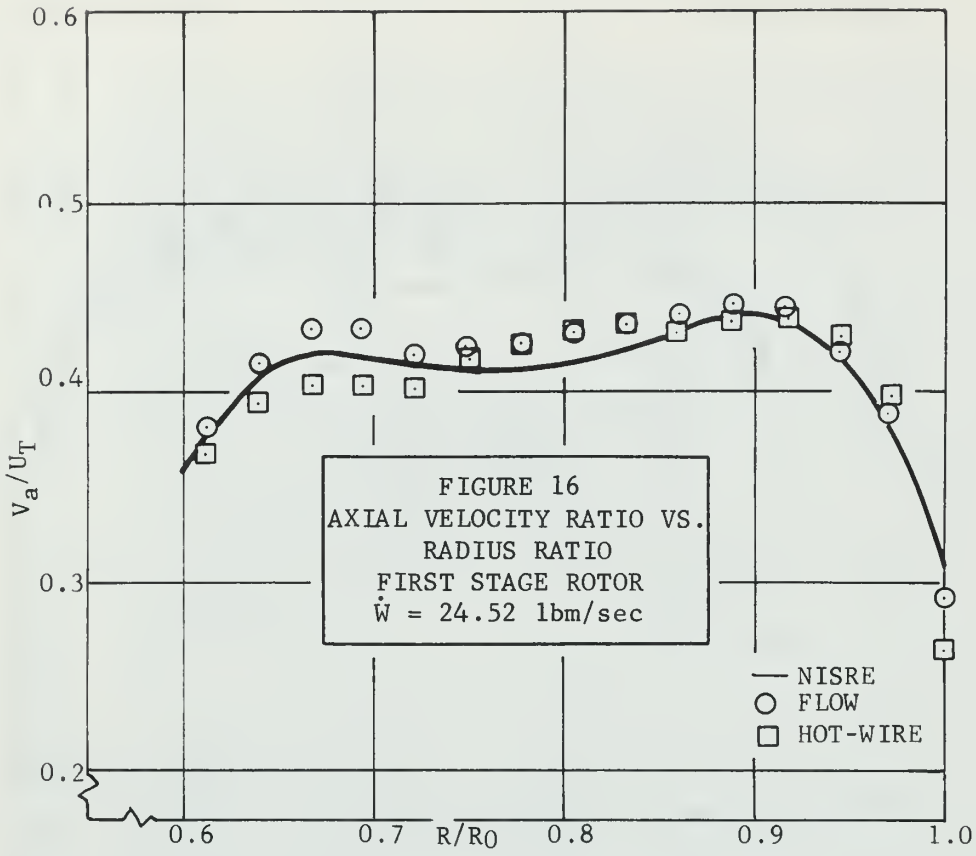

FIGURE 16
AXIAL VELOCITY RATIO VS.
RADIUS RATIO
FIRST STAGE ROTOR
$\dot{W}$ = 24.52 lbm/sec

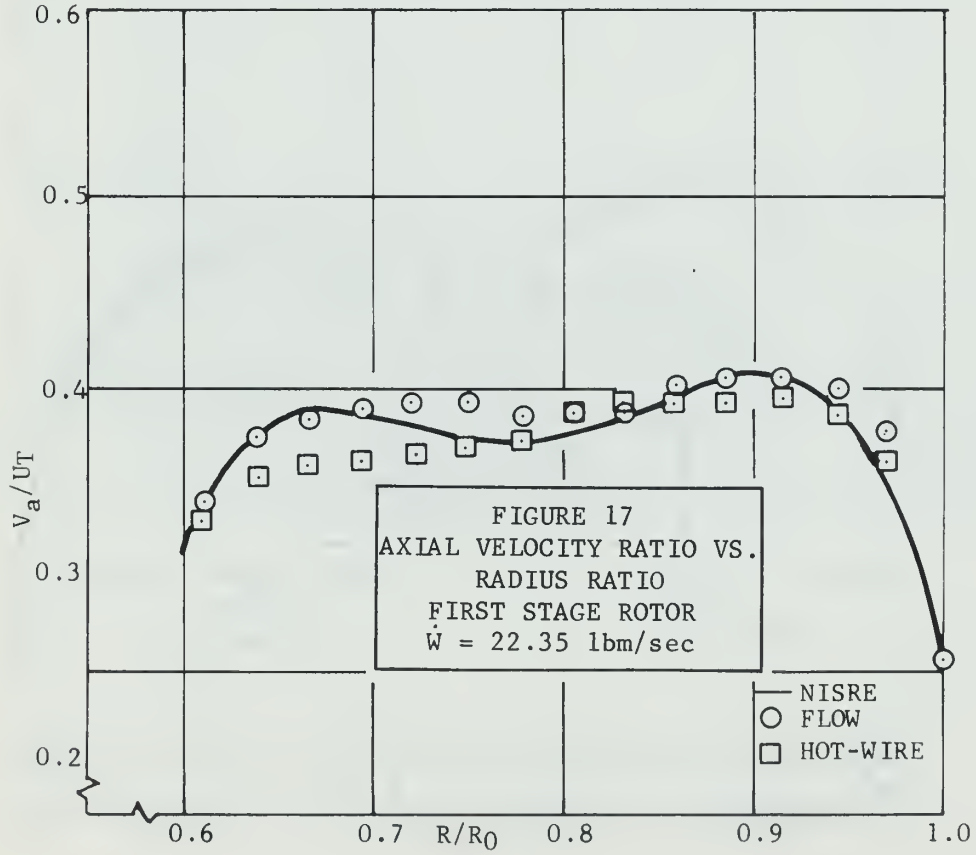

FIGURE 17
AXIAL VELOCITY RATIO VS.
RADIUS RATIO
FIRST STAGE ROTOR
$\dot{W}$ = 22.35 lbm/sec

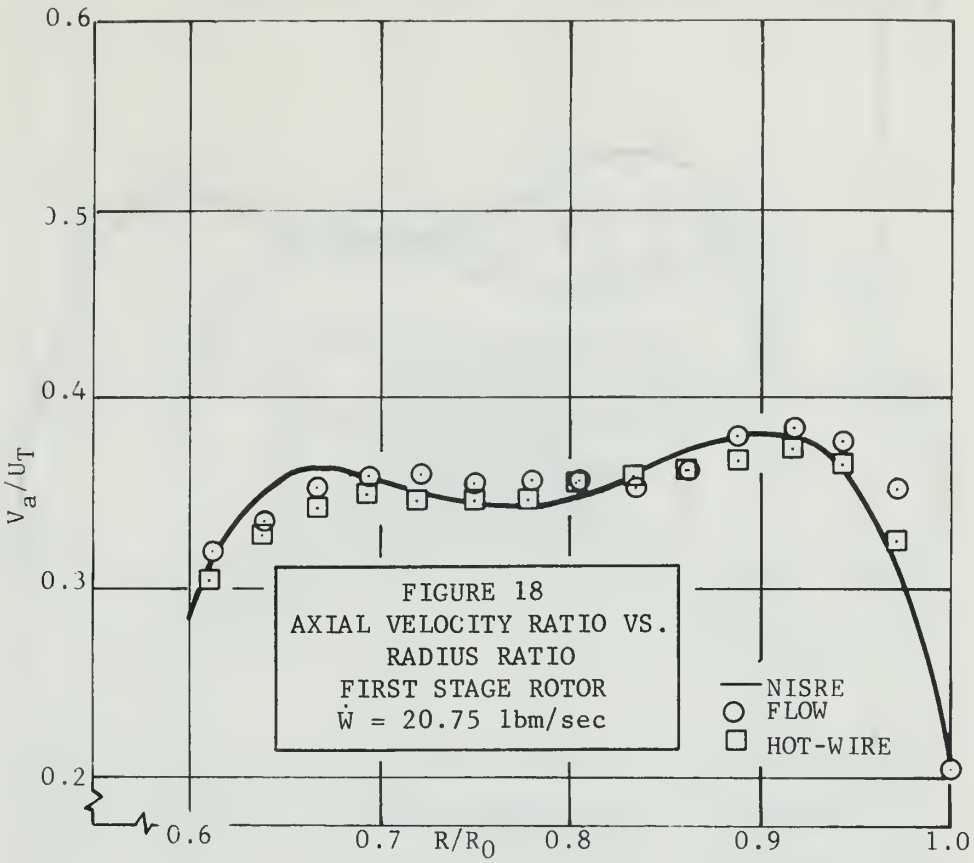

FIGURE 18
AXIAL VELOCITY RATIO VS.
RADIUS RATIO
FIRST STAGE ROTOR
$\dot{W}$ = 20.75 lbm/sec

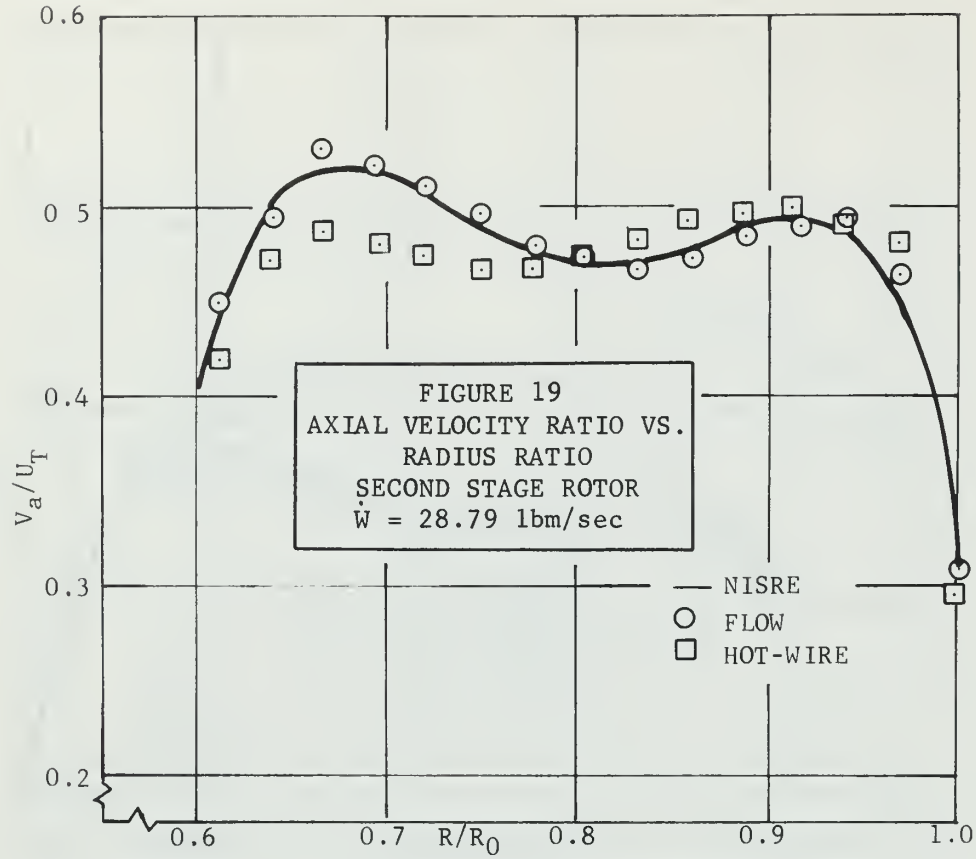

FIGURE 19
AXIAL VELOCITY RATIO VS.
RADIUS RATIO
SECOND STAGE ROTOR
$\dot{W}$ = 28.79 lbm/sec

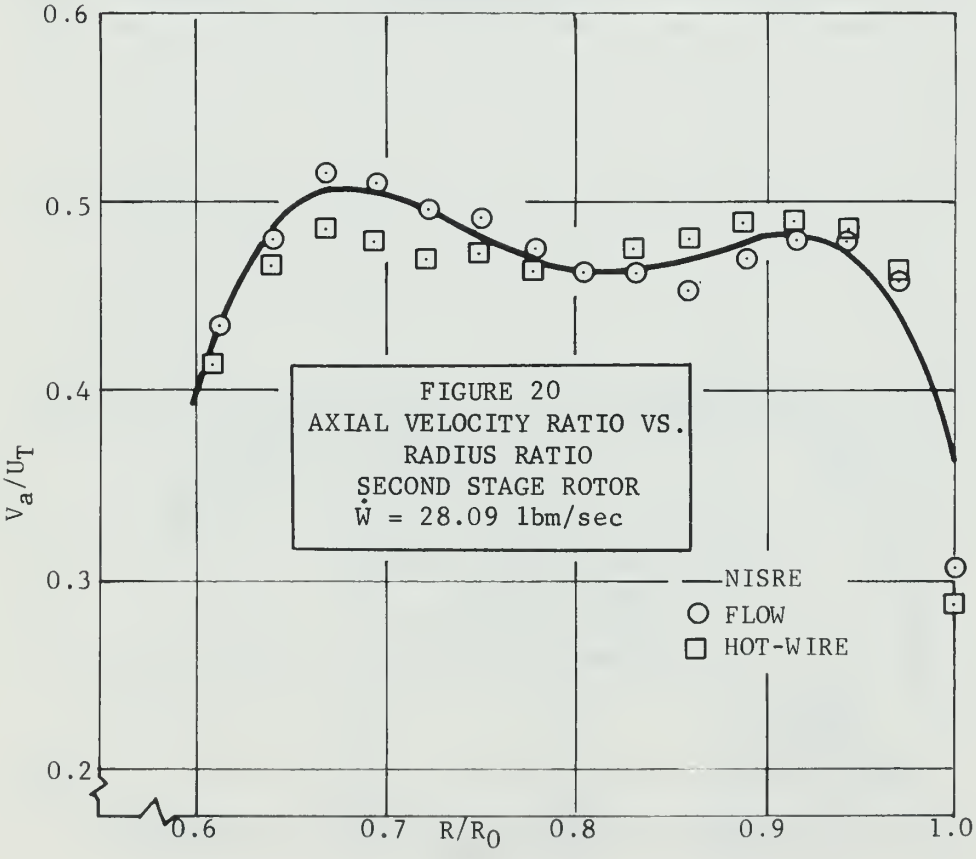

FIGURE 20
AXIAL VELOCITY RATIO VS.
RADIUS RATIO
SECOND STAGE ROTOR
$\dot{W}$ = 28.09 lbm/sec

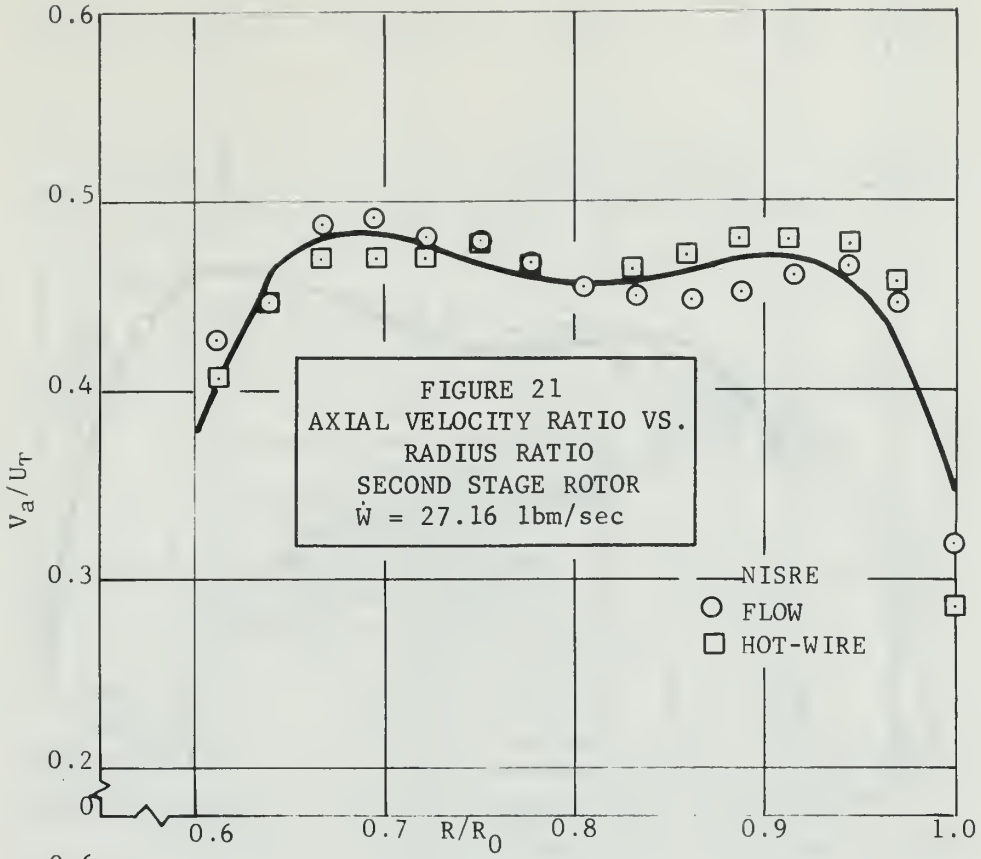

FIGURE 21
AXIAL VELOCITY RATIO VS.
RADIUS RATIO
SECOND STAGE ROTOR
$\dot{W}$ = 27.16 lbm/sec

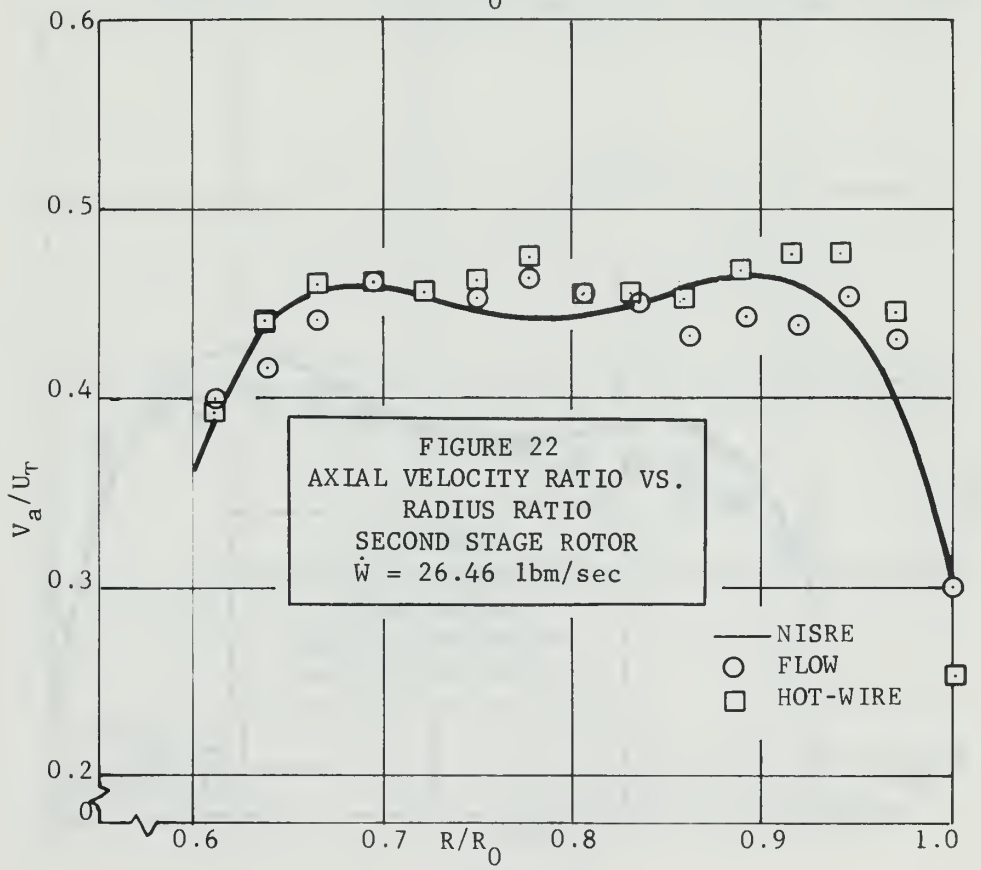

FIGURE 22
AXIAL VELOCITY RATIO VS.
RADIUS RATIO
SECOND STAGE ROTOR
$\dot{W}$ = 26.46 lbm/sec

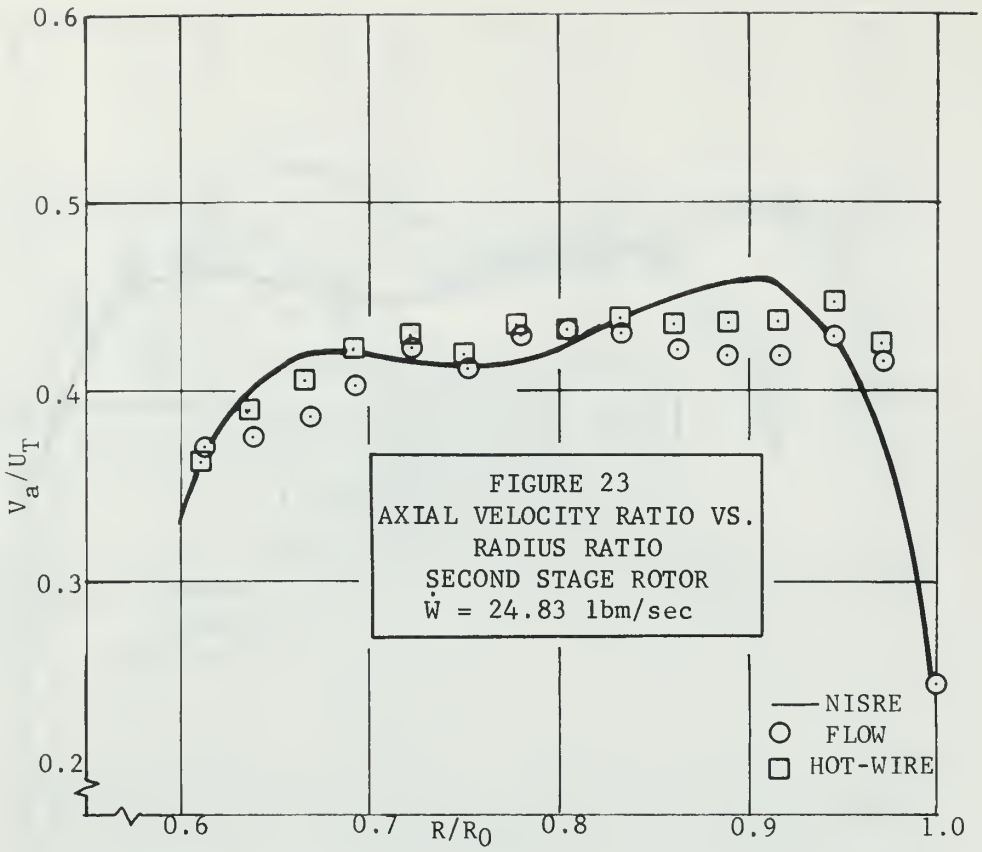

FIGURE 23
AXIAL VELOCITY RATIO VS.
RADIUS RATIO
SECOND STAGE ROTOR
$\dot{W}$ = 24.83 lbm/sec

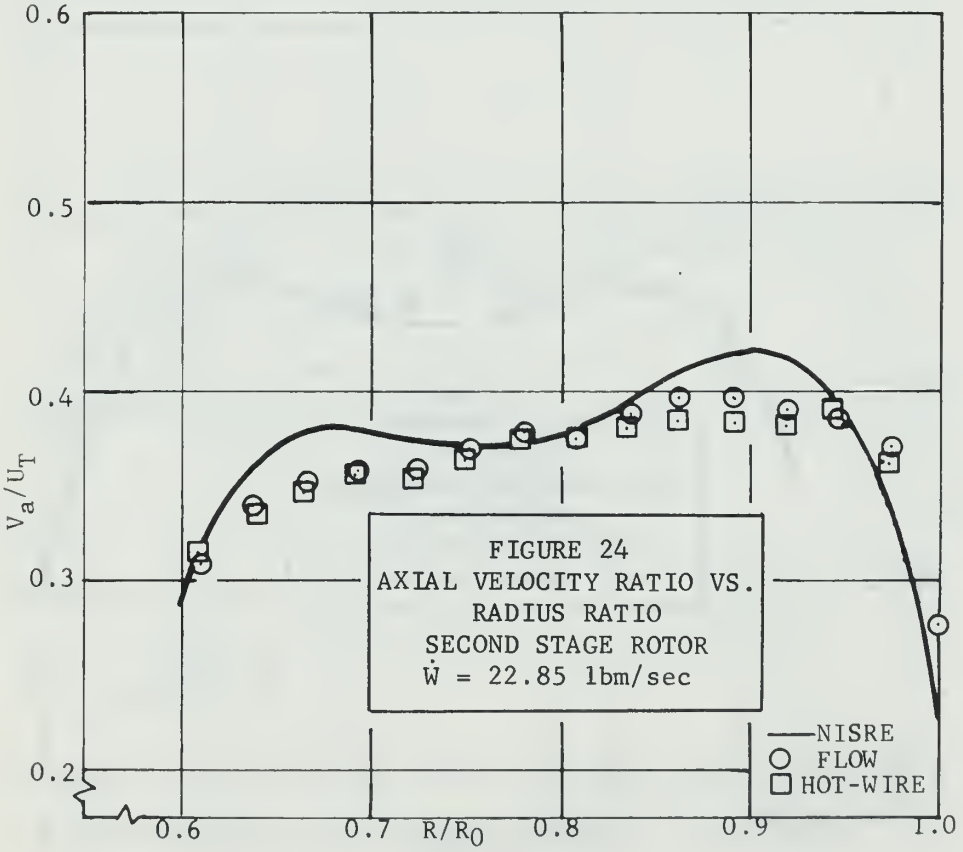

FIGURE 24
AXIAL VELOCITY RATIO VS.
RADIUS RATIO
SECOND STAGE ROTOR
$\dot{W}$ = 22.85 lbm/sec

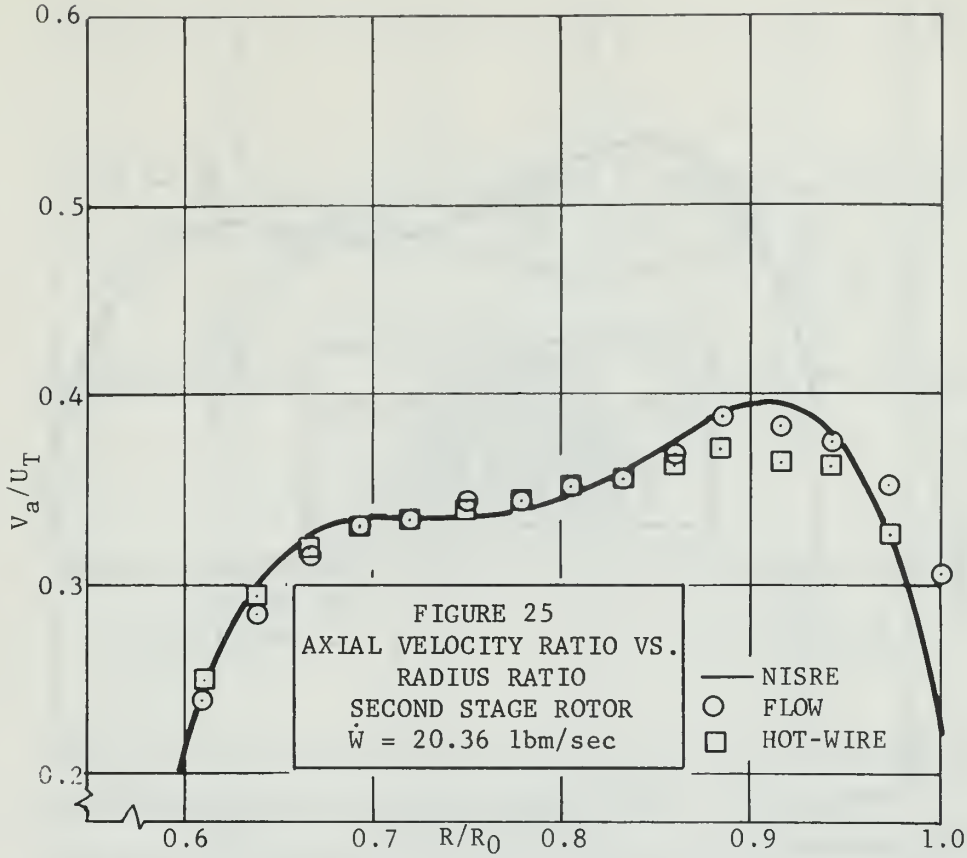

FIGURE 25
AXIAL VELOCITY RATIO VS.
RADIUS RATIO
SECOND STAGE ROTOR
$\dot{W}$ = 20.36 lbm/sec

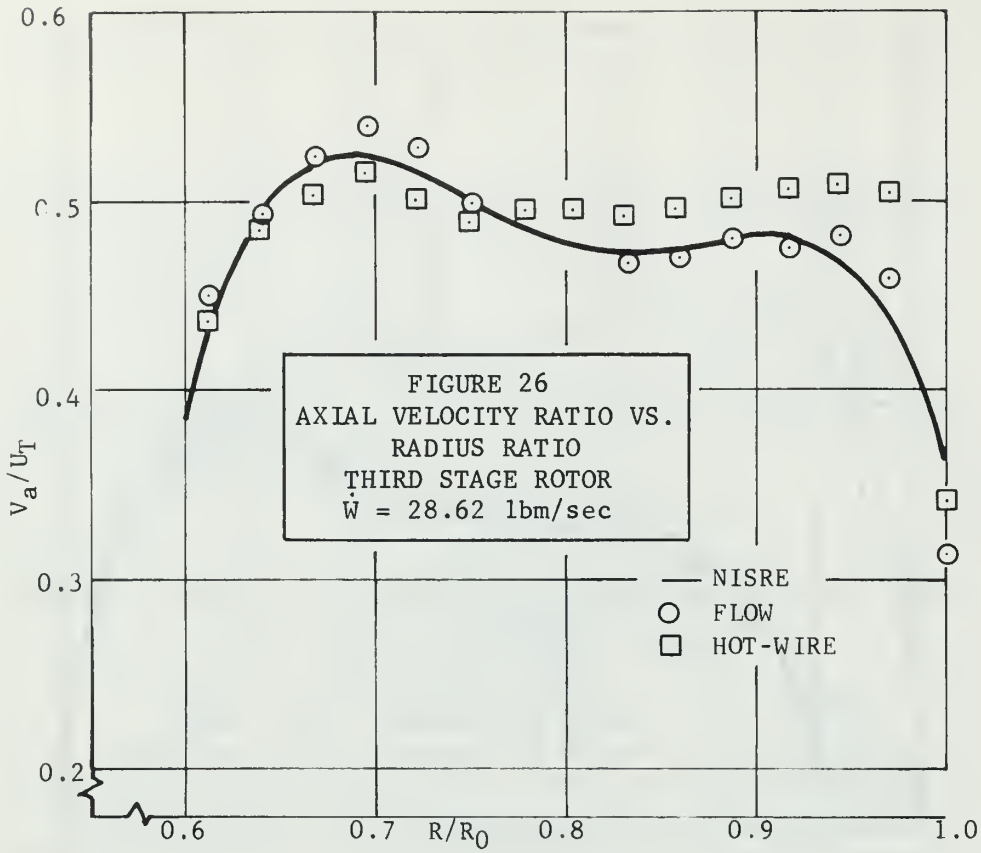

FIGURE 26
AXIAL VELOCITY RATIO VS.
RADIUS RATIO
THIRD STAGE ROTOR
$\dot{W}$ = 28.62 lbm/sec

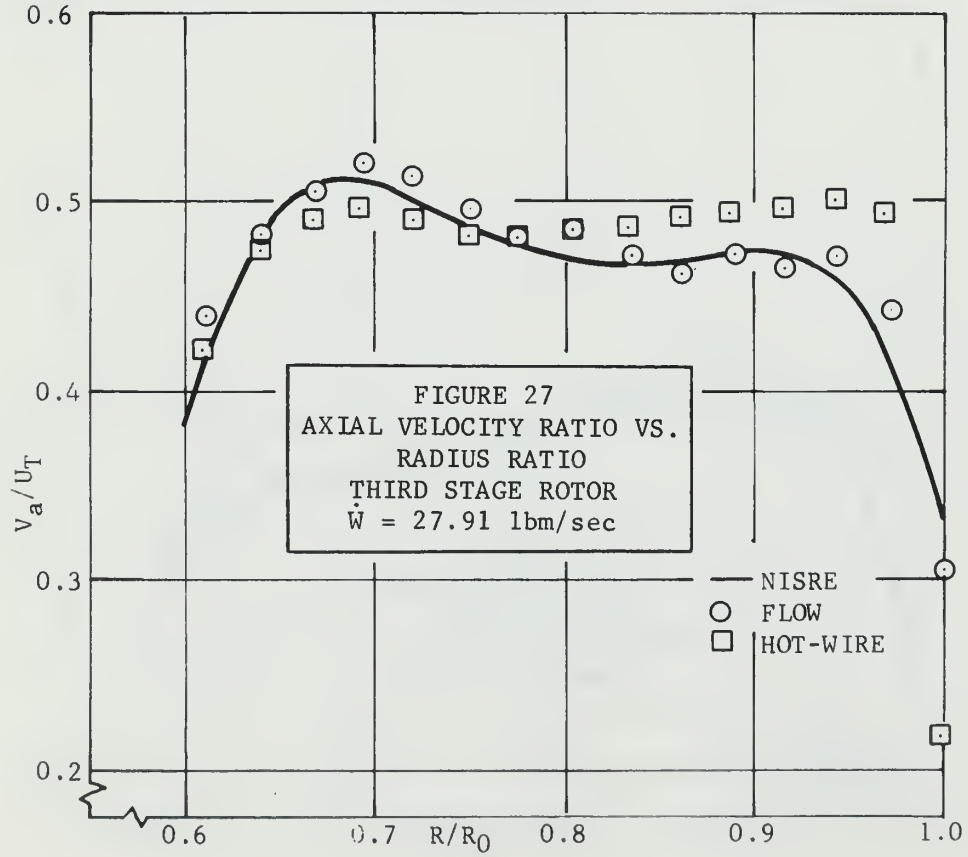

FIGURE 27
AXIAL VELOCITY RATIO VS.
RADIUS RATIO
THIRD STAGE ROTOR
$\dot{W}$ = 27.91 lbm/sec

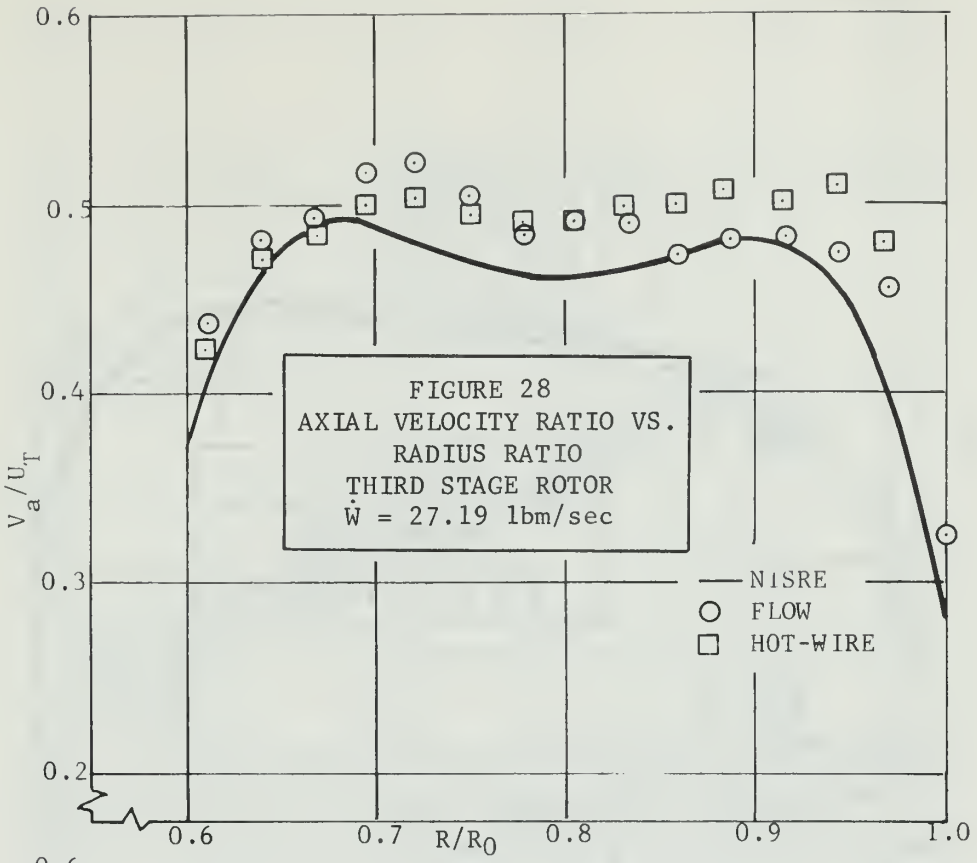

FIGURE 28
AXIAL VELOCITY RATIO VS.
RADIUS RATIO
THIRD STAGE ROTOR
$\dot{W}$ = 27.19 lbm/sec

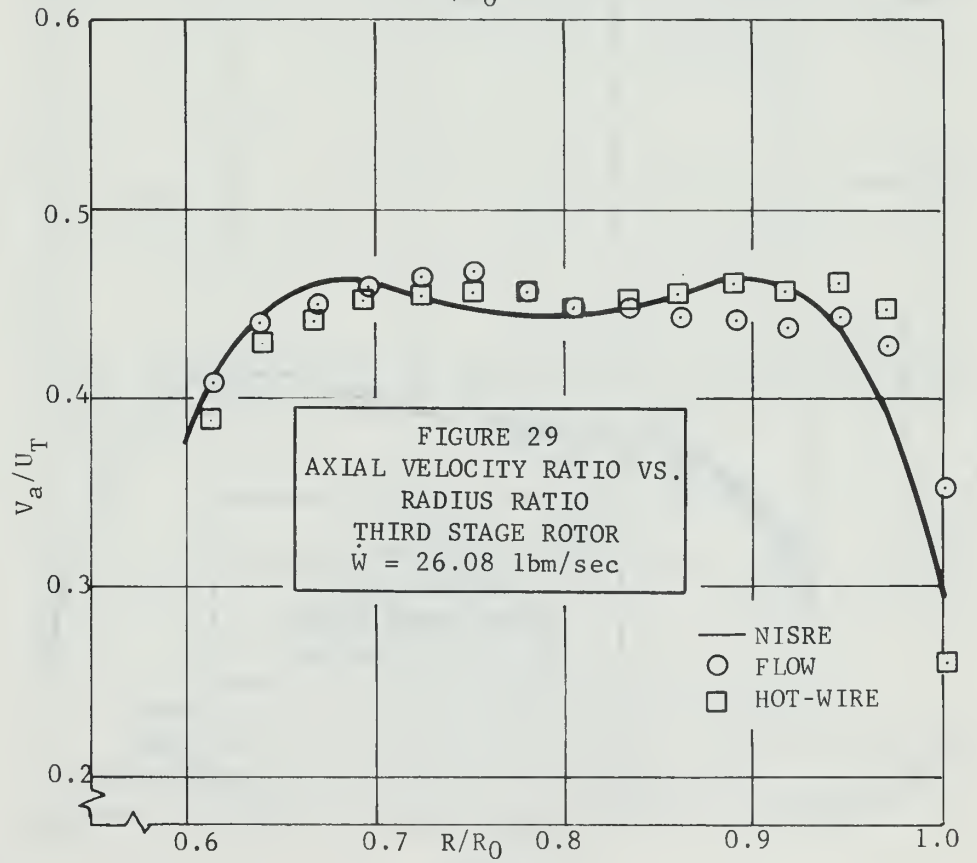

FIGURE 29
AXIAL VELOCITY RATIO VS.
RADIUS RATIO
THIRD STAGE ROTOR
$\dot{W}$ = 26.08 lbm/sec

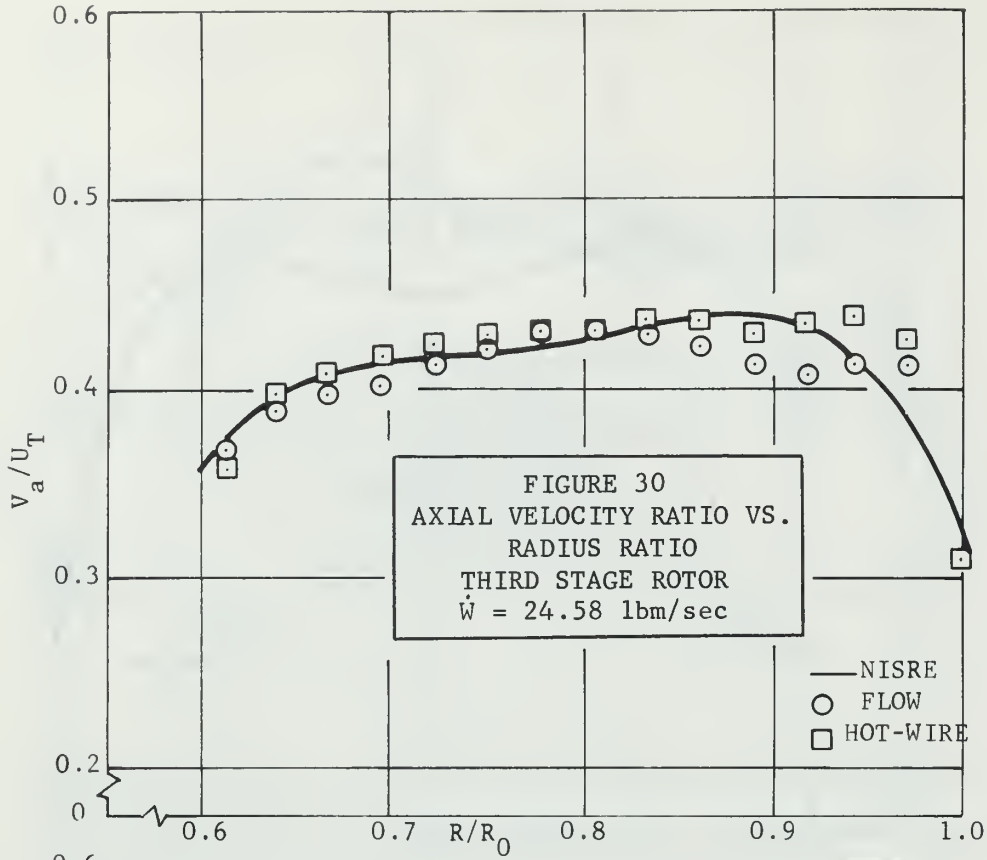

FIGURE 30
AXIAL VELOCITY RATIO VS.
RADIUS RATIO
THIRD STAGE ROTOR
$\dot{W}$ = 24.58 lbm/sec

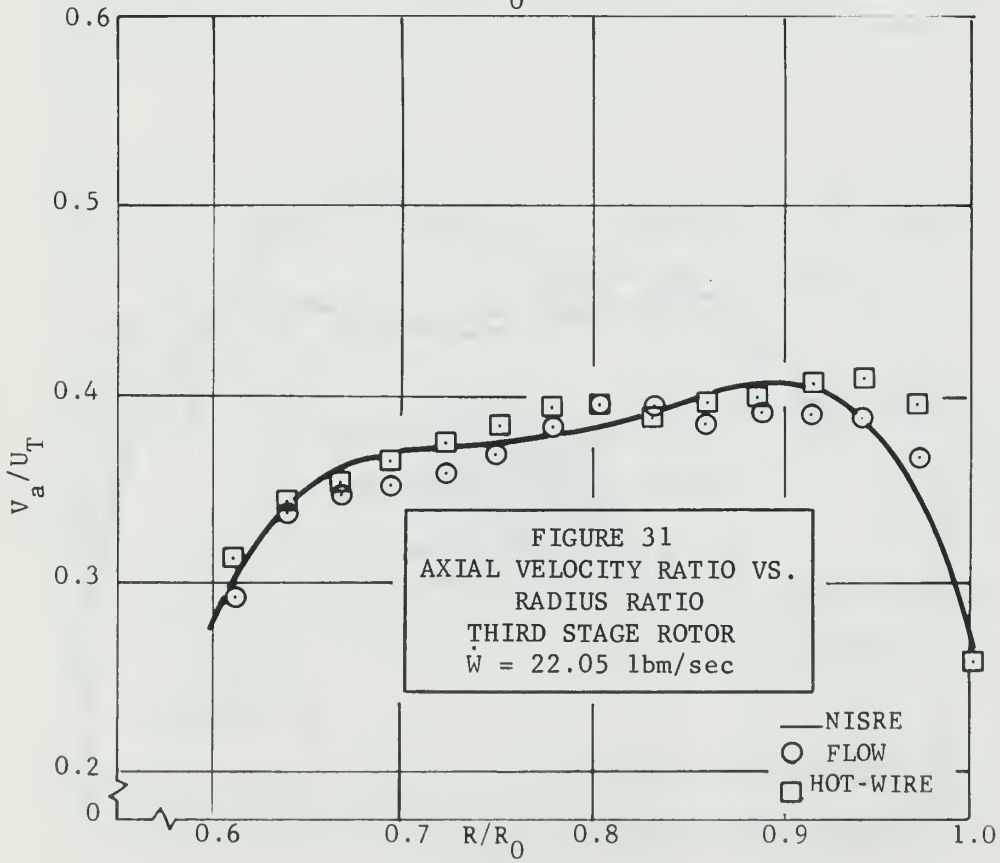

FIGURE 31
AXIAL VELOCITY RATIO VS.
RADIUS RATIO
THIRD STAGE ROTOR
$\dot{W}$ = 22.05 lbm/sec

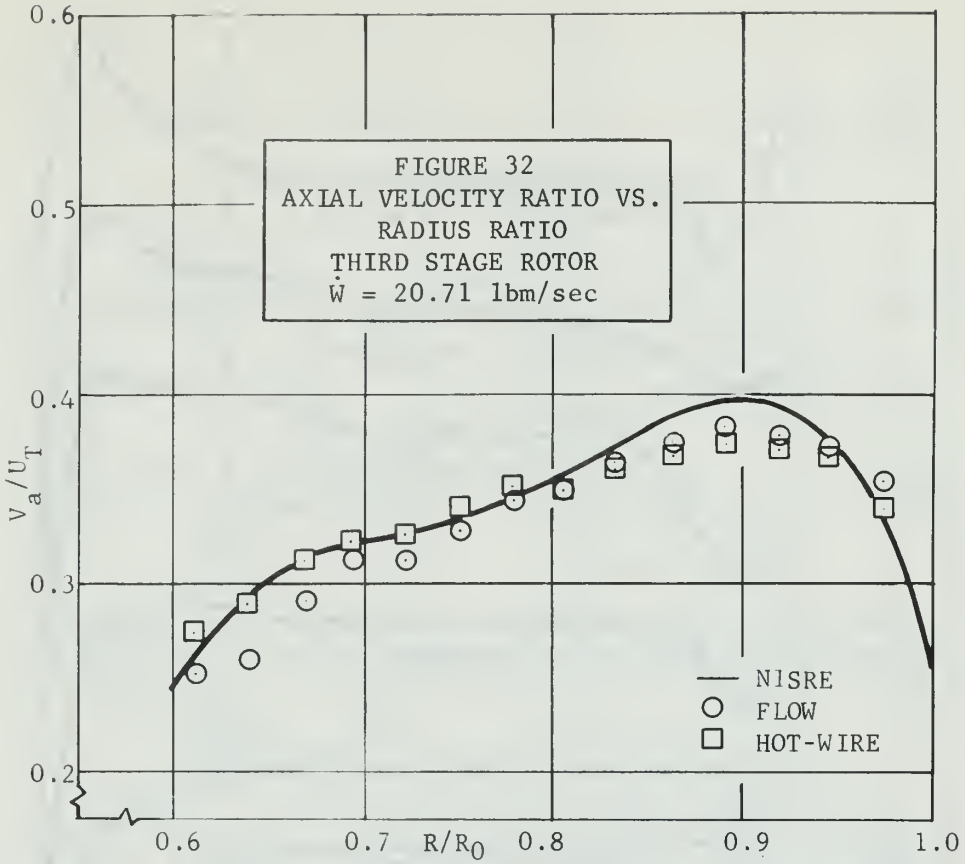
FIGURE 32
AXIAL VELOCITY RATIO VS.
RADIUS RATIO
THIRD STAGE ROTOR
$\dot{W}$ = 20.71 lbm/sec
0.6
0.5
0.4
0.3
0.2
V_a/U_T
0.6
0.7
R/R_0
0.8
0.9
1.0
NISRE
FLOW
HOT-WIRE

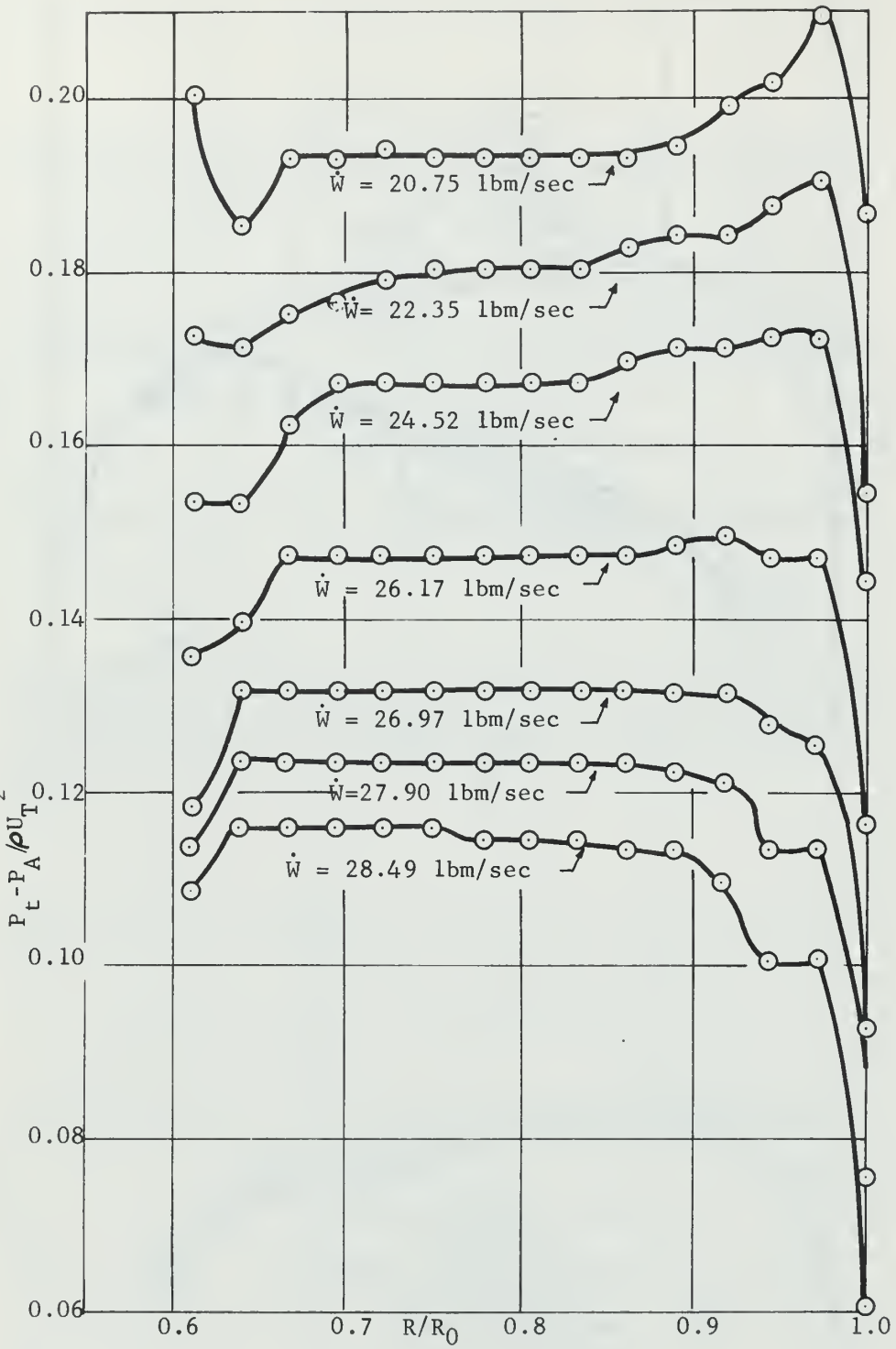

FIGURE 33
TOTAL PRESSURE COEFFICIENT VS. RADIUS RATIO
FIRST STAGE ROTOR

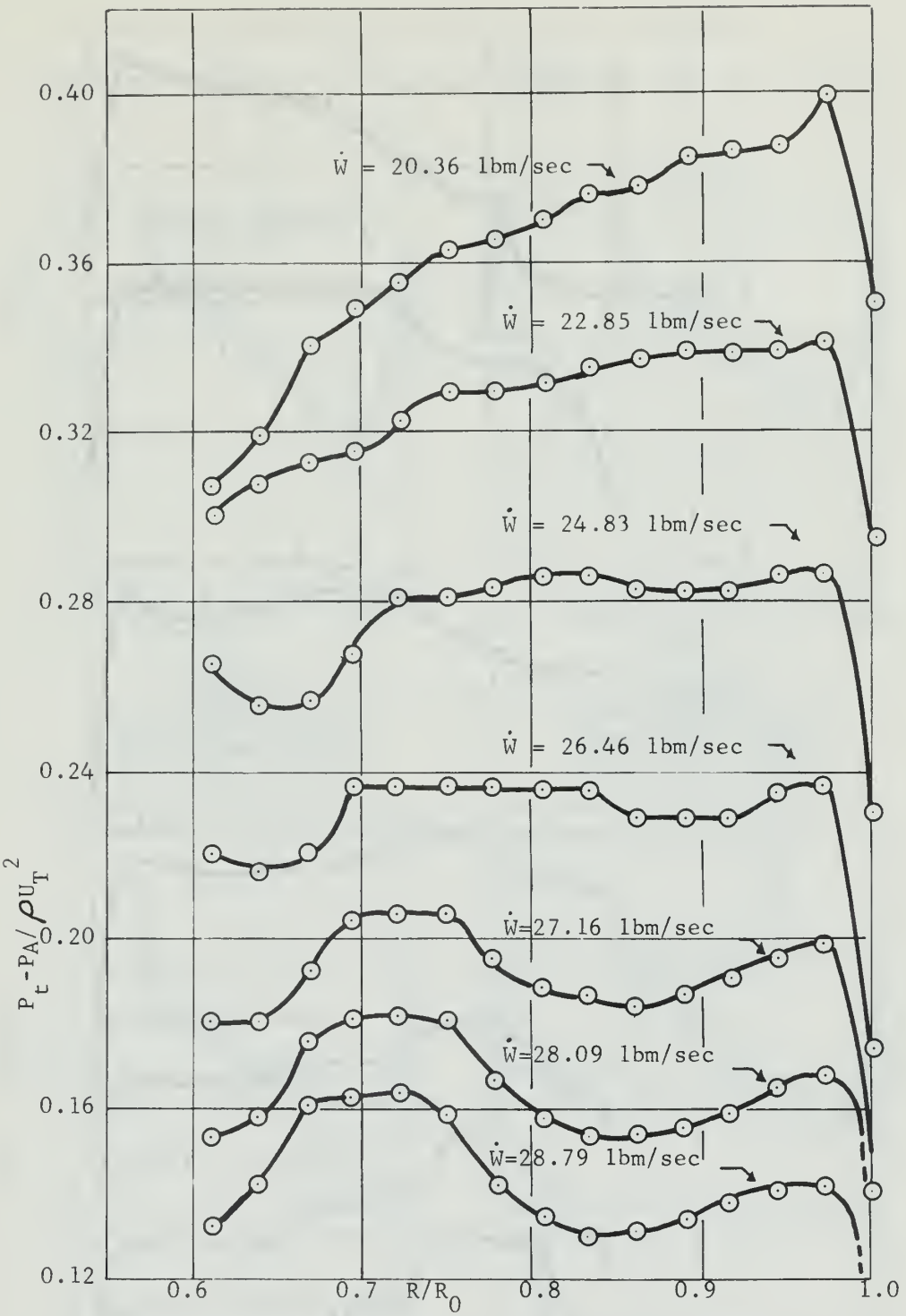

FIGURE 34
TOTAL PRESSURE COEFFICIENT VS. RADIUS RATIO
SECOND STAGE ROTOR

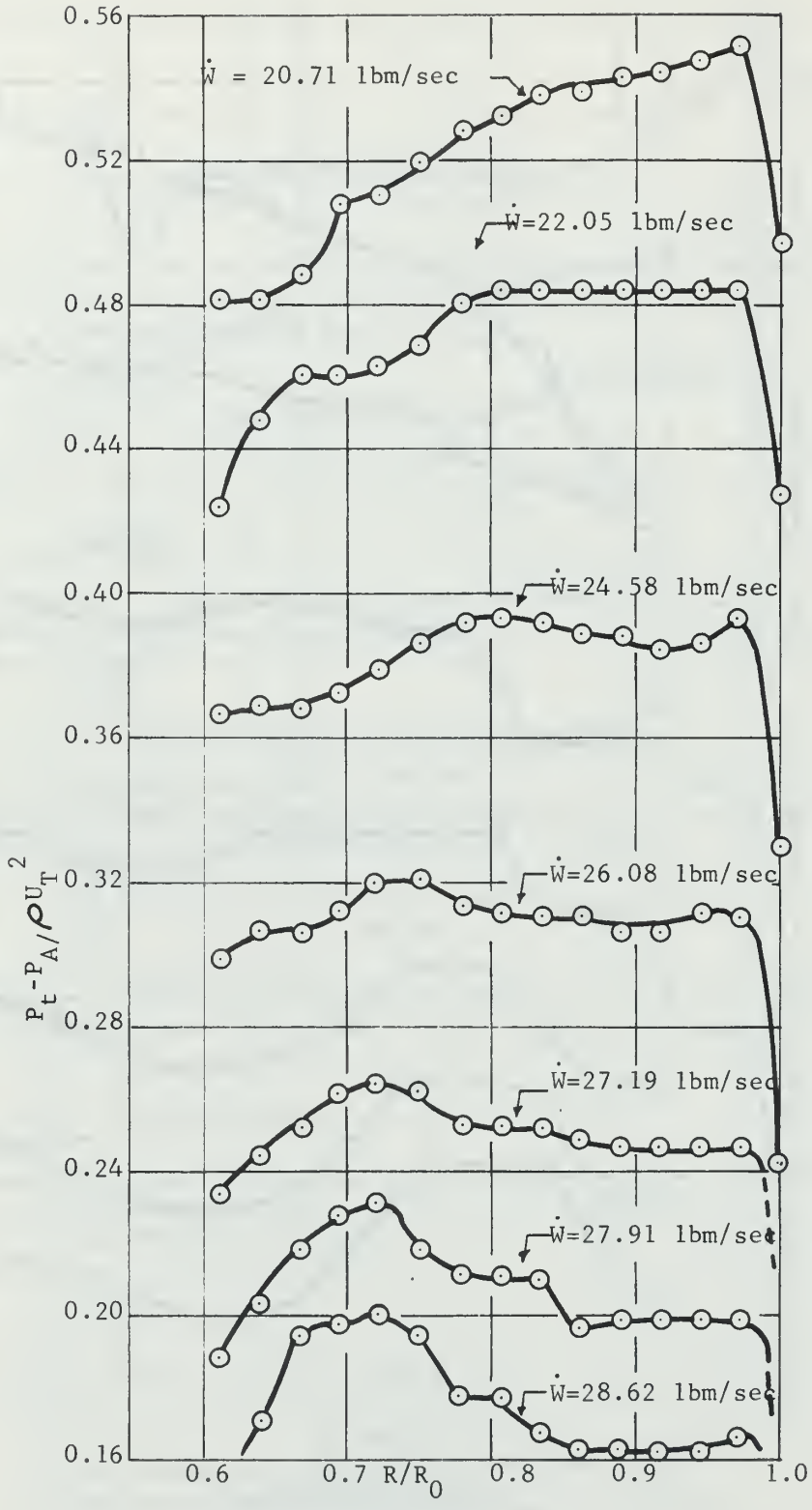

FIGURE 35
TOTAL PRESSURE COEFFICIENT VS. RADIUS RATIO
THIRD STAGE ROTOR

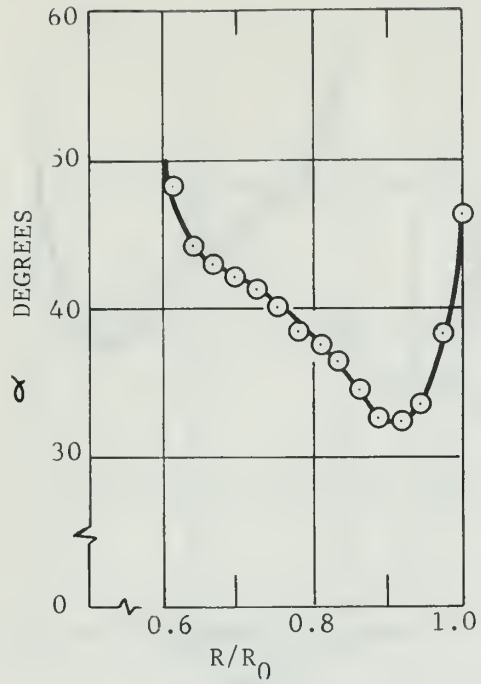

FIGURE 36
α VS. RADIUS RATIO
FIRST STAGE ROTOR
$\dot{W}$ = 28.49 lbm/sec

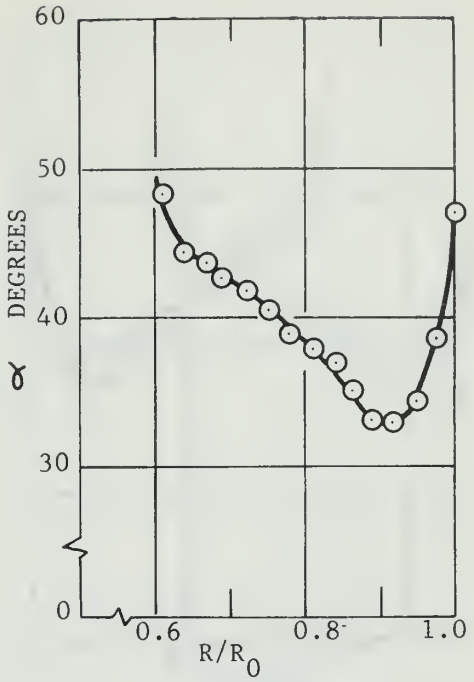

FIGURE 37
α VS. RADIUS RATIO
FIRST STAGE ROTOR
$\dot{W}$ = 27.90 lbm/sec

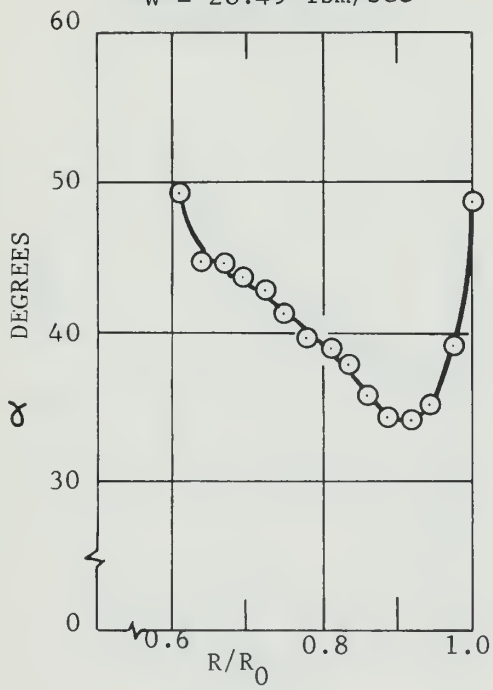

FIGURE 38
α VS. RADIUS RATIO
FIRST STAGE ROTOR
$\dot{W}$ = 26.97 lbm/sec

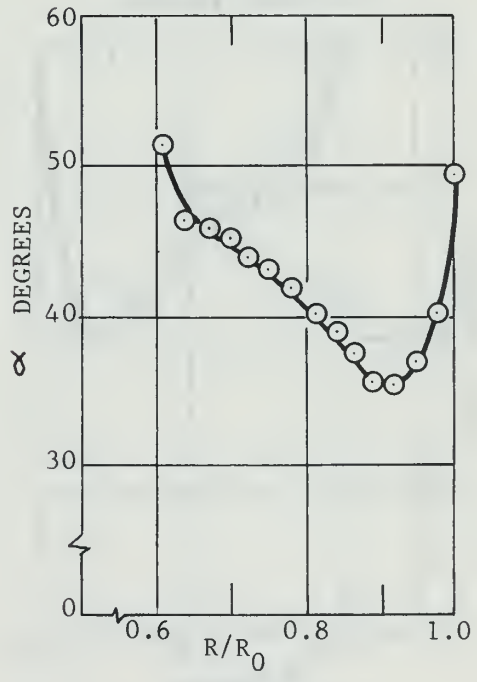

FIGURE 39
α VS. RADIUS RATIO
FIRST STAGE ROTOR
$\dot{W}$ = 26.17 lbm/sec

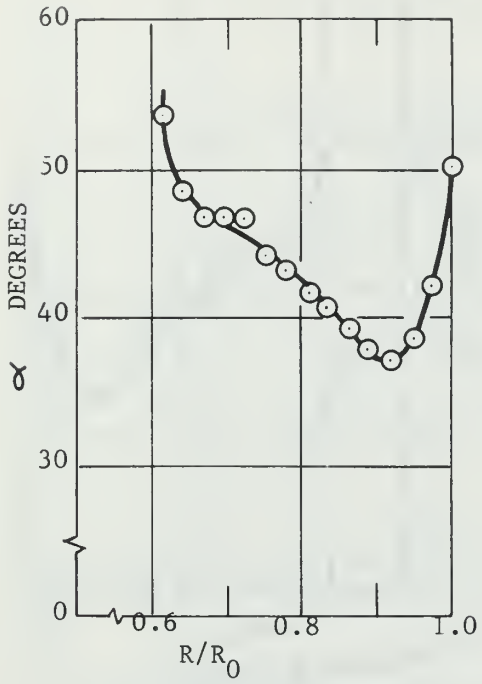

FIGURE 40
α VS. RADIUS RATIO
FIRST STAGE ROTOR
$\dot{W}$ = 24.52 lbm/sec

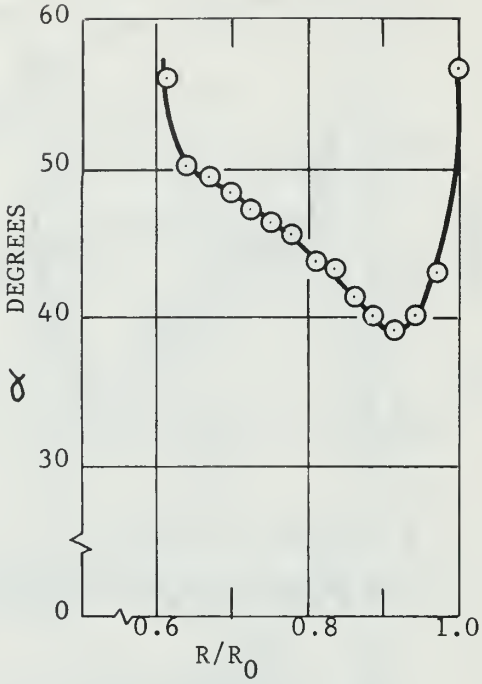

FIGURE 41
α VS. RADIUS RATIO
FIRST STAGE ROTOR
$\dot{W}$ = 22.35 lbm/sec

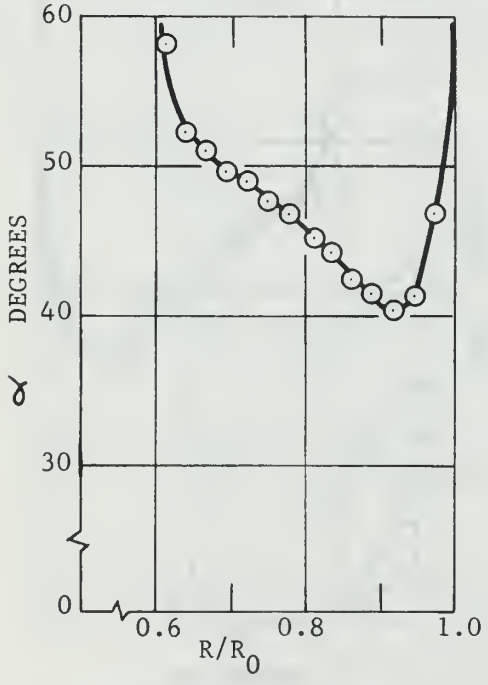

FIGURE 42
α VS. RADIUS RATIO
FIRST STAGE ROTOR
$\dot{W}$ = 20.75 lbm/sec

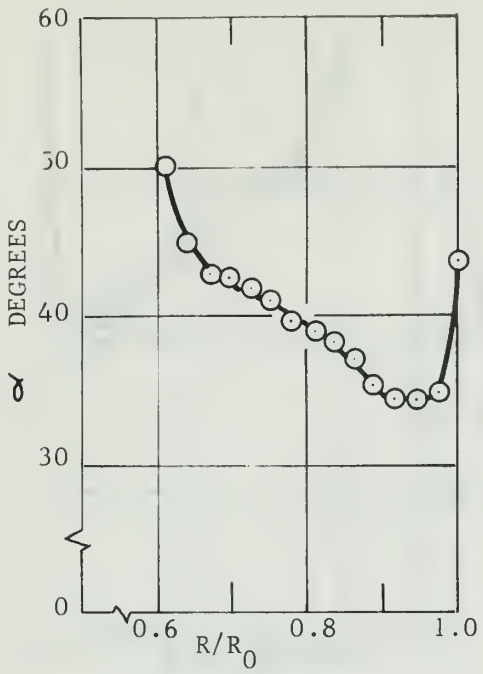

FIGURE 43
α VS. RADIUS RATIO
SECOND STAGE ROTOR
$\dot{W}$ = 28.79 lbm/sec

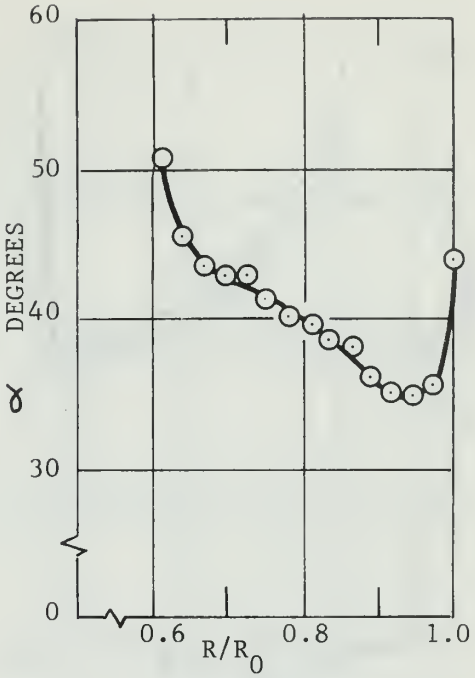

FIGURE 44
α VS. RADIUS RATIO
SECOND STAGE ROTOR
$\dot{W}$ = 28.09 lbm/sec

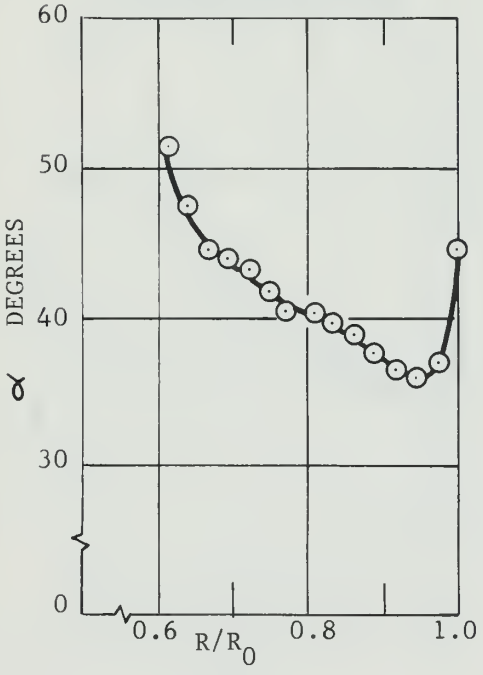

FIGURE 45
α VS. RADIUS RATIO
SECOND STAGE ROTOR
$\dot{W}$ = 27.16 lbm/sec

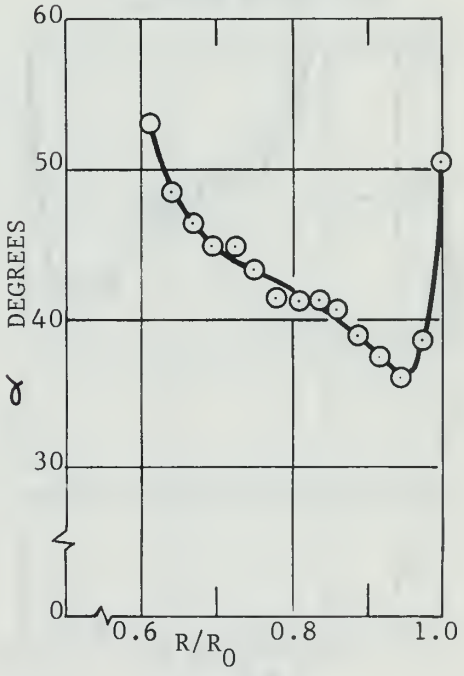

FIGURE 46
α VS. RADIUS RATIO
SECOND STAGE ROTOR
$\dot{W}$ = 26.46 lbm/sec

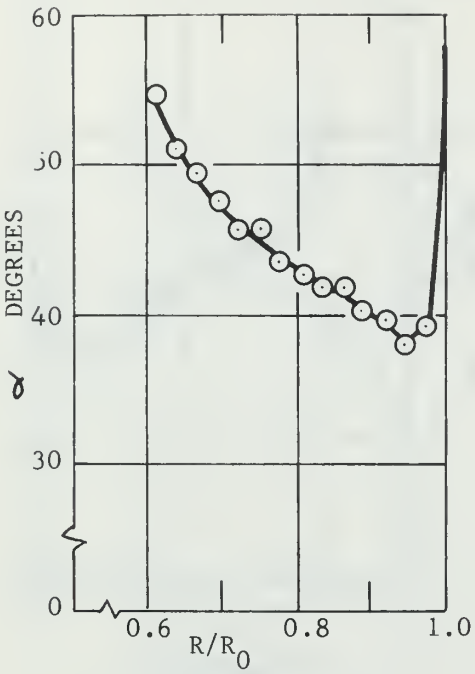

FIGURE 47
α VS. RADIUS RATIO
SECOND STAGE ROTOR
$\dot{W}$ = 24.83 lbm/sec

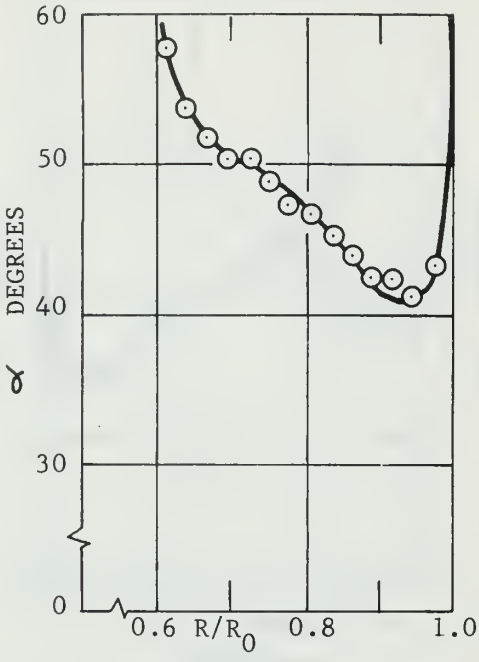

FIGURE 48
α VS. RADIUS RATIO
SECOND STAGE ROTOR
$\dot{W}$ = 22.85 lbm/sec

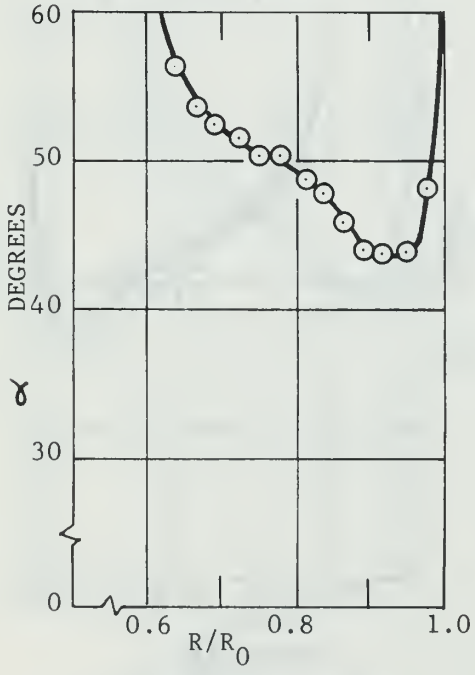

FIGURE 49
α VS. RADIUS RATIO
SECOND STAGE ROTOR
$\dot{W}$ = 20.36 lbm/sec

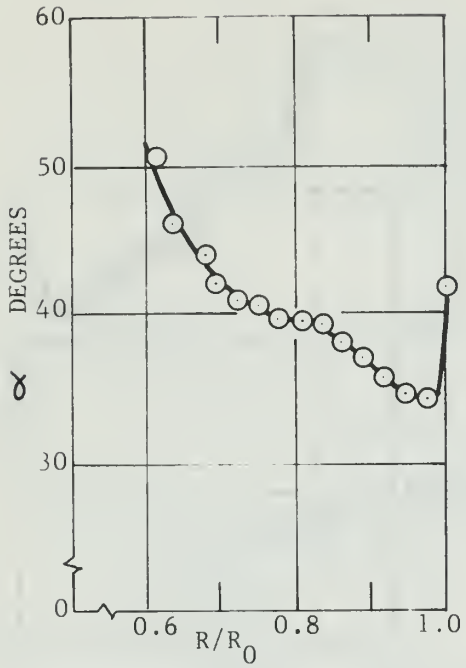

FIGURE 50
α VS. RADIUS RATIO
THIRD STAGE ROTOR
$\dot{W}$ = 28.62 lbm/sec

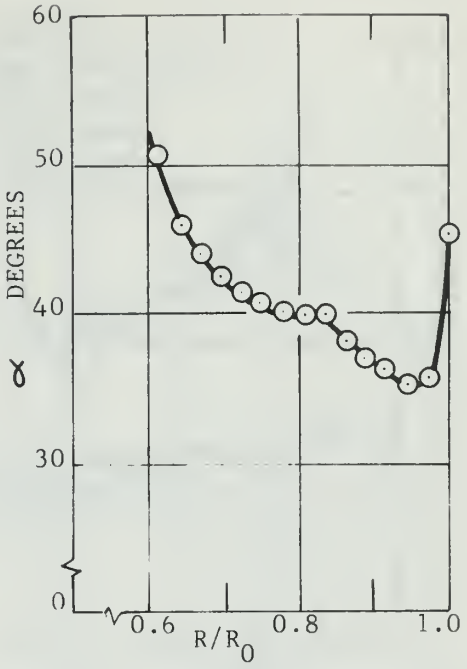

FIGURE 51
α VS. RADIUS RATIO
THIRD STAGE ROTOR
$\dot{W}$ = 27.91 lbm/sec

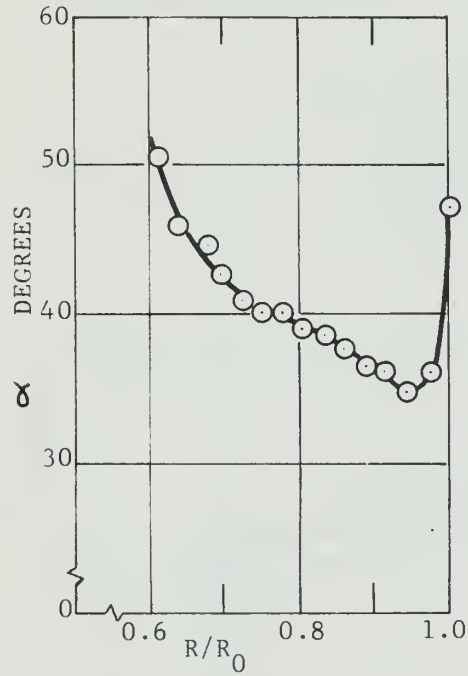

FIGURE 52
α VS. RADIUS RATIO
THIRD STAGE ROTOR
$\dot{W}$ = 27.19 lbm/sec

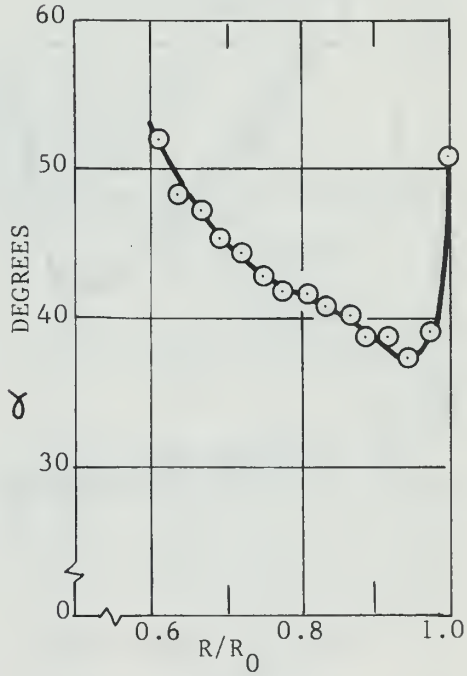

FIGURE 53
α VS. RADIUS RATIO
THIRD STAGE ROTOR
$\dot{W}$ = 26.08 lbm/sec

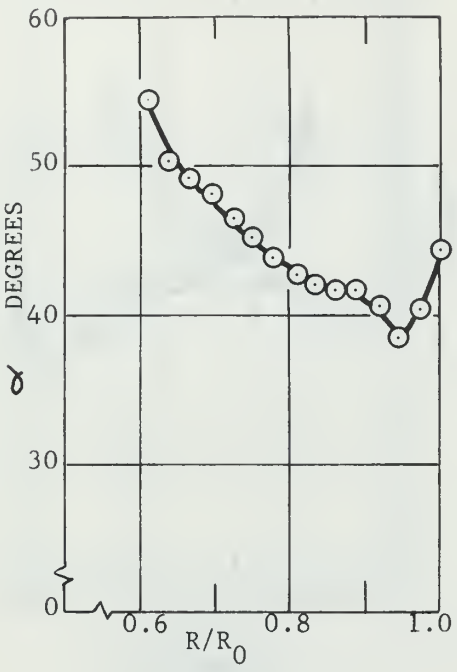

FIGURE 54
α VS. RADIUS RATIO
THIRD STAGE ROTOR
$\dot{W}$ = 24.58 lbm/sec

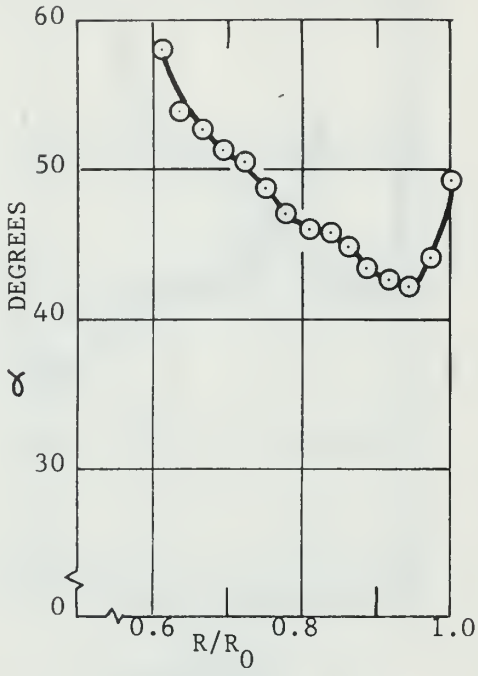

FIGURE 55
α VS. RADIUS RATIO
THIRD STAGE ROTOR
$\dot{W}$ = 22.05 lbm/sec

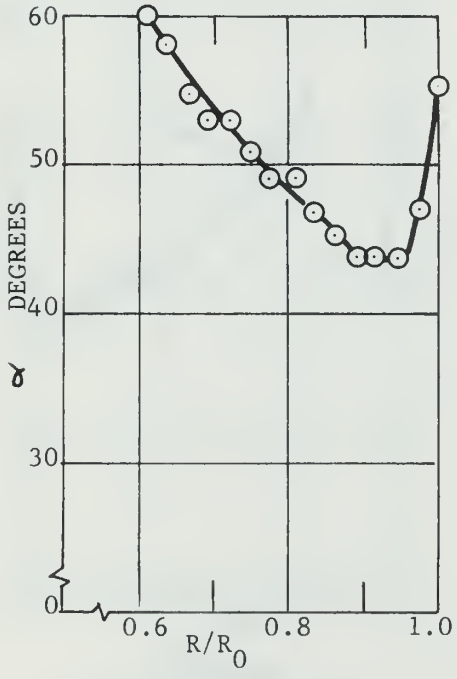

FIGURE 56
α VS. RADIUS RATIO
THIRD STAGE ROTOR
$\dot{W}$ = 20.71 lbm/sec

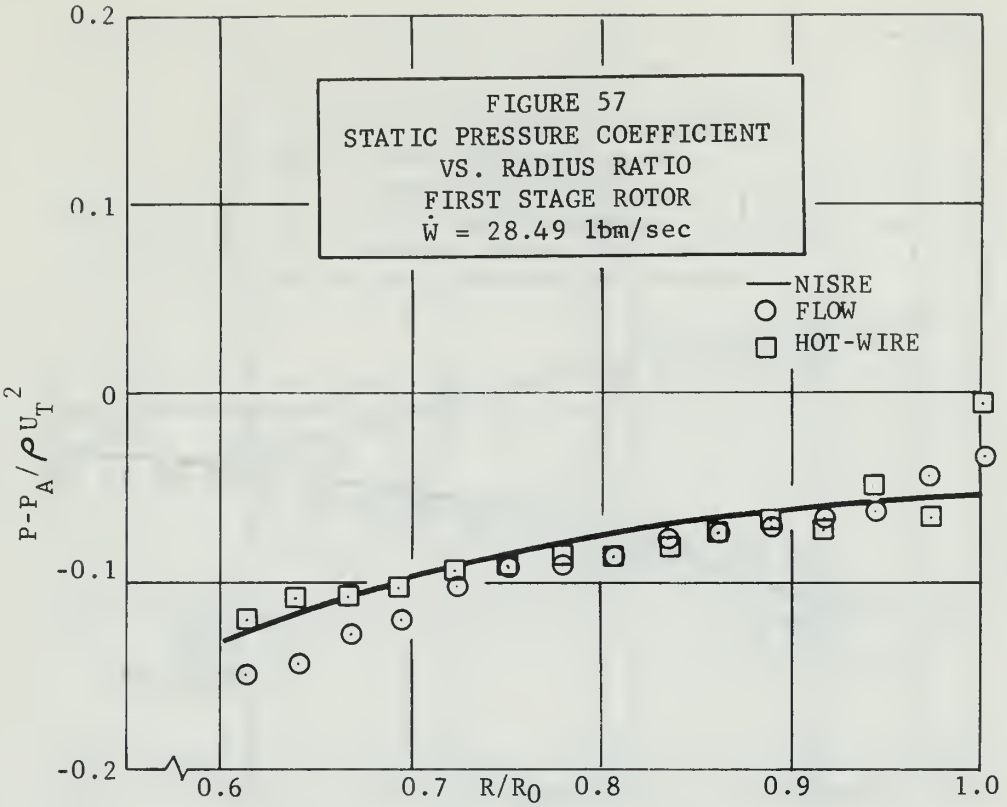
FIGURE 57
STATIC PRESSURE COEFFICIENT
VS. RADIUS RATIO
FIRST STAGE ROTOR
$\dot{W}$ = 28.49 lbm/sec
NISRE
FLOW
HOT-WIRE
$P-P_A/\rho U_T^2$
0.2
0.1
0
-0.1
-0.2
0.6
0.7
R/R_0
0.8
0.9
1.0

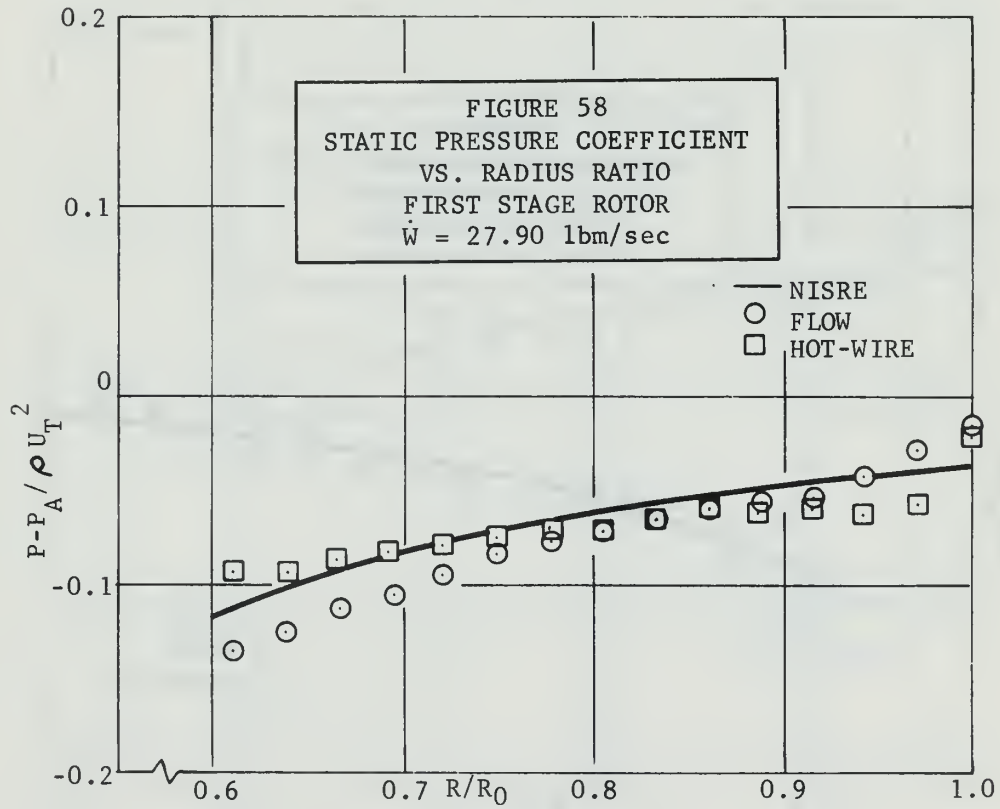
FIGURE 58
STATIC PRESSURE COEFFICIENT
VS. RADIUS RATIO
FIRST STAGE ROTOR
$\dot{W}$ = 27.90 lbm/sec
NISRE
FLOW
HOT-WIRE
$P-P_A/\rho U_T^2$
0.2
0.1
0
-0.1
-0.2
0.6
0.7
R/R_0
0.8
0.9
1.0

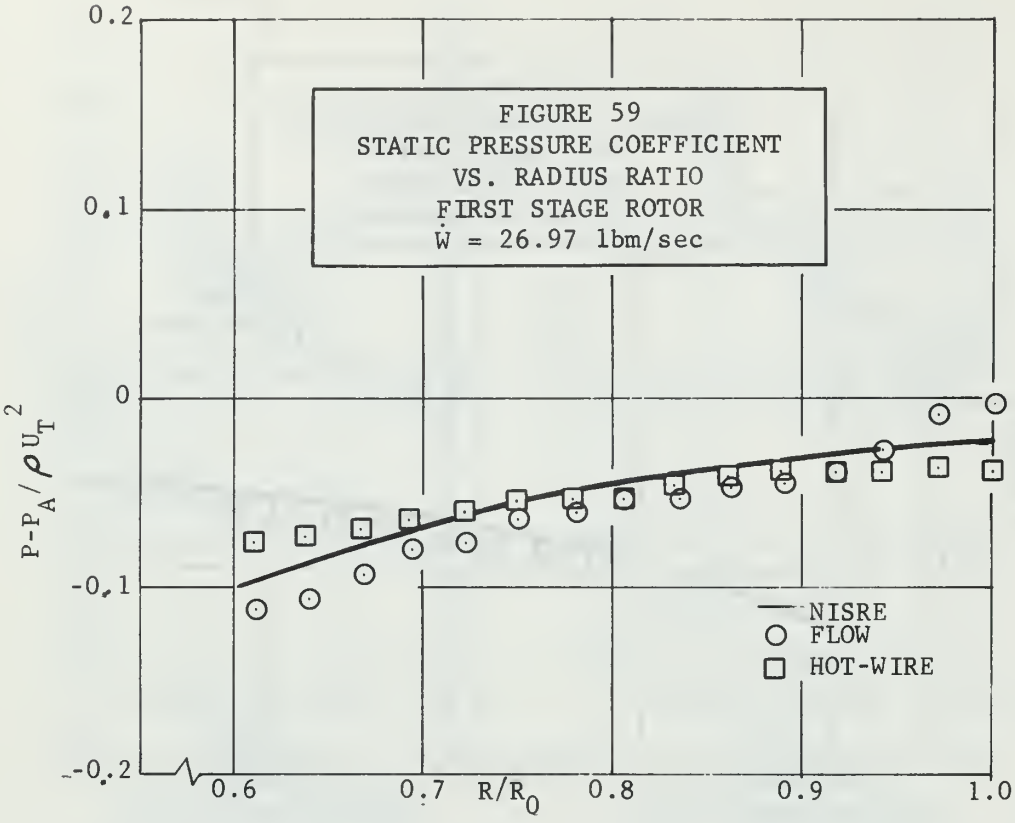
FIGURE 59
STATIC PRESSURE COEFFICIENT
VS. RADIUS RATIO
FIRST STAGE ROTOR
$\dot{W}$ = 26.97 lbm/sec
$P-P_A/\rho U_T^2$
0.2
0.1
0
-0.1
-0.2
0.6
0.7
R/R_0
0.8
0.9
1.0
NISRE
FLOW
HOT-WIRE

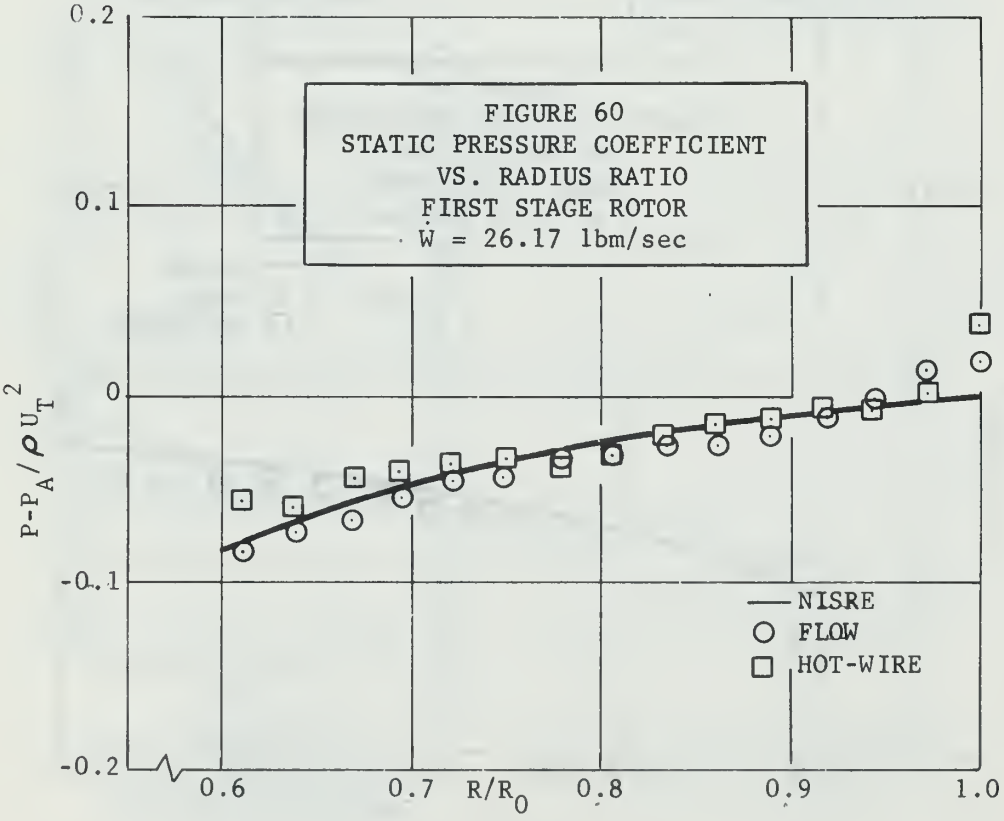
FIGURE 60
STATIC PRESSURE COEFFICIENT
VS. RADIUS RATIO
FIRST STAGE ROTOR
$\dot{W}$ = 26.17 lbm/sec
$P-P_A/\rho U_T^2$
0.2
0.1
0
-0.1
-0.2
0.6
0.7
R/R_0
0.8
0.9
1.0
NISRE
FLOW
HOT-WIRE

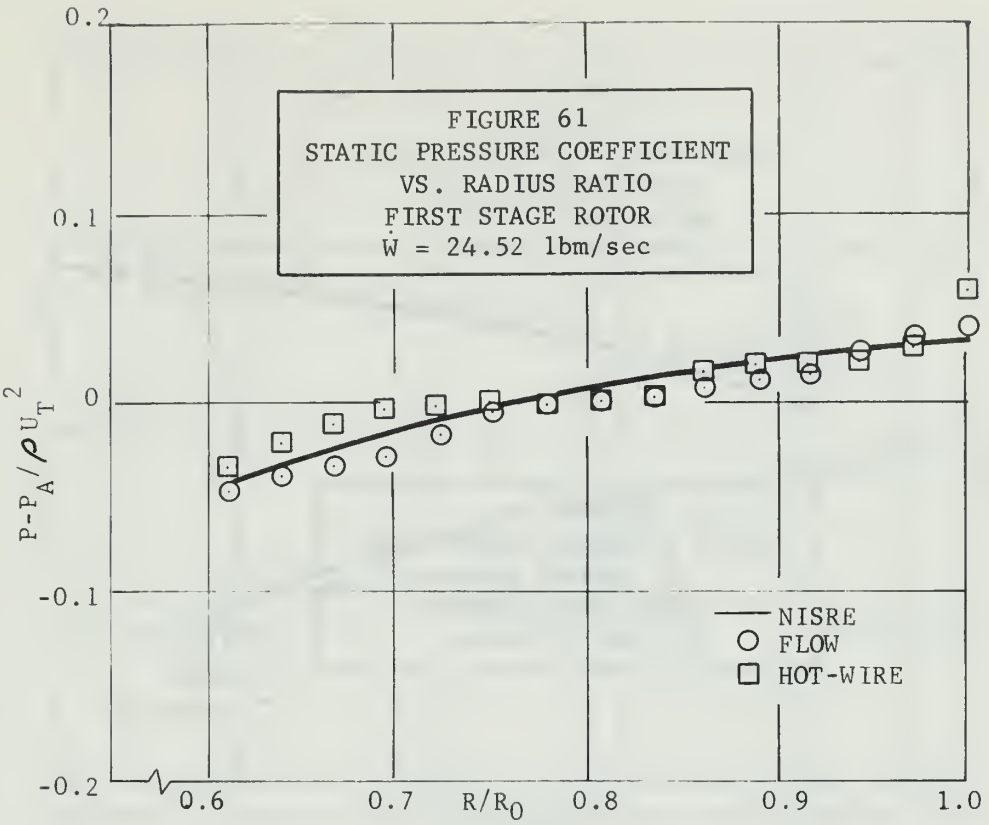
FIGURE 61
STATIC PRESSURE COEFFICIENT
VS. RADIUS RATIO
FIRST STAGE ROTOR
$\dot{W}$ = 24.52 lbm/sec
$P-P_A/\rho U_T^2$
0.2
0.1
0
-0.1
-0.2
0.6
0.7
R/R_0
0.8
0.9
1.0
NISRE
FLOW
HOT-WIRE

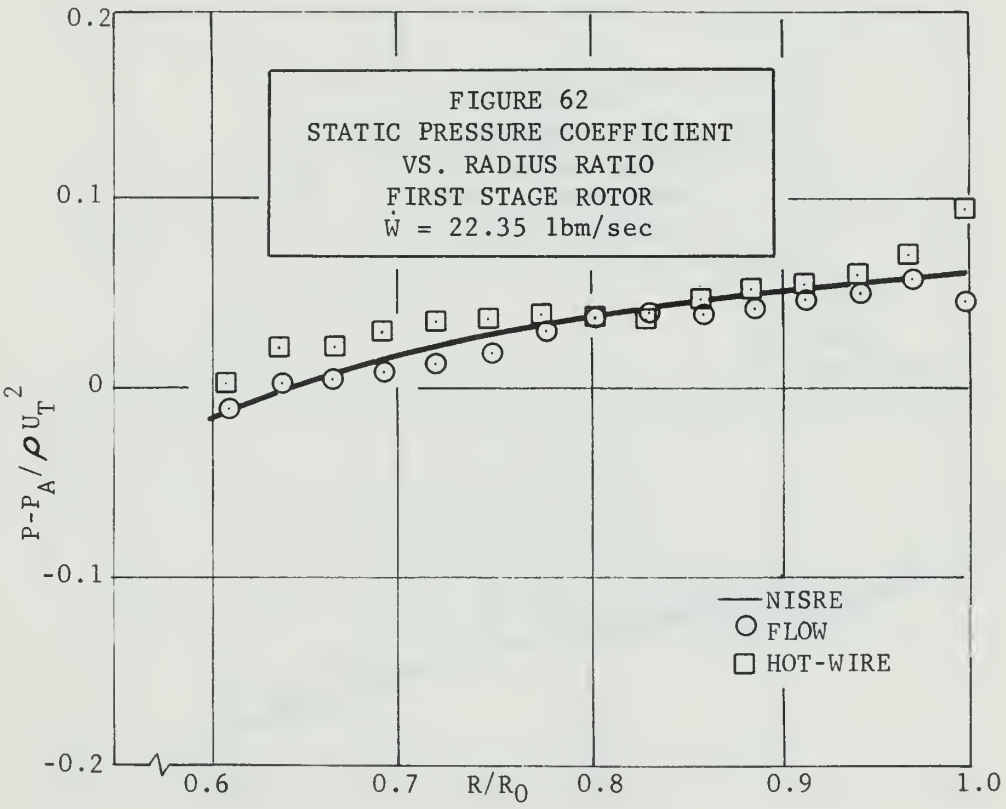
FIGURE 62
STATIC PRESSURE COEFFICIENT
VS. RADIUS RATIO
FIRST STAGE ROTOR
$\dot{W}$ = 22.35 lbm/sec
$P-P_A/\rho U_T^2$
0.2
0.1
0
-0.1
-0.2
0.6
0.7
R/R_0
0.8
0.9
1.0
NISRE
FLOW
HOT-WIRE

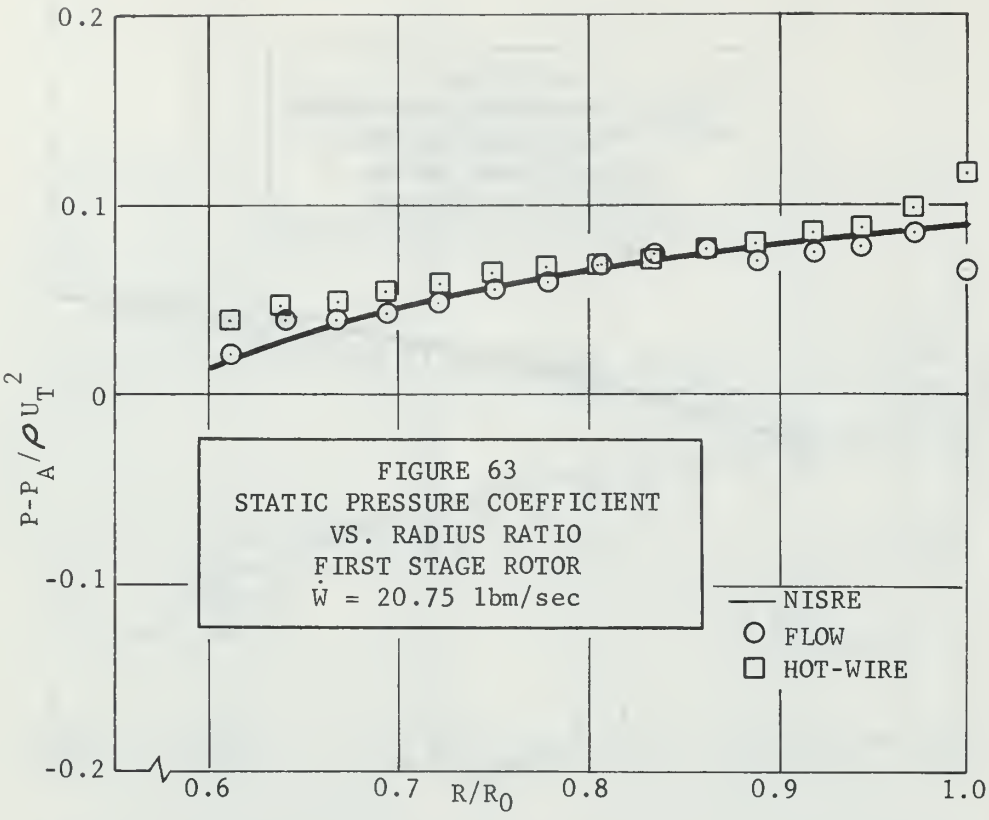

FIGURE 63
STATIC PRESSURE COEFFICIENT
VS. RADIUS RATIO
FIRST STAGE ROTOR
$\dot{W}$ = 20.75 lbm/sec

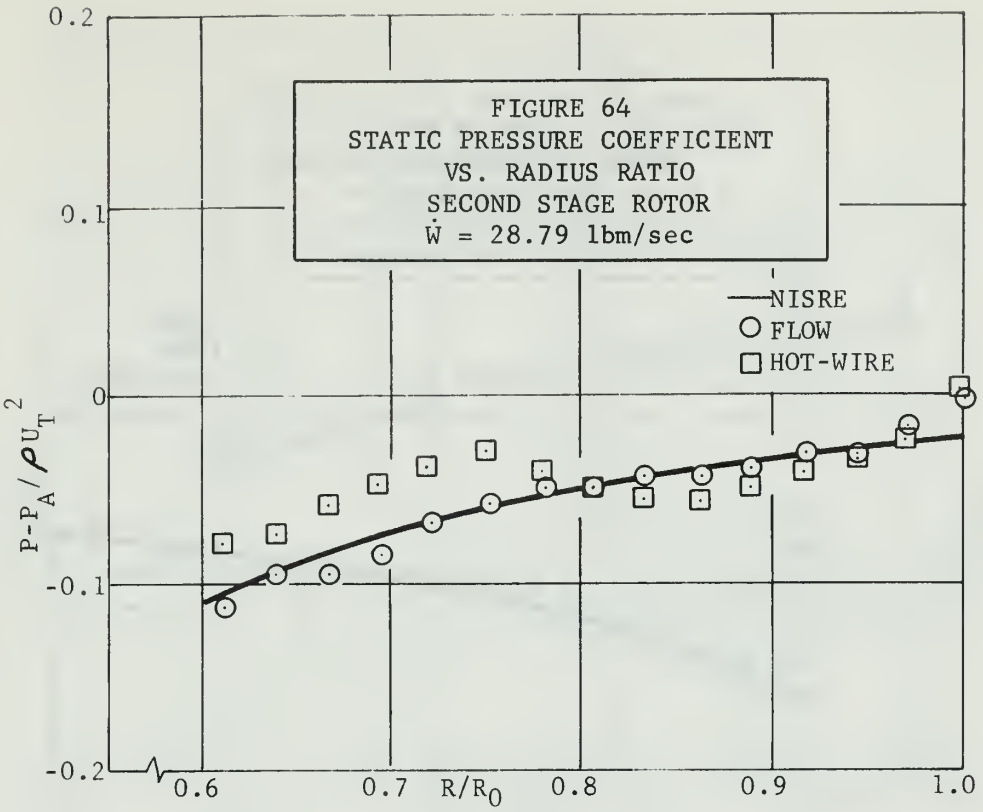
FIGURE 64
STATIC PRESSURE COEFFICIENT
VS. RADIUS RATIO
SECOND STAGE ROTOR
$\dot{W}$ = 28.79 lbm/sec
NISRE
FLOW
HOT-WIRE
$P-P_A/\rho U_T^2$
0.2
0.1
0
-0.1
-0.2
0.6
0.7
R/R_0
0.8
0.9
1.0

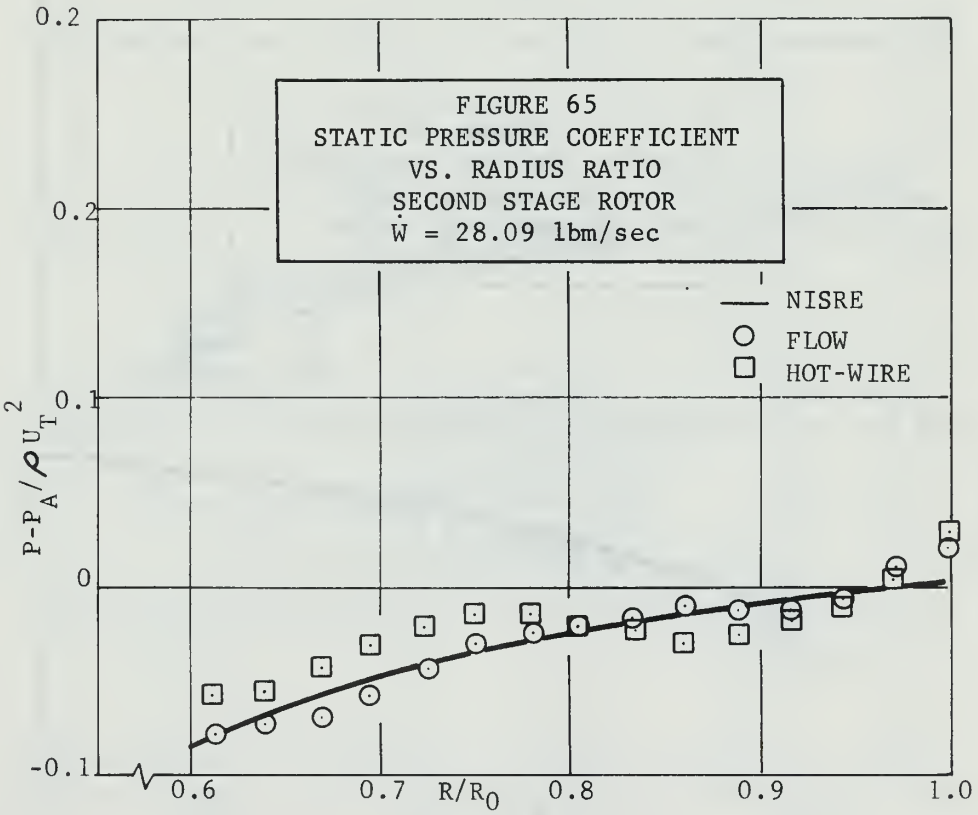
FIGURE 65
STATIC PRESSURE COEFFICIENT
VS. RADIUS RATIO
SECOND STAGE ROTOR
$\dot{W}$ = 28.09 lbm/sec
NISRE
FLOW
HOT-WIRE
$P-P_A/\rho U_T^2$
0.2
0.2
0.1
0
-0.1
0.6
0.7
R/R_0
0.8
0.9
1.0

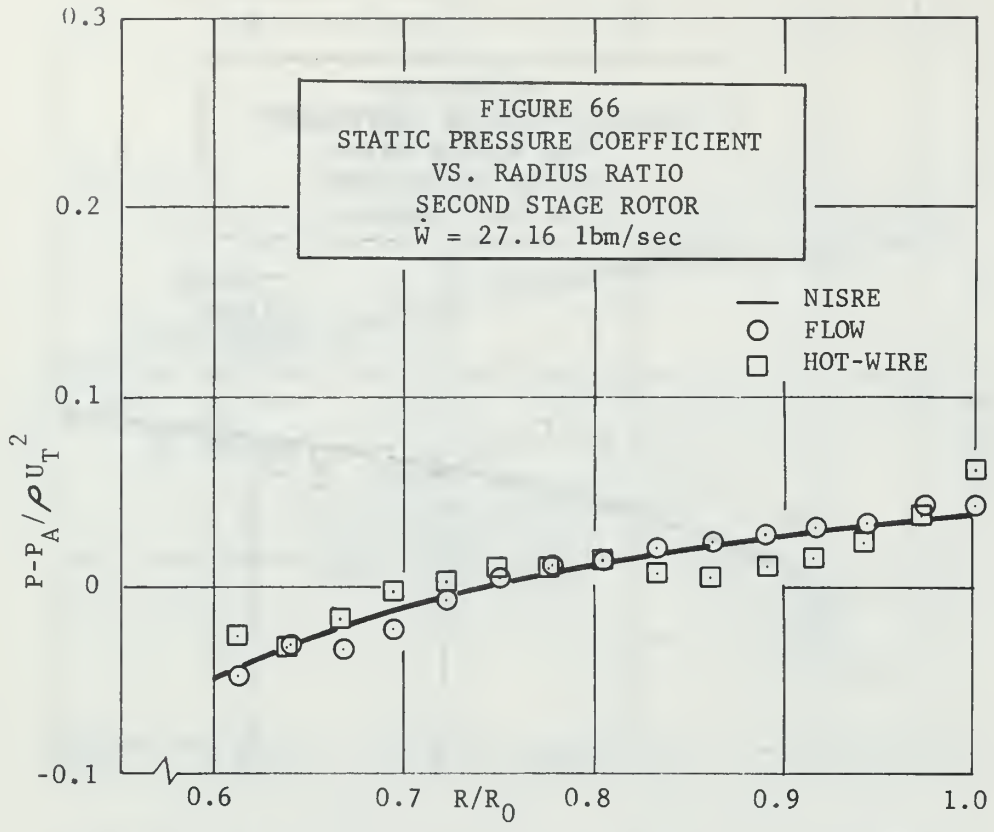
FIGURE 66
STATIC PRESSURE COEFFICIENT
VS. RADIUS RATIO
SECOND STAGE ROTOR
$\dot{W}$ = 27.16 lbm/sec
NISRE
FLOW
HOT-WIRE
0.3
0.2
0.1
0
-0.1
$P-P_A/\rho U_T^2$
0.6
0.7
R/R_0
0.8
0.9
1.0

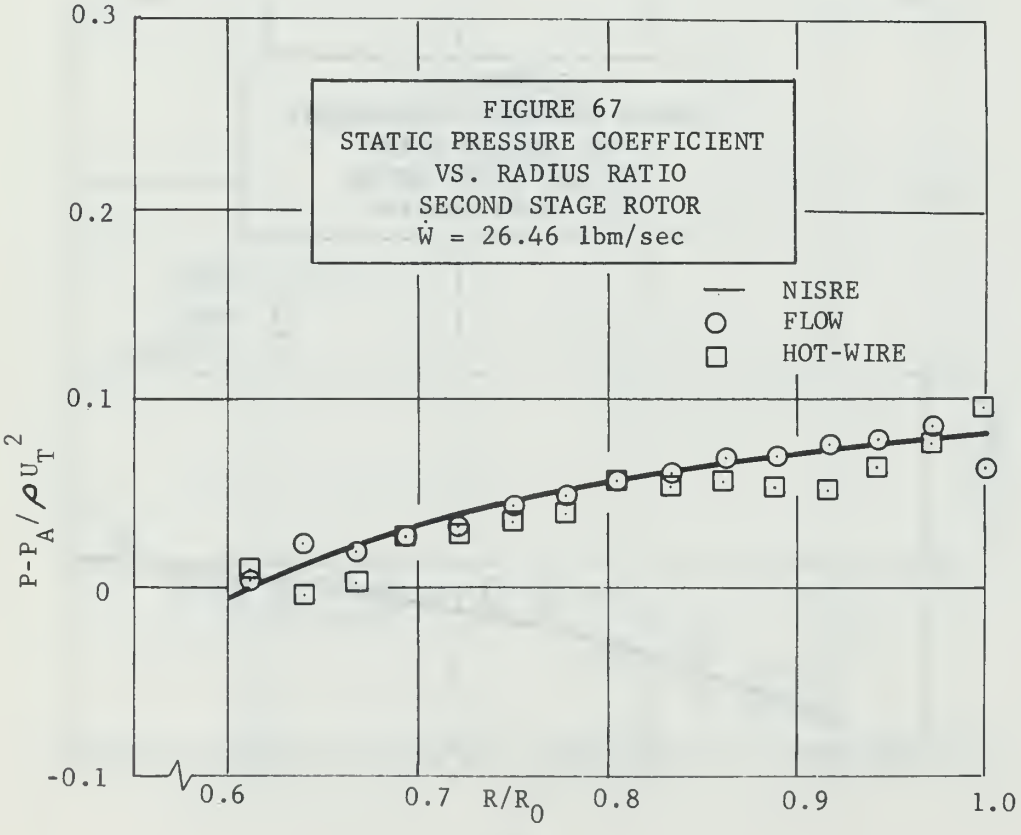
FIGURE 67
STATIC PRESSURE COEFFICIENT
VS. RADIUS RATIO
SECOND STAGE ROTOR
$\dot{W}$ = 26.46 lbm/sec
NISRE
FLOW
HOT-WIRE
0.3
0.2
0.1
0
-0.1
$P-P_A/\rho U_T^2$
0.6
0.7
R/R_0
0.8
0.9
1.0

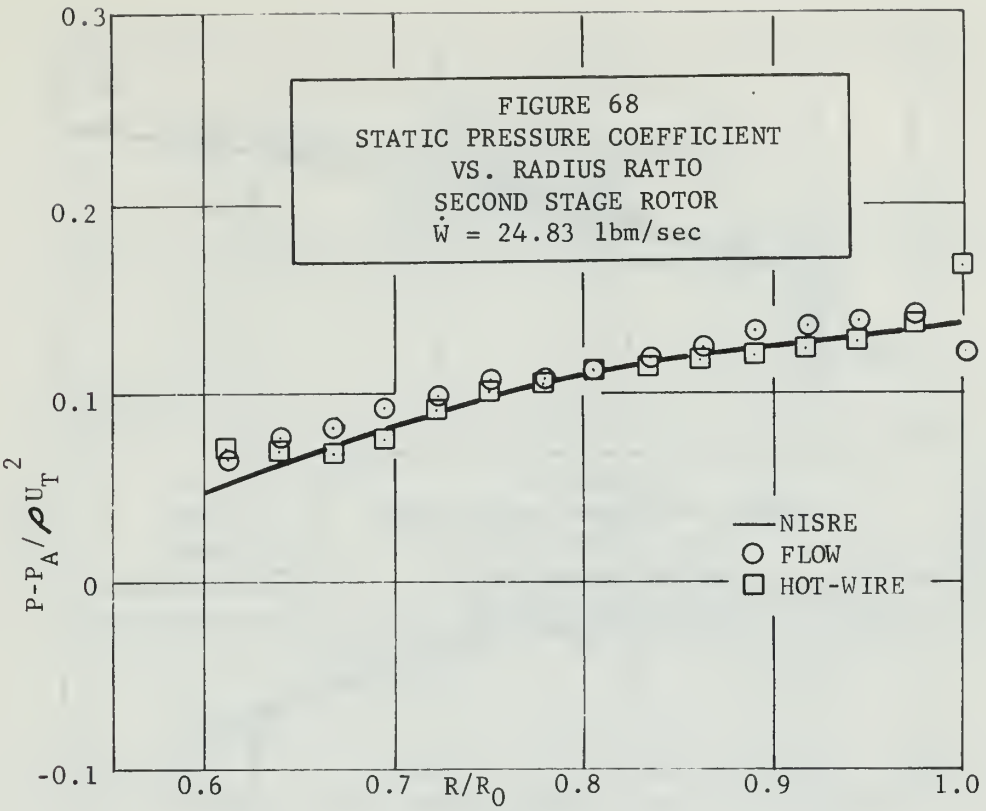

FIGURE 68
STATIC PRESSURE COEFFICIENT
VS. RADIUS RATIO
SECOND STAGE ROTOR
$\dot{W}$ = 24.83 lbm/sec

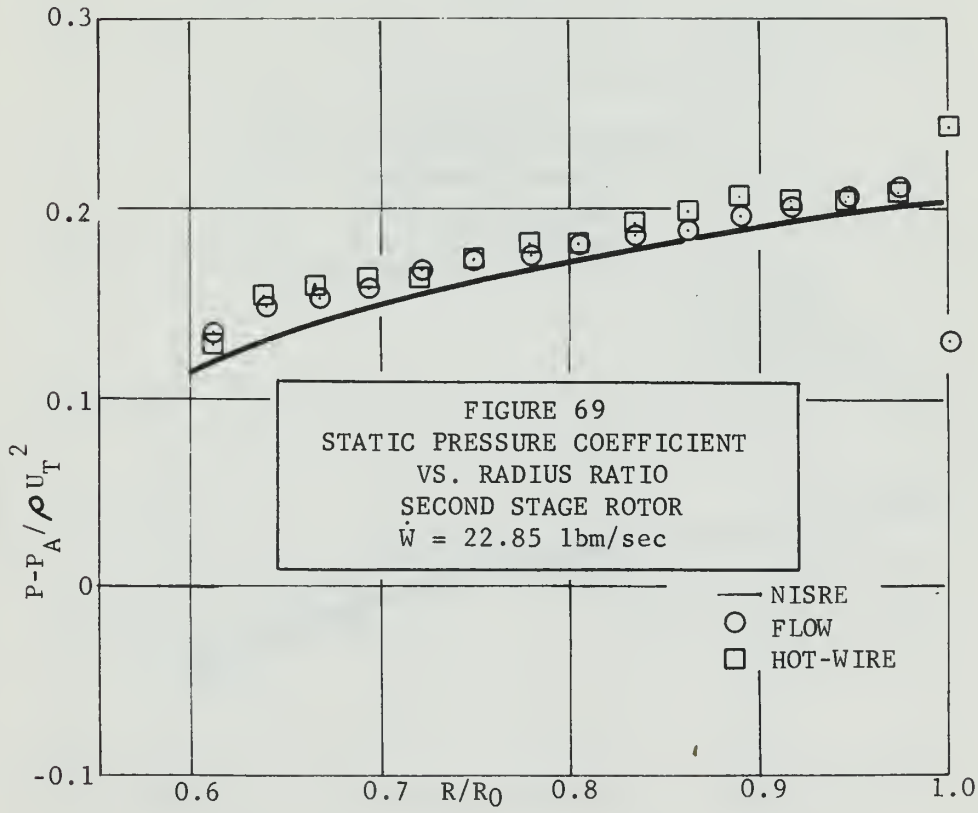

FIGURE 69
STATIC PRESSURE COEFFICIENT
VS. RADIUS RATIO
SECOND STAGE ROTOR
$\dot{W}$ = 22.85 lbm/sec

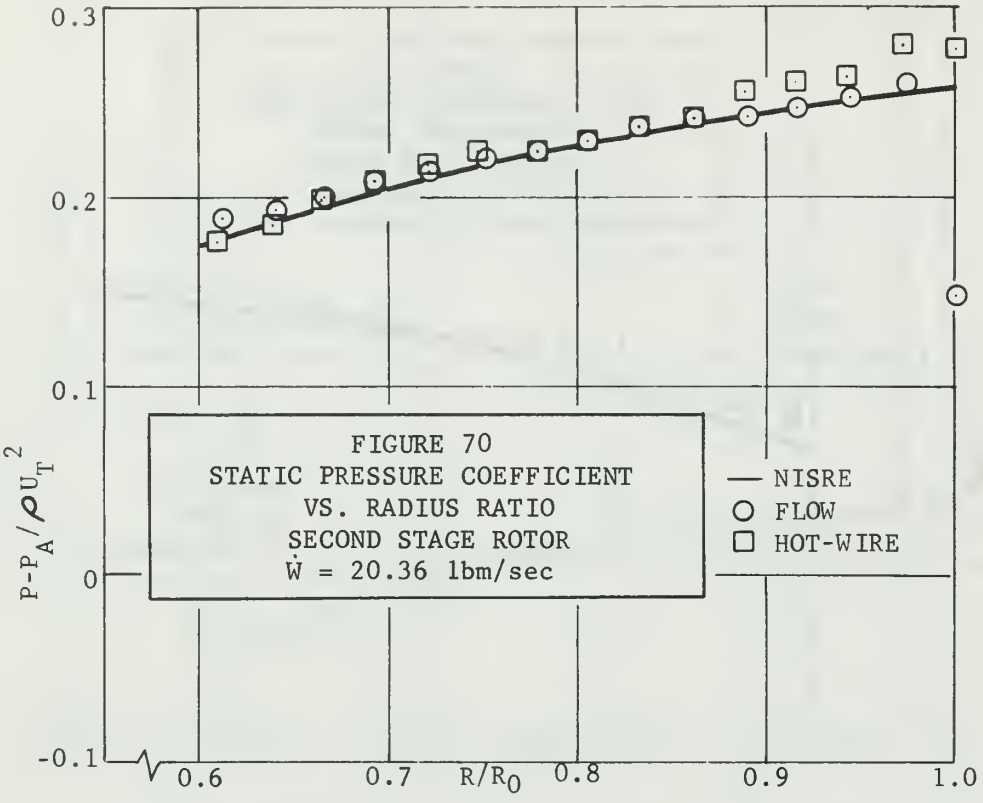

FIGURE 70
STATIC PRESSURE COEFFICIENT
VS. RADIUS RATIO
SECOND STAGE ROTOR
$\dot{W}$ = 20.36 lbm/sec

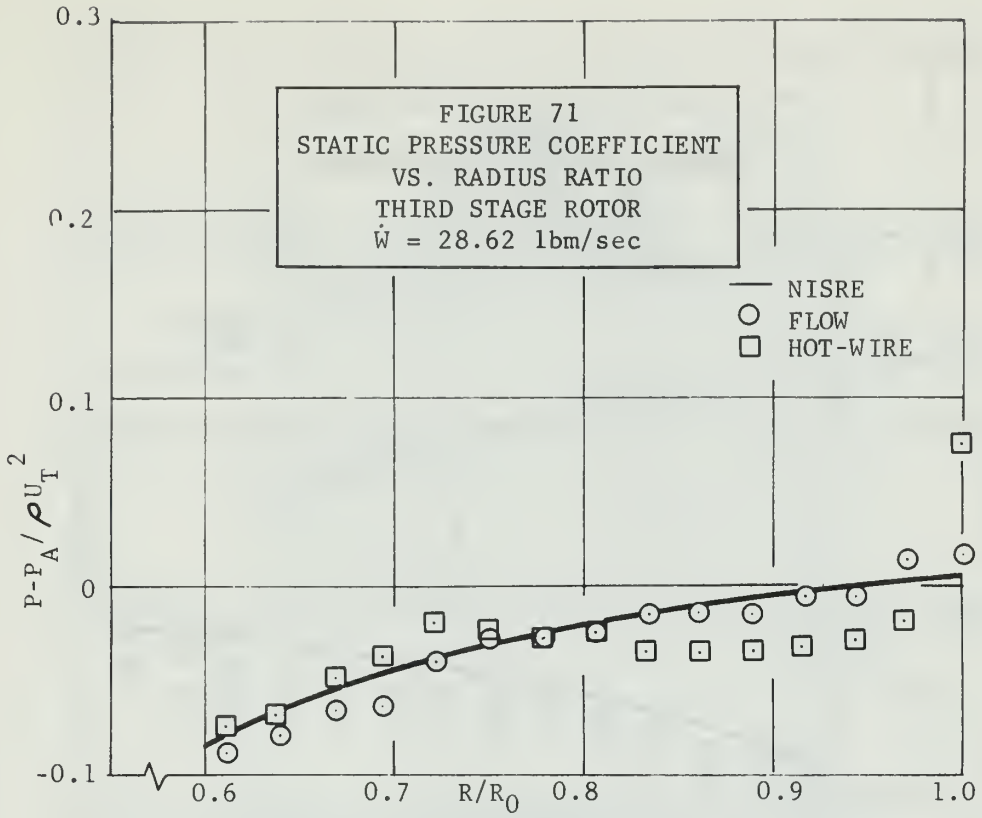
FIGURE 71
STATIC PRESSURE COEFFICIENT
VS. RADIUS RATIO
THIRD STAGE ROTOR
$\dot{W}$ = 28.62 lbm/sec
NISRE
FLOW
HOT-WIRE
$P-P_A/\rho U_T^2$
0.3
0.2
0.1
0
-0.1
0.6
0.7
R/R_0
0.8
0.9
1.0

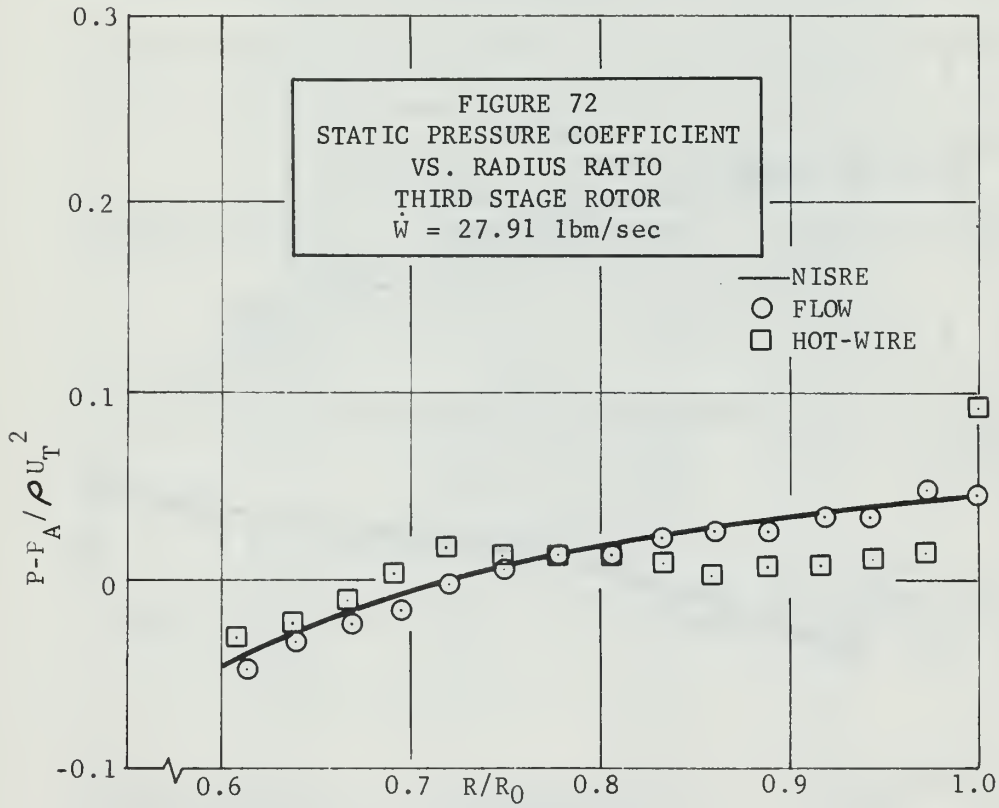
FIGURE 72
STATIC PRESSURE COEFFICIENT
VS. RADIUS RATIO
THIRD STAGE ROTOR
$\dot{W}$ = 27.91 lbm/sec
NISRE
FLOW
HOT-WIRE
$P-P_A/\rho U_T^2$
0.3
0.2
0.1
0
-0.1
0.6
0.7
R/R_0
0.8
0.9
1.0

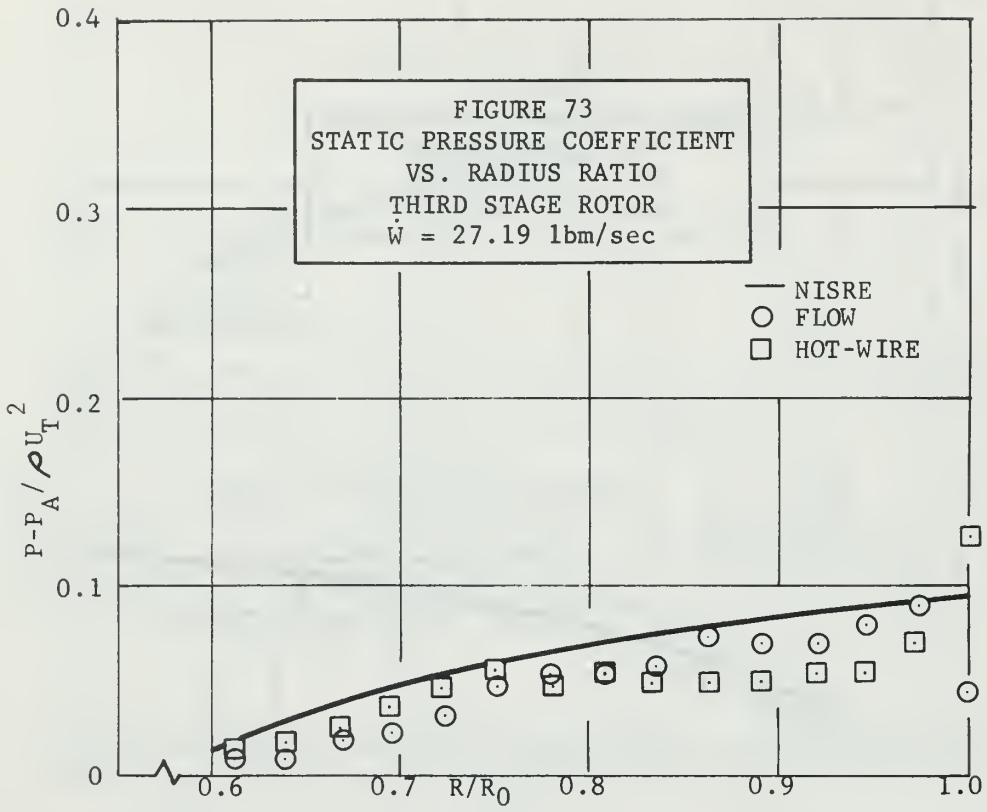
FIGURE 73
STATIC PRESSURE COEFFICIENT
VS. RADIUS RATIO
THIRD STAGE ROTOR
$\dot{W}$ = 27.19 lbm/sec
NISRE
FLOW
HOT-WIRE
$P-P_A/\rho U_T^2$
0.4
0.3
0.2
0.1
0
0.6
0.7
R/R_0
0.8
0.9
1.0

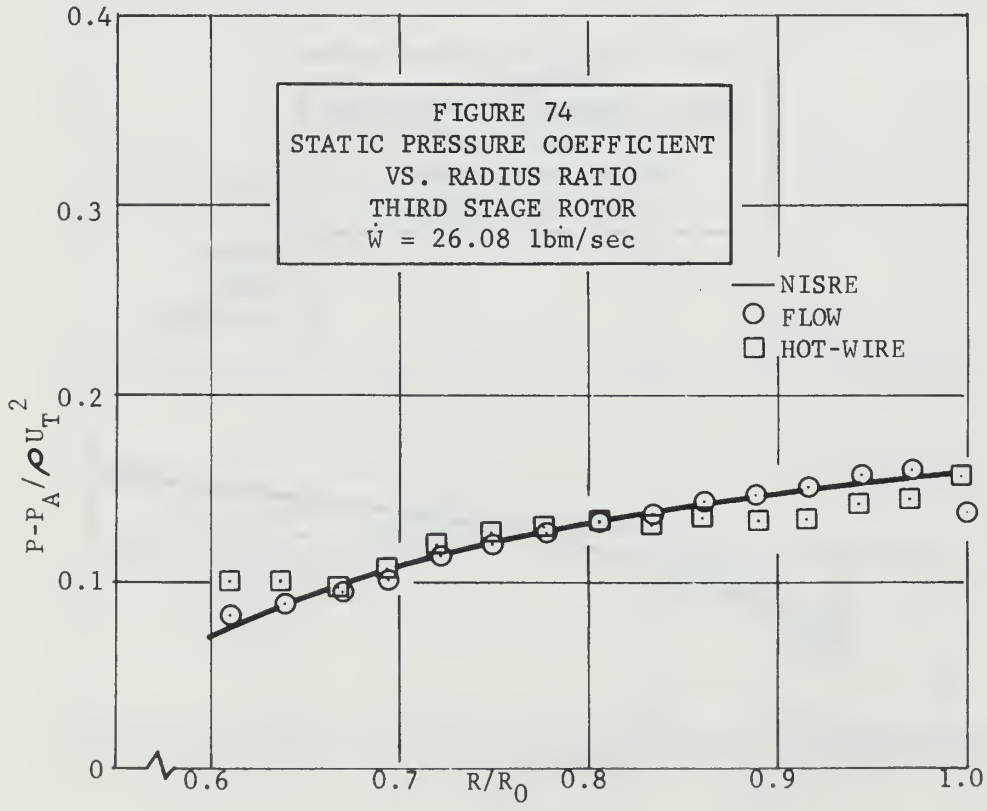
FIGURE 74
STATIC PRESSURE COEFFICIENT
VS. RADIUS RATIO
THIRD STAGE ROTOR
$\dot{W}$ = 26.08 lbm/sec
NISRE
FLOW
HOT-WIRE
$P-P_A/\rho U_T^2$
0.4
0.3
0.2
0.1
0
0.6
0.7
R/R_0
0.8
0.9
1.0

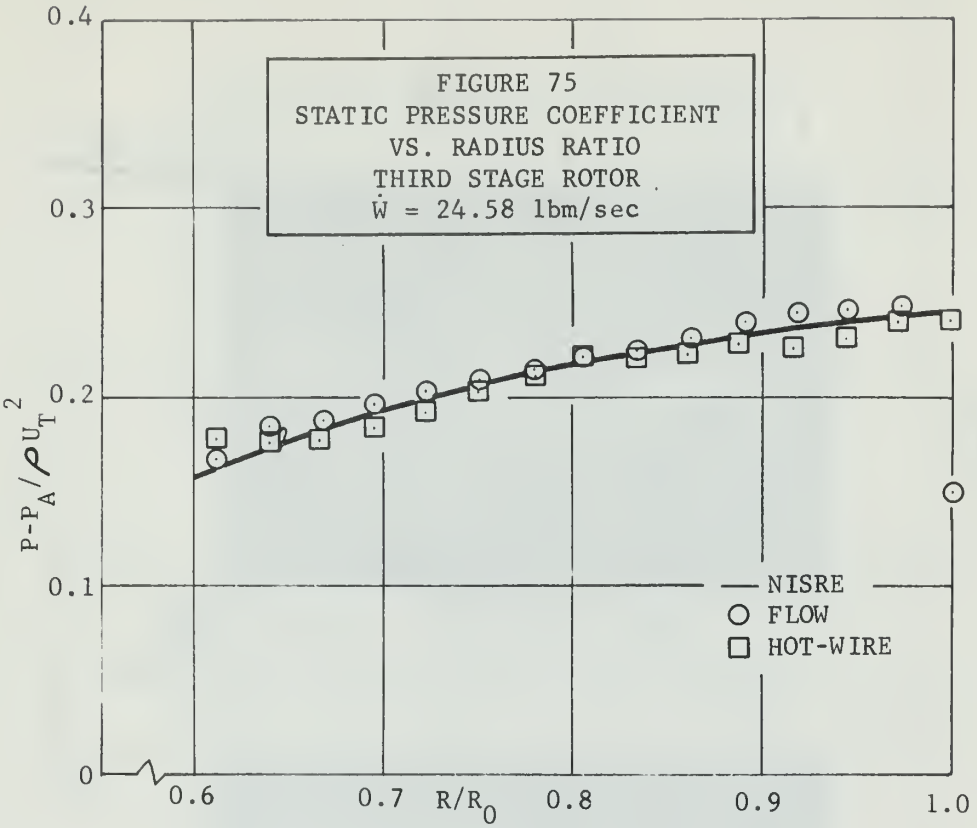
FIGURE 75
STATIC PRESSURE COEFFICIENT
VS. RADIUS RATIO
THIRD STAGE ROTOR
$\dot{W}$ = 24.58 lbm/sec
$P-P_A/\rho U_T^2$
0.4
0.3
0.2
0.1
0
0.6
0.7
R/R_0
0.8
0.9
1.0
NISRE
FLOW
HOT-WIRE

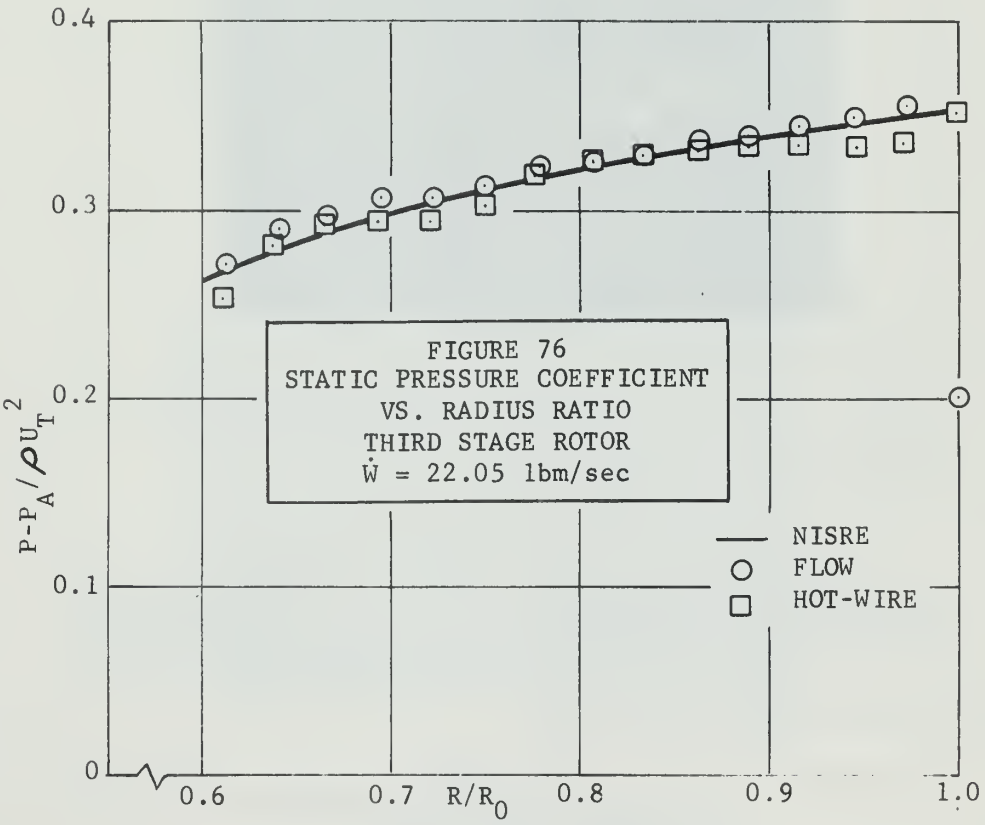
FIGURE 76
STATIC PRESSURE COEFFICIENT
VS. RADIUS RATIO
THIRD STAGE ROTOR
$\dot{W}$ = 22.05 lbm/sec
$P-P_A/\rho U_T^2$
0.4
0.3
0.2
0.1
0
0.6
0.7
R/R_0
0.8
0.9
1.0
NISRE
FLOW
HOT-WIRE

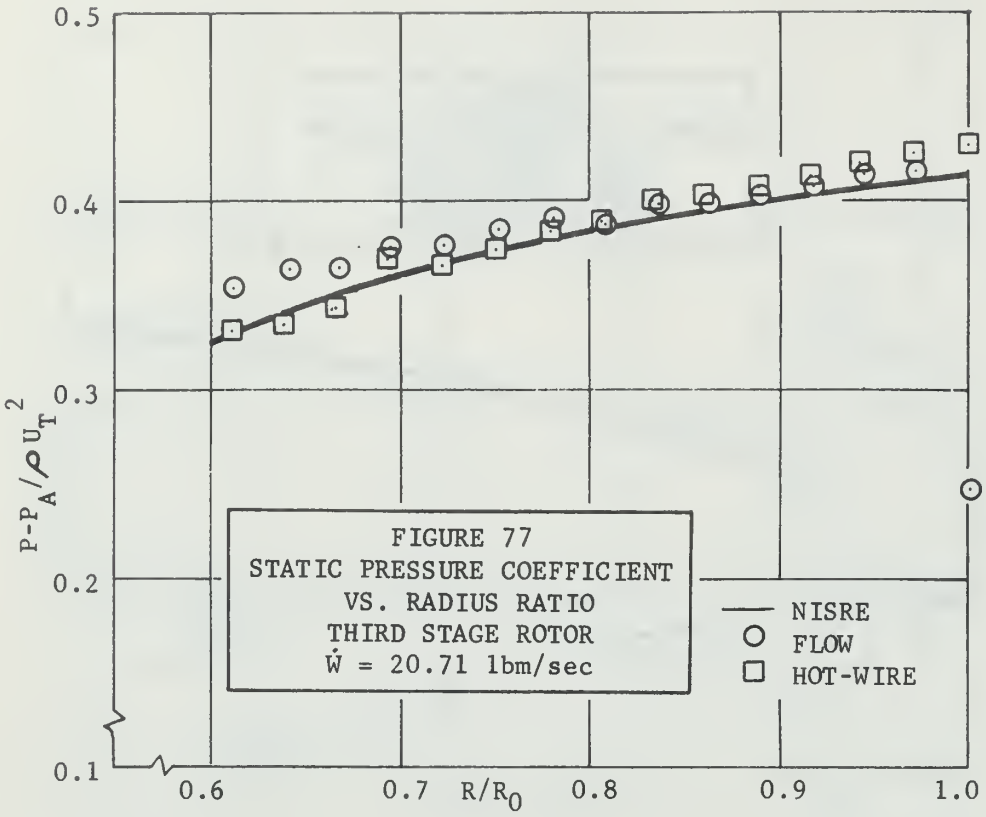

FIGURE 77
STATIC PRESSURE COEFFICIENT
VS. RADIUS RATIO
THIRD STAGE ROTOR
$\dot{W}$ = 20.71 lbm/sec

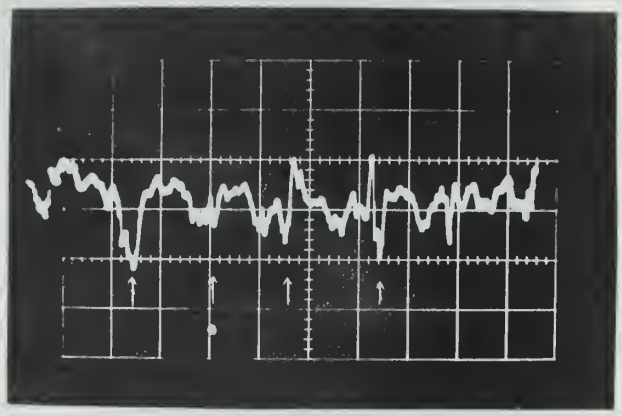

1.675 cm

(a) $\dot{W}$ = 28.37 lbm/sec

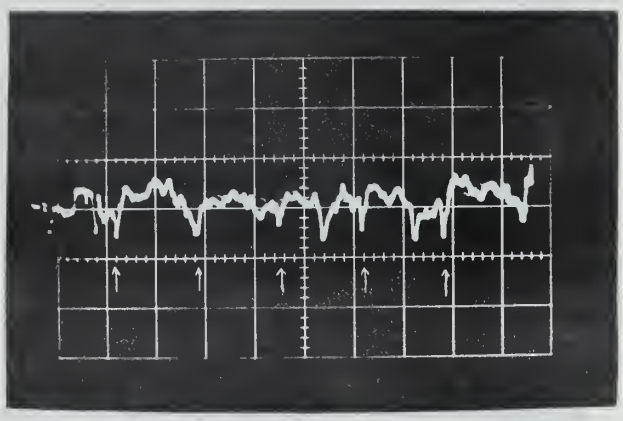

1.675 cm

cm 0 1 2

(b) $\dot{W}$ = 27.91 lbm/sec

PROBE POSITION
DOWNSTREAM OF
SECOND STAGE ROTOR
RADIUS = 13 inches

OSCILLOSCOPE SETTINGS
TIME SCALE 1 millisec/cm
AMPLITUDE 10 millivolt/cm

HOT-WIRE CURRENT 25 milliamps

FIGURE 76
HOT-WIRE ANEMOMETER OSCILLOGRAMS
SECOND STAGE ROTOR

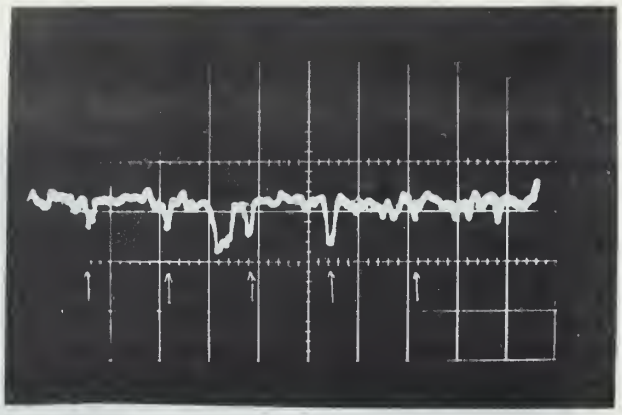

1.675 cm →| |←

(c) $\dot{W}$ = 27.12 lbm/sec

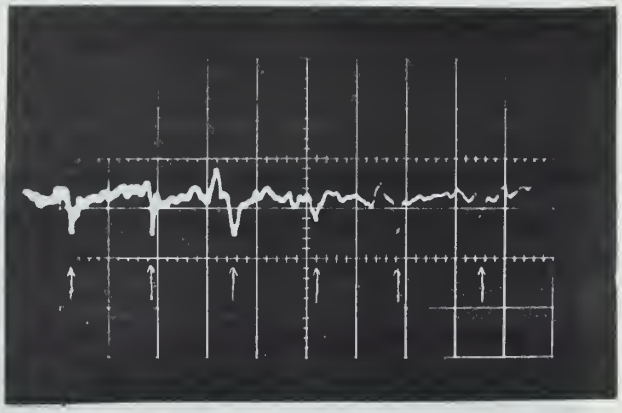

1.675 cm →| |←

(d) $\dot{W}$ = 25.93 lbm/sec

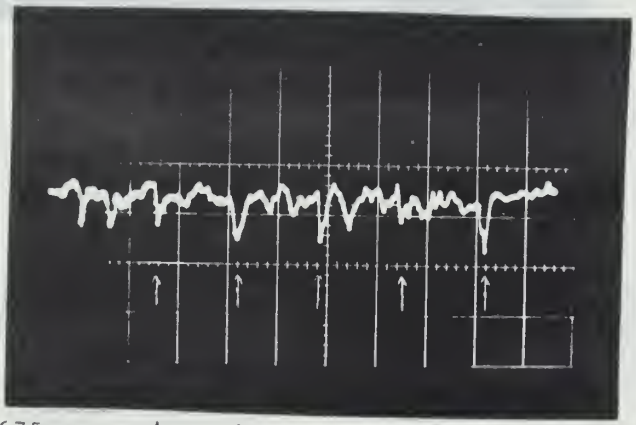

1.675 cm →| |←

(e) $\dot{W}$ = 24.80 lbm/sec

cm 0 1 2

FIGURE 78 (continued)

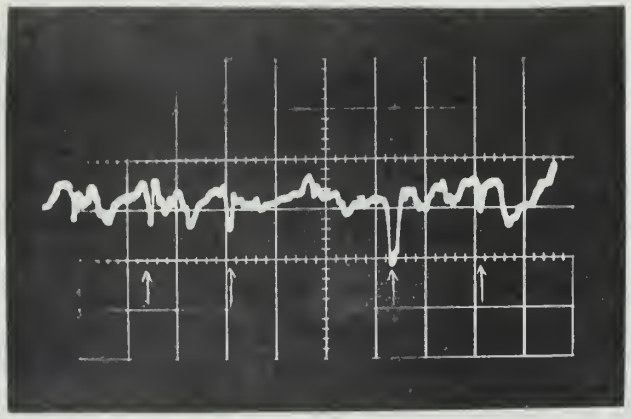

1.675 cm

(f) $\dot{W}$ = 22.52 lbm/sec

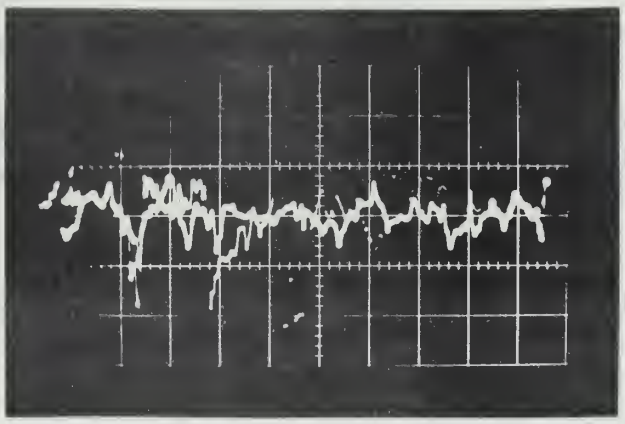

(g) $\dot{W}$ = 19.26 lbm/sec

cm 0 1 2

FIGURE 78 (continued)

REFERENCES

1. Vavra, M. H., Aero-Thermodynamics and Flow in Turbomachines, John Wiley & Sons, Inc., New York, N. Y., 1960.

2. Harrison, Robert Glen, "An Analysis of Single Stage Axial-Flow Turbine Performance Using Three-Dimensional Calculating Methods," Naval Postgraduate School Thesis, September 1967.

3. Giamati, Charles C. Jr. and Finger, Harold B., "Design Velocity Distribution in Meridional Plane," Chapter VIII of NASA SP-36, Washington, D. C., 1965.

4. Bowen, John T., Sabersky, Rolf H. and Rannie, Duncan W., "Theoretical and Experimental Investigations of Axial Flow Compressors (Summary Report)," California Institute of Technology, January 1949.

5. Marshall, Bruce Cameron, "Effect of Stator Blade Orientation on the Performance of an Axial Flow Compressor," Naval Postgraduate School Thesis, September 1967.

6. National Research Council, International Critical Tables, McGraw-Hill, 1928.

7. Iura, T. and Rannie, W. D., "Observations of Propagating Stall in Axial-Flow Compressors," California Institute of Technology, April 1953.

APPENDIX A

DETAILS OF FLOW RATE CALIBRATION COMPUTER PROGRAM

This program uses the data obtained from the hot-wire anemometer surveys of the inlet to calculate volume flow rate. Reference velocity for the hot-wire reference setting is obtained from the inlet survey Pitot-static probe mounted at the inlet centerline. Inlet guide vane velocity is obtained from the permanently mounted Pitot-static probe ahead of the inlet guide vanes.

This program assumes that the hot-wire instrument is set to 90 per cent of full scale for the reference velocity at the inlet centerline and that the hot-wire instrument is linear.

Input

Card No.	Format	Fortran	Description
1	12	KKK	Number of runs to be considered.
2	3I3,2I10	M	Number of radial data points - symmetric on either side of centerline (maximum 99)
		MM	Number of readings of total pressure and velocity head taken at the inlet centerline (maximum 99)
		MMM	Number of readings of total pressure and velocity head taken ahead of the inlet guide vanes (maximum 99)

		IRUN	Run number
		ISPEED	Rotor speed (rpm)
3	4F10.4	TI	Temperature in the inlet (°F)
		TW	Temperature in test cell (°F)
		BAR	Barometric pressure (inches Hg.)
		TBAR	Temperature of mercury column of barometer (°F)
4	8F10.4	PT1R	Total pressure at the inlet centerline (inches H_2O)
		Q1R	Velocity head at the inlet centerline (inches H_2O)
5	8F10.4	PT2R	Total pressure ahead of the inlet guide vanes (inches H_2O)
6	8F10.4	Q2R	Velocity head ahead of the inlet guide vanes (inches H_2O)
7	8F10.4	R	Radii at which data are taken from the centerline outward - data points must be symmetric on either side of centerline (inches)
8	8F10.4	VRL	Values of velocity ratio of hot-wire anemometer to the left side of centerline looking downstream (dimensionless)

9	8F10.4	VRR	Values of velocity ratio of hot-wire anemometer to the right side of centerline looking downstream (dimensionless)

Output

The computer program output prints the input data in the same format as they are read in.

The calculated information is presented as follows:

Description	Units
Barometric pressure	(lb/ft^2)
Inlet temperature	(°R)
Volume flow rate	(ft^3/sec)
Mass flow rate	(lbm/sec)
Velocity at inlet centerline	(ft/sec)
Velocity ahead of inlet guide vanes	(ft/sec)
Mass density at inlet centerline	(lbm/ft^3)
$CCC = \frac{\text{(volume flow rate)}}{\text{(velocity ahead of inlet guide vanes)}}$	$\frac{(ft^3/sec)}{(ft/sec)}$

TABLE A-1 LISTING OF PROGRAM FLORAT

```
      DIMENSION PT1R(99),Q1R(99),PT2R(99),Q2R(99),R(99),VRL(99),VRR(99),
     1PT1(99),Q1(99),P1(99),RHO1(99),V(99),PT2(99),Q2(99),P2(99),RHO2(99
     2)
      G=32.16
      RGAS=53.35
      READ(5,1)KKK
    1 FORMAT(I2)
      DO 2 II=1,KKK
      READ(5,3)M,MM,MMM,IRUN,ISPEED
    3 FORMAT(3I3,2I10)
      READ(5,4)TI,TW,BAR,TBAR
    4 FORMAT(4F10.4)
      READ(5,5)(PT1R(I),Q1R(I),I=1,MM)
    5 FORMAT(8F10.4)
      READ(5,5)(PT2R(I),I=1,MMM)
      READ(5,5)(Q2R(I),I=1,MMM)
      READ(5,5)(R(I),I=1,M)
      READ(5,5)(VRL(I),I=1,M)
      READ(5,5)(VRR(I),I=1,M)
      WRITE(6,14)
   14 FORMAT(1H1)
      WRITE(6,3)M,MM,MMM,IRUN,ISPEED
      WRITE(6,4)TI,TW,BAR,TBAR
      WRITE(6,5)(PT1R(I),Q1R(I),I=1,MM)
      WRITE(6,5)(PT2R(I),I=1,MMM)
      WRITE(6,5)(Q2R(I),I=1,MMM)
      WRITE(6,5)(R(I),I=1,M)
      WRITE(6,5)(VRL(I),I=1,M)
      WRITE(6,5)(VRR(I),I=1,M)
      GWRM=.99837633+1.0605756*TW/10000.-1.593186*TW**2/1000000.
      GHGRM=13.63905-.0013630303*TBAR
      CHGC=.4891585*GHGRM/13.54*144.
      PAMB=BAR*CHGC
      TI=TI+459.7
      TOTAR=0.
      DO 6 I=1,MM
      PT1(I)=PT1R(I)*GWRM/12.*62.42732+PAMB
      Q1(I)=Q1R(I)*GWRM/12.*62.42732
      P1(I)=PT1(I)-Q1(I)
      RHO1(I)=P1(I)/(RGAS*TI*G)
      V1=SQRT(2.*Q1(I)/RHO1(I))
      TOTAR=TOTAR+V1
    6 CONTINUE
      RMM=MM
      V1=TOTAR/RMM
```

TABLE A-1 (continued)

```
      DO 7 I=1,M
      V(I)=(VRL(I)+VRR(I))/2.*V1/.9
    7 CONTINUE
      R(M+1)=18.
      TOTAR=V(1)*3.1416*(R(2)/2.)**2/144.
      K=M-1
      DO 8 I=2,K
      SEGAR=V(I)*3.1416*(((R(I)+R(I+1))/2.)**2-((R(I)+R(I-1))/2.)**2)/14
     14.
      TOTAR=TOTAR+SEGAR
    8 CONTINUE
      SEGAR=V(M)*3.1416*(R(M+1)**2-((R(M)+R(M-1))/2.)**2)/144.
      TOTAR=TOTAR+SEGAR
      VOLFL=TOTAR
      TOTAR=0.
      DO 9 I=1,MMM
      PT2(I)=PT2R(I)*GWRM/12.*62.42732+PAMB
      Q2(I)=Q2R(I)*GWRM/12.*62.42732
      P2(I)=PT2(I)-Q2(I)
      RHO2(I)=P2(I)/(RGAS*TI*G)
      V2=SQRT(2.*Q2(I)/RHO2(I))
      TOTAR=TOTAR+V2
    9 CONTINUE
      RMMM=MMM
      V2=TOTAR/RMMM
      CCC=VOLFL/V2
      TOTAR=0.
      DO 10 I=1,MM
      TOTAR=TOTAR+RHO1(I)
   10 CONTINUE
      WDOT=VOLFL*TOTAR/RMM*G
      GRHO1=TOTAR/RMM*G
      WRITE(6,11)
   11 FORMAT(' NAVAL POSTGRADUATE SCHOOL'/' TURBO-PROPULSION LABORATORY'
     1/5X'CNR COMPRESSOR'/5X'FLOW CALIBRATION'/)
      WRITE(6,12)IRUN,ISPEED,PAMB,TI
   12 FORMAT(' RUN NUMBER 'I3,I10,' RPM'/' BAROMETRIC PRESSURE='F10.4,'
     1PSFA   INLET TEMPERATURE='F10.4,' DEG-R'/)
      WRITE(6,13)VOLFL,WDOT,CCC
   13 FORMAT(' VOLUME FLOW RATE='F10.4,' FT3/SEC   MASS FLOW RATE='F10.4
     1,' LBM/SEC    CCC='F10.4,' FT3/SEC PER FT/SEC')
      WRITE(6,16)V1,V2,GRHO1
   16 FORMAT(/' VELOCITY AT INLET CENTERLINE='F10.4' FT/SEC'/' VELOCITY
     1AHEAD OF INLET GUIDE VANES='F10.4' FT/SEC'/' MASS DENSITY IN INLET
     2='F10.4' LBM/FT3')
```

TABLE A-1 (continued)

```
      WRITE(6,15)
   15 FORMAT(1H1)
    2 CONTINUE
      STOP
      END
```

TABLE A-2 SAMPLE OUTPUT OF PROGRAM FLORAT

```
20  1  1          18        1195
  75.7500    71.6000    30.1100    74.0000
  -0.1035     0.6940
  -0.6000
   1.6800
   0.0          3.0000     6.0000     9.0000    12.0000    15.0000    15.2000    15.4000
  15.6000    15.8000    16.0000    16.2000    16.4000    16.6000    16.8000    17.0000
  17.2000    17.4000    17.6000    17.8000
   0.9000     0.9000     0.8950     0.8900     0.8950     0.8900     0.8800     0.8750
   0.8800     0.8750     0.8750     0.8650     0.8700     0.8550     0.8450     0.8500
   0.8450     0.8200     0.7800     0.6700
   0.9000     0.9000     0.9000     0.8900     0.8900     0.8750     0.8750     0.8750
   0.8750     0.8700     0.8650     0.8600     0.8700     0.8600     0.8600     0.8450
   0.8350     0.8100     0.7600     0.7100
NAVAL POSTGRADUATE SCHOOL
TURBO-PROPULSION LABORATORY
    ONR COMPRESSOR
    FLOW CALIBRATION

RUN NUMBER  18       1195 RPM
BAROMETRIC PRESSURE= 2120.6272 PSFA    INLET TEMPERATURE=  535.4500 DEG-R

VOLUME FLOW RATE=  383.5956 FT3/SEC    MASS FLOW RATE=    28.4504 LBM/SEC     CCC=     4.4052 FT3/SEC PER FT/SEC

VELOCITY AT INLET CENTERLINE=    55.9230 FT/SEC
VELOCITY AHEAD OF INLET GUIDE VANES=    87.1678 FT/SEC
MASS DENSITY IN INLET=     0.0741 LBM/FT3
```

APPENDIX B

DETAILS OF FLOW PROPERTIES COMPUTER PROGRAM

This program uses the total pressure, total temperature, velocity head, velocity ratio from the hot-wire anemometer, and absolute flow angle data obtained from the radial surveys downstream of rotor blade rows and calculates flow properties based on the NISRE solution, flow probe velocity and hot-wire anemometer velocity. The NISRE solution also requires total pressure and velocity head data from the permanent Pitot-static probe ahead of the inlet guide vanes in order to calculate mass flow rate.

Input

Card No.	Format	Fortran	Description
1	I2	KKK	Number of sets of data to be read.
2	3I3,7F10.3	IRUN	Run number
		MD	Number of radial data points (maximum 50)
		N	Number of radial points required from NISRE solution (maximum 100)
		BAR	Barometric pressure (inches Hg.)
		TBAR	Temperature of mercury column of barometer (°F)
		RPM	Rotor speed (rpm)
		BKG	Assumed gross weight flow blockage factor (BKG $\leq$ 1)

		GAM	Specific heat ratio (dimensionless)
		RGAS	Gas constant (ft-lb)/lbm-°R)
		FARB	Arbitrary multiplication factor for reference axial velocity in NISRE solution, required to start Newton Raphson iteration ($1 < FARB \leq 1.2$)
3	6F10.3,3I3	VA1	Reference axial velocity at root mean square radius for NISRE solution, which must be estimated within 50 per cent of true value (ft/sec)
		ACC	Accuracy to which the NISRE solution is to match the actual flow rate. $\left(ACC \quad \left\lvert 1-\frac{\text{Flow rate calculated}}{\text{Actual flow rate}} \right\rvert\right.$, $0 < ACC \leq .00001$)
		TW	Temperature in the test cell (°F)
		TI	Inlet air temperature (°F)
		RO	Outer radius of the annulus (inches)
		RI	Inner radius of the annulus (inches)

		MMM	Number of readings of total pressure and velocity head taken ahead of the inlet guide vanes (maximum 50)
		NREF	The number of the data point at which the hot wire anemometer was set to 90 per cent, counting from the hub outward.
		NS	Stage number
4	8F10.3	PTIR	Total pressure ahead of the inlet guide vanes (inches (H_2O)
		QIR	Velocity head ahead of the inlet guide vanes (inches H_2O)

The remaining input data are from the radial surveys downstream of a particular rotor. Data must be entered into the program from the hub outward, one card per radial station.

5	6F10.4	PTR	Total pressure (inches H_2O)
		QR	Velocity head (inches H_2O)
		TTR	Total temperature (millivolts determined from an iron-constantan thermocouple with a 32°F reference junction)

ALPHA	Absolute flow angle, taken positive from the axial direction to the direction of rotation (degrees)
VR	Velocity ratio from hot-wire anemometer (dimensionless)
R	Radius (inches)

Output

The computer program output gives the input data in the same format as read in for the purpose of checking input data for errors.

The major part of the output is divided into three sections, the NISRE, flow probe, and hot-wire calculations respectively. The calculated data for each of the three methods are presented in dimensional and in dimensionless form. The method used to obtain the dimensionless quantities is described in Section 8.

Dimensional Form

Name	Description
RADIUS	(inches)
PT	Total pressure (psfa)
P	Static pressure (psfa)
TT	Total temperature (°R)
T	Static temperature (°R)
V	Absolute velocity (ft/sec)
VA	Axial component of absolute velocity (ft/sec)
VU	Peripheral component of absolute velocity (ft/sec)
VMACH	Mach number of absolute velocity based on calculated static temperature (dimensionless)

W	Relative velocity (ft/sec)
WA	Axial component of relative velocity (ft/sec)
WU	Peripheral component of relative velocity (ft/sec)
WMACH	Mach number of relative velocity based on calculated static temperature (dimensionless)
U	Peripheral velocity (ft/sec)
ALPHA	Angle of absolute velocity - positive from the axial direction to the direction of rotation (degrees)
BETA	Angle of relative velocity - positive from the axial direction to the direction of rotation (degrees)

Dimensionless Form

All velocities are made dimensionless by dividing by the peripheral tip velocity (U_T). All temperatures are made dimensionless by dividing by the compressor inlet temperature.

R/RO	Radius ratio - Radius divided by tip radius
DPT/RHO*UT **2	$(P_t-P_a)/(\frac{1}{2}\rho U_T^2)$
DP/RHO*UT **2	$(P-P_a)/(\frac{1}{2}\rho U_T^2)$
PHIAV	Numerical average of the dimensionless axial velocity components.

TABLE B-1 LISTING OF PROGRAM FLOW

```
      REAL*8 RD,TTD,PTD,ALPHD,BT,BP,BA,TL,CL,AL,YL,RDN
      DIMENSION DELY(99),SB(6),TL(6),ST(6),CL(6),SC(6),AL(30,30),WL(99),
     1YL(99),RD(99),TTD(99),PTD(99),ALPHD(99),BT(6),BP(6),BA(6),RDN(100)
     2,PT(50),TT(50),ALPH(100),RN(100),V(100),VA(100),VU(100),W(100),WA(
     3100),WU(100),BETA(100),VMACH(100),WMACH(100),U(100),T(100),P(100),
     4PTIR(50),QIR(50),PTR(50),QR(50),TTR(50),ALPHA(50),VR(50),R(50),TTN
     5(100),PTN(100),QM(50),PM(50)
      READ(5,6)KKK
    6 FORMAT(I2)
      DO 100 K1=1,KKK
      READ(5,1)IRUN,MD,N,BAR,TBAR,RPM,BKG,GAM,RGAS,FARB
    1 FORMAT(3I3,7F10.3)
      READ(5,2)VA1,ACC,TW,TI,RO,RI,MMM,NREF,NS
    2 FORMAT(6F10.3,3I3)
      READ(5,9)(PTIR(I),QIR(I),I=1,MMM)
    9 FORMAT(8F10.3)
      READ(5,3)(PTR(I),QR(I),TTR(I),ALPHA(I),VR(I),R(I),I=1,MD)
    3 FORMAT(6F10.4)
      WRITE(6,1)IRUN,MD,N,BAR,TBAR,RPM,BKG,GAM,RGAS,FARB
      WRITE(6,2)VA1,ACC,TW,TI,RO,RI,MMM,NREF,NS
      WRITE(6,3)(PTR(I),QR(I),TTR(I),ALPHA(I),VR(I),R(I),I=1,MD)
      WRITE(6,9)(PTIR(I),QIR(I),I=1,MMM)
      CALL CONVER(PTIR,QIR,PTI,QI,PI,TTR,TT,PTR,QR,PT,QM,PM,BAR,TBAR,MD,
     1TW,MMM,PAMB)
      WRITE(6,4)PTI,QI,PI
    4 FORMAT(3F10.3)
      WRITE(6,5)(TT(I),PT(I),QM(I),PM(I),I=1,MD)
    5 FORMAT(4F10.3)
      CALL FLOW(TI,PI,QI,WDES,RGAS)
      WRITE(6,7)WDES
    7 FORMAT(' WDES='F10.4'LBM/SEC'/)
      DO 8 I=1,MD
      PTD(I)=PT(I)
      TTD(I)=TT(I)
      ALPHD(I)=ALPHA(I)
      RD(I)=R(I)
    8 CONTINUE
      IW=0
      ISW=1
      LP=0
      KM=4
      CALL LSQPOL(MD,KM,IW,ISW,LP,SIGMA,RD,PTD,WL,YL,DELY,BP,SB,TL,ST,C,
     1SC,AL)
      CALL LSQPOL(MD,KM,IW,ISW,LP,SIGMA,RD,TTD,WL,YL,DELY,BT,SB,TL,ST,C,
     1SC,AL)
```

TABLE B-1 (continued)

```
      CALL LSQPOL(MD,KM,IW,ISW,LP,SIGMA,RD,ALPHD,WL,YL,DELY,BA,SB,TL,ST,
     1C,SC,AL)
      CALL RADDET(RO,RI,N,M,RDN,RN)
      WRITE(6,200)(RN(I),I=1,N)
  200 FORMAT(12F10.5)
      WRITE(6,201)M
  201 FORMAT(I4)
      CALL POLRET(N,BP,RDN,PTN)
      CALL POLRET(N,BT,RDN,TTN)
      CALL POLRET(N,BA,RDN,ALPH)
      CALL NISRE(PTN,TTN,WDES,ALPH,RN,VA1,FARB,ACC,RPM,V,VA,VU,W,WA,WU,B
     1ETA,WCALC,BKG,VMACH,WMACH,U,T,P,IN,M,RGAS,GAM,N)
      IF(IN.EQ.1)STOP
      JJ=1
      CALL OUTPUT(PTN,P,TTN,T,V,VA,VU,VMACH,W,WA,WU,WMACH,RN,U,ALPH,BETA
     1,WDES,BKG,RPM,IRUN,PAMB,TI,JJ,N,NS)
      CALL NONDIM(PTN,P,TTN,T,V,VA,VU,VMACH,W,WA,WU,WMACH,RN,U,ALPH,BETA
     1,PAMB,TI,N,IRUN)
      CALL PITOT(PM,QM,RGAS,GAM,ALPHA,BETA,TT,T,V,VA,VU,W,WA,WU,VMACH,WM
     1ACH,U,MD,RPM,R)
      JJ=3
      CALL OUTPUT(PT,PM,TT,T,V,VA,VU,VMACH,W,WA,WU,WMACH,R,U,ALPHA,BETA,
     1WDES,BKG,RPM,IRUN,PAMB,TI,JJ,MD,NS)
      CALL NONDIM(PT,PM,TT,T,V,VA,VU,VMACH,W,WA,WU,WMACH,R,U,ALPHA,BETA,
     1PAMB,TI,MD,IRUN)
      CALL HOTWIR(NREF,VR,GAM,RGAS,RPM,ALPHA,V,VA,VU,T,VMACH,U,W,WA,WU,W
     1MACH,BETA,MD,R,TT,P,PT)
      JJ=2
      CALL OUTPUT(PT,P ,TT,T,V,VA,VU,VMACH,W,WA,WU,WMACH,R,U,ALPHA,BETA,
     1WDES,BKG,RPM,IRUN,PAMB,TI,JJ,MD,NS)
      CALL NONDIM(PT,P,TT,T,V,VA,VU,VMACH,W,WA,WU,WMACH,R,U,ALPHA,BETA,P
     1AMB,TI,MD,IRUN)
  100 CONTINUE
      STOP
      END



      SUBROUTINE CONVER(PTIR,QIR,PTI,QI,PI,TTR,TT,PTR,QR,PT,QM,PM,BAR,TB
     1AR,MD,TW,MMM,PAMB)
      DIMENSION TT(1),PT(1),QM(1),PM(1),TTR(1),PTR(1),QR(1),PTIR(1),QIR(
     11)
      GWRM=.99837633+1.0605756*TW/10000.-1.5931861*TW**2/1000000.
```

TABLE B-1 (continued)

```
      GHGRM=13.63905-.0013630303*TBAR
      CHGC=.4891585*GHGRM/13.54*144.
      PAMB=BAR*CHGC
      DO 1 I=1,MD
      TEMP=32.+39.98*TTR(I)-.435*TTR(I)**2
      TT(I)=TEMP+459.7
      PT(I)=PTR(I)*GWRM/12.*62.42732+PAMB
      QM(I)=QR(I)*GWRM/12.*62.42732*1.09
      PM(I)=PT(I)-QM(I)
    1 CONTINUE
      SUM1=0.
      SUM2=0.
      SUM3=0.
      DO 2 I=1,MMM
      PTI=PTIR(I)*GWRM/12.*62.42732+PAMB
      QI=QIR(I)*GWRM/12.*62.42732
      PI=PTI-QI
      SUM1=SUM1+PTI
      SUM2=SUM2+QI
      SUM3=SUM3+PI
    2 CONTINUE
      RMMM=MMM
      PTI=SUM1/RMMM
      QI=SUM2/RMMM
      PI=SUM3/RMMM
      RETURN
      END



      SUBROUTINE FLOW(TI,PI,QI,WDES,RGAS)
      TIA=TI+459.7
      RHOI=PI/(RGAS*TIA*32.17)
      CCC=4.405
      VI=SQRT(2.*QI/RHOI)
      VF=CCC*VI
      WDES=RHOI*32.17*VF
      RETURN
      END
```

TABLE B-1 (continued)

```
      SUBROUTINE RADDET(RO,RI,N,M,RDN,R)
      REAL*8 RDN
      DIMENSION RDN(1),R(1),A(100)
      RMS=14.8432
      RN=N-1
      DR=(RO-RI)/RN
      R(1)=RMS
      I=2
    1 R(I)=R(I-1)-DR
      IF(R(I).LT.RI)GO TO 2
      I=I+1
      GO TO 1
    2 R(I)=RI
      M=I
      DO 3 I=1,M
      A(I)=R(M-I+1)
    3 CONTINUE
      DO 4 I=1,M
      R(I)=A(I)
    4 CONTINUE
      I=M+1
    5 R(I)=R(I-1)+DR
      IF(R(I).GT.RO)GO TO 6
      I=I+1
      GO TO 5
    6 R(I)=RO
      IF(I.GT.N)R(I-1)=RO
      DO 7 I=1,N
      RDN(I)=R(I)
    7 CONTINUE
      RETURN
      END
```

```
      SUBROUTINE LSQPOL(M,KM,IW,ISW,LP,SIGMA,X,F2,W,Y,DELY,B,SB,T,ST,C,
     1SC,A)
      REAL*8 X,F2,Y,B,T,C,A,F,P,BM,D,FBAR,XBAR,PXF,PXP,XPXP,XPXPM,XP,
     1ALPHA,BETA,PPXF,PPXPP,PT,VARA,POLYE1
      DIMENSION S(30),X(1),F2(1),ST(1),SB(1),F(100),PM(100),P(100),B(1),
     1DELY(1),W(1),A(30,30),T(1),Y(1),BM(11,11),D(11,11),C(1),SC(1)
      DO 7 I=1,11
```

TABLE B-1 (continued)

```
      DO 4 J=1,11
      D(I,J)=0.0D0
    4 CONTINUE
    7 CONTINUE
      LL=0
    9 FM=0.0
      SUMEV2=0.0
      A(1,1)=1.0
      A(2,2)=1.0
      FBAR=0.0
      XBAR=0.0
      DO10I=1,M
      IF(IW)1009,1010,1009
1010  W2=1.0
      W(I)=1.0
      GOTO1011
1009  W2=SQRT(W(I))
1011  FM=FM+W(I)
      F(I)=W2*F2(I)
      PM(I) = W2
      FBAR=FBAR+F(I)*PM(I)
   10 XBAR=XBAR+X(I)*PM(I)**2
      XBAR=XBAR/FM
      T(1)=FBAR/FM
      A(2,1)=-XBAR
      PXF=0.0
      PXP=0.0
      DO20I=1,M
      P(I)=(X(I)-XBAR)*PM(I)
      PXF=PXF+P(I)*F(I)
   20 PXP=PXP+P(I)*P(I)
      T(2)=PXF/PXP
      PMXPM=FM
      S(1)=PMXPM
      KM=KM+1
      B(1)=T(1)*A(1,1)+T(2)*A(2,1)
      B(2)=T(2)*A(2,2)
   60 DO190K=2,KM
      IF(K-2)40,165,65
   40 WRITE(6,4000)
4000  FORMAT(7HSTOP 40)
      STOP
   65 XPXP=0.0
      XPXPM=0.0
      B(K)=0.0
```

TABLE B-1 (continued)

```
      DO70J=1,M
      XP=X(J)*P(J)
      XPXP=XPXP+XP*P(J)
   70 XPXPM=XPXPM+XP*PM(J)
      ALPHA=XPXP/PXP
      BETA=XPXPM/PMXPM
      PPXF=0.0
      PPXPP=0.0
      DO90I=1,M
   80 PT=P(I)
   81 P(I)=X(I)*PT-ALPHA*PT-BETA*PM(I)
   82 PPXF=PPXF+P(I)*F(I)
   83 PPXPP=PPXPP+P(I)*P(I)
   90 PM(I)=PT
      T(K)=PPXF/PPXPP
      PMXPM=PXP
      PXP=PPXPP
      A(K,1)=-ALPHA*A(K-1,1)-BETA*A(K-2,1)
      A(K,K-1)=A(K-1,K-2)-A(K-1,K-1)*ALPHA
      A(K,K)=1.0
      IF(K-3)150,150,110
  110 K1=K-2
      DO120I=2,K1
  120 A(K,I)=A(K-1,I-1)-ALPHA*A(K-1,I)-BETA*A(K-2,I)
  150 DO160I=1,K
  160 B(I)=B(I)+T(K)*A(K,I)
  165 SIG3=0.0
      DO180I=1,M
      Y(I)=POLYE1(X(I),K,B)
  175 DELY(I)=Y(I)-F2(I)
  180 SIG3 = SIG3 + (DELY(I)**2)*W(I)
      SIG3=SIG3/FM
      SIG2=SIG3*FLOAT(M)/FLOAT(M-K)
      IF(K-2)40,1650,1651
 1650 FLEV = 0.
      GO TO 1652
 1651 FLEV=(SUMEV2-SIG3)/SIG2
 1652 SUMEV2=SIG3
      SIGMA=SQRT (SIG2)
      S(K) = PXP
      DO499I=1,K
  499 ST(I)=SIGMA/SQRT(S(I))
      DO501I=1,K
      SB(I)=0.0
      DO500J=I,K
```

TABLE B-1 (continued)

```
500 SB(I)=SB(I)+(A(J,I)*ST(J))**2
501 SB(I)=SQRT(SB(I))
    IF(LP)658,183,658
658 IF(K-2)652,651,652
651 D(1,1)=1.0D0
    D(2,2)=1.0D0
    D(2,1)=0.0D0
    D(3,3)=1.5D0
    D(3,2)=0.0D0
    D(3,1)=-0.5D0
    D(4,4)=3.5D0
    D(4,3)=0.0D0
    D(4,2)=-1.5D0
    D(4,1)=0.0D0
    D(5,5)=35.0D0/8.0D0
    D(5,4)=0.0D0
    D(5,3)=-30.0D0/8.0D0
    D(5,2)=0.0D0
    D(5,1)=3.0D0/8.0D0
    D(6,6)=63.0D0/8.0D0
    D(6,5)=0.0D0
    D(6,4)=-70.0D0/8.0D0
    D(6,2)=15.0D0/8.0D0
    D(7,7)=231.0D0/16.0D0
    D(7,5)=-315.0D0/16.0D0
    D(7,3)=105.0D0/16.0D0
    D(7,1)=-5.0D0/16.0D0
    D(8,8)=429.0D0/16.0D0
    D(8,6)=-693.0D0/16.0D0
    D(8,4)=315.0D0/16.0D0
    D(8,2)=-35.0D0/16.0D0
    D(9,9)=6435.0D0/128.0D0
    D(9,7)=-12012.0D0/128.0D0
    D(9,5)=6930.0D0/128.0D0
    D(9,3)=-1260.0D0/128.0D0
    D(9,1)=35.0D0/128.0D0
    D(10,10)=12155.0D0/128.0D0
    D(10,8)=-25740.0D0/128.0D0
    D(10,6)=18018.0D0/128.0D0
    D(10,4)=-4620.0D0/128.0D0
    D(10,2)=315.0D0/128.0D0
    D(11,11)=46189.0D0/256.0D0
    D(11,9)=-109395.0D0/256.0D0
    D(11,7)=90090.0D0/256.0D0
    D(11,5)=-30030.0D0/256.0D0
```

TABLE B-1 (continued)

```
      D(11,3)=3465.0D0/256.0D0
      D(11,1)=-63.0D0/256.0D0
652   DO700II=1,K
      J=K-II+1
      VARA=0.0
      III=K-J
      IF(III)702,701,702
702   DO703JJ=1,III
      JK=K-JJ+1
703   VARA=VARA+D(JK,J)*BM(K,JK)
701   BM(K,J)=(A(K,J)-VARA)/D(J,J)
      IF(K-2)700,704,700
704   BM(1,1)=A(1,1)/D(1,1)
700   CONTINUE
705   DO708I=1,K
      C(I)=0.0
      SC(I)=0.0
      DO707J=1,K
      C(I)=C(I)+BM(J,I)*T(J)
707   SC(I)=SC(I)+(BM(J,I)*ST(J))**2
708   SC(I)=SQRT(SC(I))
183   CONTINUE
192   WRITE(6,600)
      WRITE(6,1) (I,B(I),SB(I),I=1,K)
185   WRITE(6,186) SIGMA,FLEV,SUMEV2
      WRITE(6,601) (I,T(I),ST(I),I=1,K)
      IF(LP)187,670,187
187   WRITE(6,188)
      WRITE(6,602) (I,C(I),SC(I),I=1,K)
670   WRITE(6,2)
      WRITE(6,603) (I,X(I),F2(I),Y(I),DELY(I),W(I),I=1,M)
190   CONTINUE
211   IF(ISW) 210,220,210
210   DO215I=2,KM
215   WRITE(6,5) I,(A(I,J),J=1,I)
220   KM=KM-1
      RETURN
    1 FORMAT(3H B(0PI2,2H)=1PE15.7,6H ERRB=E10.3,3H B(0PI2,2H)=1PE15.7,
     16H ERRB=E10.3,3H B(0PI2,2H)=1PE15.7,6H ERRB=E10.3)
    2 FORMAT(4H0  I 11X 4HX(I) 12X4HF(I)12X4HY(I)12X7HDELY(I)10X4HW(I)/)
    5 FORMAT(36H0 ORTHOGONAL POLYNOMIAL COEFF FOR K=I5//(1P8E15.6))
186   FORMAT(7H0SIGMA=1PE16.7,9H F LEVEL=1PE16.7,12H SUM SQ DEV=,1PE16.7
     *                      //  45H COEFFICIENTS OF Y=T1*P1+T2*P2+ETC AND
     1 ERRORS/)
188   FORMAT(23H0  LEGENDRE POLYNOMIALS/45H COEFFICIENTS OF Y=C1*L1+C2*L
```

TABLE B-1 (continued)

```
   12+ETC AND ERRORS/)
600 FORMAT(41H1COEFFICIENTS OF Y=B1+B2*X+ETC AND ERRORS/)
601 FORMAT(3H T(I2,2H)=1PE15.7,6H ERRT=E10.3,3H T(0PI2,2H)=1PE15.7,6H
   1ERRT=E10.3,3H T(0PI2,2H)=1PE15.7,6H ERRT=E10.3)
602 FORMAT(3H C(I2,2H)=1PE15.7,6H ERRC=E10.3,3H C(0PI2,2H)=1PE15.7,6H
   1ERRC=E10.3,3H C(0PI2,2H)=1PE15.7,6H ERRC=E10.3)
603 FORMAT(I6,1P5E16.7)
    END
    REAL FUNCTION POLYE1*8(X,K,B)
    REAL*8 X,B,S
    DIMENSION B(30)
 10 S=B(K)
    KK=K-1
 20 DO 40 I=1,KK
 30 IK=K-I
 40 S=X*S+B(IK)
    POLYE1=S
    RETURN
     END



    SUBROUTINE POLRET(N,C,R,VAL)
    REAL*8 C,R,V
    DIMENSION C(1),R(1),V(100),VAL(1)
    DO 1 I=1,N
    V(I)=C(1)+C(2)*R(I)+C(3)*R(I)**2+C(4)*R(I)**3+C(5)*R(I)**4
    VAL(I)=V(I)
  1 CONTINUE
    RETURN
    END



    SUBROUTINE NISRE(PT,TT,WDES,ALPH,R,VAL,FARB,ACC,SPEED,V,VA,VU,W,WA
   1,WU,BETA,WCALC,BKG,ZACH ,WMACH,U,T,P,IN,M,RGAS,GAM,N)
    DIMENSION PT(1),TT(1),ALPH(1),R(1),V(1),VA(1),VU(1),W(1),WA(1),WU(
   11),BETA(1), ZACH(1),WMACH(1),U(1),TANAL(100),EE(100),GRHO(100),P(1
   2),T(1)
    IN=0
    IP=0
```

TABLE B-1 (continued)

```
      G=32.16
      GAM1=1./(GAM-1.)
      GAM2=(GAM-1.)/(2.*GAM)
      GAM3=GAM*GAM1
      BKSF=BKG*2.*3.1416
      DO 400 I=1,N
      ALP=ALPH(I)/57.296
      TANAL(I)=TAN(ALP)
      U(I)=3.1416/360.*SPEED*R(I)
  400 CONTINUE
      MP1=M+1
      DO 401 I=MP1,N
  401 EF(I)=ALOG((TT(I)/TT(I-1))**GAM3/(PT(I)/PT(I-1)))
      MM1=M-1
      DO 430 I=1,MM1
  430 EF(I)=ALOG((TT(I)/TT(I+1))**GAM3/(PT(I)/PT(I+1)))
      EF(M)=0.
      FIRST=0.
      KOUNT=0
      VA(M)=VA1
  402 VU(M)=VA(M)*TANAL(M)
      VF=VA(M)**2+VU(M)**2
      V(M)=SQRT(VF)
      GRHO(M)=(PT(M)/(RGAS*TT(M)))*(1.-GAM2*VF/(G*RGAS*TT(M)))**GAM1
      ZACH(M)= SQRT(VF/(GAM*G*RGAS*(TT(M)-(GAM2*VF/(G*RGAS)))))
      RAKM=GRHO(M)*VA(M)*R(M)/12.
      RAK1=RAKM
C     END OF MEAN LINE CALCULATIONS
      TOTAR=0.
      DO 403 I=MP1,N
      F=EF(I)
      TERM1=2.*G*RGAS*GAM3*(TT(I)-TT(I-1))
      TERM2=F*G*RGAS*(TT(I)+TT(I-1))
      TERM3=VA(I-1)**2*(F*GAM2+1.)
      TERM4=VU(I-1)**2*(F*GAM2+2.-R(I)/R(I-1))
      SUM1=TERM1-TERM2+TERM3+TERM4
      TERM5=1.-F*GAM2
      TERM6=TANAL(I)**2*(2.-R(I-1)/R(I)-F*GAM2)
      SUM2=TERM5+TERM6
      VASQ=SUM1/SUM2
      VA(I)=SQRT(VASQ)
      VFN=VA(I)**2*(1.+TANAL(I)**2)
      VU(I) =VA(I)*TANAL(I)
      V(I)=SQRT(VFN)
      GRHO(I)=(PT(I)/(RGAS*TT(I)))*(1.-GAM2*VFN/(G*RGAS*TT(I)))**GAM1
```

TABLE B-1 (continued)

```
      ZACH(I)=SQRT(VFN/(GAM*G*RGAS*(TT(I)-(GAM2*VFN/(G*RGAS)))))
      DELTR=(R(I)-R(I-1))/12.
      RAK2=GRHO(I)*VA(I)*R(I)/12.
      SEGAR=(RAK1+RAK2)*DELTR*.5
      TOTAR=TOTAR+SEGAR
      RAK1=RAK2
  403 CONTINUE
      RAK1=RAKM
      I=M-1
  431 F=EF(I)
      TERM1=2.*G*RGAS*GAM3*(TT(I)-TT(I+1))
      TERM2=F*G*RGAS*(TT(I)+TT(I+1))
      TERM3=VA(I+1)**2*(F*GAM2+1.)
      TERM4=VU(I+1)**2*(F*GAM2+2.-R(I)/R(I+1))
      SUM1=TERM1-TERM2+TERM3+TERM4
      TERM5=1.-F*GAM2
      TERM6=TANAL(I)**2*(2.-R(I+1)/R(I)-F*GAM2)
      SUM2=TERM5+TERM6
      VASQ=SUM1/SUM2
      VA(I)=SQRT(VASQ)
      VFN=VA(I)**2*(1.+TANAL(I)**2)
      VU(I) =VA(I)*TANAL(I)
      V(I)=SQRT(VFN)
      GRHO(I)=(PT(I)/(RGAS*TT(I)))*(1.-GAM2*VFN/(G*RGAS*TT(I)))**GAM1
      ZACH(I)=SQRT(VFN/(GAM*G*RGAS*(TT(I)-(GAM2*VFN/(G*RGAS)))))
      DELTR=(R(I+1)-R(I))/12.
      RAK2=GRHO(I)*VA(I)*R(I)/12.
      SEGAR=(RAK1+RAK2)*DELTR*.5
      TOTAR=TOTAR+SEGAR
      RAK1=RAK2
      IF(I.EQ.1)GO TO 432
      I=I-1
      GO TO 431
  432 WCALC=BKSF*TOTAR
      IF(IP)415,404,415
  404 IF(FIRST)406,405,406
  405 VZN1=VA(M)
      WN1=WCALC
      TOTAR=0.
      FIRST=1.
      VA(M)=VA(M)*FARB
      GO TO 402
  406 VZN2=VA(M)
      DELVZ=VZN2-VZN1
      WN2=WCALC
```

TABLE B-1 (continued)

```
      DELWC=WN2-WN1
      IF(DELWC)409,407,409
  407 IN=1
      WRITE(6,408)
  408 FORMAT(' DESIRED FLOW RATE IS NOT HIGH ENOUGH FOR NISRES STATOR SO
     1LUTION-PROGRAM STOPPED')
      GO TO 421
  409 DELWD=WDES-WN2
      VA(M)=(DELWD*DELVZ/DELWC)+VZN2
      IF(VA(M))410,411,411
  410 VA(M)=0.0
  411 CONTINUE
      RATIO=(WCALC/WDES)-1.
      RATIO=ABS(RATIO)
      IF(ACC-RATIO)412,419,419
  412 VZN1=VZN2
      WN1=WN2
      TOTAR=0.
      KOUNT=KOUNT+1
      IF(20-KOUNT)413,402,402
  413 IN=1
      WRITE(6,414)
  414 FORMAT('NO SOLUTION TO NISRE STATOR FLOW RATE TO ACC. REQUIRED IN
     1 20 ITERATIONS-PROGRAM STOPPED')
      GO TO 421
  415 K=1
  420 DO 418 I=1,N
      WSQ=(VU(I)-U(I))**2+VA(I)**2
      W(I)=SQRT(WSQ)
      WA(I)=VA(I)
      WU(I)=VU(I)-U(I)
      BETA(I)=ARSIN((VU(I)-U(I))/W(I))
      BETA(I)=BETA(I)*57.296
      IF(ABS(BETA(I))-180.)417,417,416
  416 BETA(I)=BETA(I)-360.
  417 CONTINUE
      T(I)=TT(I)-V(I)**2/(2.*G*RGAS*GAM3)
      P(I)=GRHO(I)*RGAS*T(I)
      AS=SQRT(GAM*G*RGAS*T(I))
      WMACH(I)=W(I)/AS
  418 CONTINUE
      GO TO (404,421),K
  419 K=2
      GO TO 420
  421 CONTINUE
```

TABLE B-1 (continued)

```
      RETURN
      END



      SUBROUTINE PITOT(PM,QM,RGAS,GAM,ALPHA,BETA,TT,T,V,VA,VU,W,WA,WU,VM
     1ACH,WMACH,U,MD,SPEED,R)
      DIMENSION PM(1),QM(1),ALPHA(1),BETA(1),TT(1),T(1),V(1),VA(1),VU(1)
     1,W(1),WA(1),WU(1),VMACH(1),WMACH(1),U(1),R(1)
      G=32.17
      DO 3 I=1,MD
      ALP=ALPHA(I)/57.296
      ALSIN=SIN(ALP)
      ALCOS=COS(ALP)
      VSQ=2.*G*RGAS*QM(I)*TT(I)/(PM(I)+(GAM-1.)/GAM*QM(I))
      V(I)=SQRT(VSQ)
      T(I)=TT(I)-VSQ/(2.*G*(GAM/(GAM-1.))*RGAS)
      VA(I)=V(I)*ALCOS
      VU(I)=V(I)*ALSIN
      AS=SQRT(GAM*G*RGAS*T(I))
      VMACH(I)=V(I)/AS
      U(I)=3.1416/360.*SPEED*R(I)
      WSQ=(VU(I)-U(I))**2+VA(I)**2
      W(I)=SQRT(WSQ)
      BETA(I)=ARSIN((VU(I)-U(I))/W(I))
      BETA(I)=BETA(I)*57.296
      IF(ABS(BETA(I))-180.)1,1,2
    2 BETA(I)=BETA(I)-360.
    1 CONTINUE
      WA(I)=VA(I)
      WU(I)=VU(I)-U(I)
      WMACH(I)=W(I)/AS
    3 CONTINUE
      RETURN
      END



      SUBROUTINE HOTWIR(NREF,VR,GAM,RGAS,SPEED,ALPHA,V,VA,VU,T,VMACH,U,W
     1,WA,WU,WMACH,BETA,MD,R,TT,P,PT)
      DIMENSION VR(1),ALPHA(1),V(1),VA(1),VU(1),T(1),VMACH(1),U(1),W(1),
```

TABLE B-1 (continued)

```
     1WA(1),WU(1),WMACH(1),BETA(1),R(1),TT(1),P(1),PT(1)
      GAM2=(GAM-1.)/(2.*GAM)
      VREF=V(NREF)
      G=32.17
      DO 3 I=1,MD
      ALP=ALPHA(I)/57.296
      ALSIN=SIN(ALP)
      ALCOS=COS(ALP)
      V(I)=VR(I)*VREF/.9
      VF=V(I)**2
      GRHO=(PT(I)/(RGAS*TT(I)))*(1.-GAM2*VF/(G*RGAS*TT(I)))**(1./(GAM-1.
     1))
      VA(I)=V(I)*ALCOS
      VU(I)=V(I)*ALSIN
      T(I)=TT(I)-V(I)**2/(2.*G*(GAM/(GAM-1.))*RGAS)
      P(I)=GRHO*RGAS*T(I)
      AS=SQRT(GAM*G*RGAS*T(I))
      VMACH(I)=V(I)/AS
      U(I)=3.1416/360.*SPEED*R(I)
      WSQ=(VU(I)-U(I))**2+VA(I)**2
      W(I)=SQRT(WSQ)
      BETA(I)=ARSIN((VU(I)-U(I))/W(I))
      BETA(I)=BETA(I)*57.296
      IF(ABS(BETA(I))-180.)1,1,2
    2 BETA(I)=BETA(I)-360.
    1 CONTINUE
      WA(I)=VA(I)
      WU(I)=VU(I)-U(I)
      WMACH(I)=W(I)/AS
    3 CONTINUE
      RETURN
      END



      SUBROUTINE OUTPUT(PT,P,TT,T,V,VA,VU,VMACH,W,WA,WU,WMACH,R,U,ALPHA,
     1BETA,WDES,BKG,RPM,IRUN,PAMB,TI,MM,NP,NS)
      DIMENSION PT(1),P(1),TT(1),T(1),V(1),VA(1),VU(1),VMACH(1),W(1),WA(
     11),WU(1),WMACH(1),R(1),U(1),ALPHA(1),BETA(1)
      WRITE(6,1)
    1 FORMAT(1H1,50X' NAVAL POSTGRADUATE SCHOOL'/54X' MONTEREY, CALIFORN
     1IA'//)
      GO TO (2,3,4),MM
```

TABLE B-1 (continued)

```
    2 WRITE(6,5)
    5 FORMAT(28X' RADIAL FLUID CONDITIONS BASED ON NON-ISENTROPIC RADIAL
     1 EQUILIBRIUM EQUATION'/28X' WITH INPUT OF TOTAL TEMPERATURE, TOTAL
     1 PRESSURE, ALPHA AND MASS FLOW RATE'/)
      WRITE(6,6)BKG
    6 FORMAT(' ASSUMED BLOCKAGE FACTOR='F5.4/)
      GO TO 9
    3 WRITE(6,7)
    7 FORMAT(39X' RADIAL FLUID CONDITIONS BASED ON HOT WIRE INFORMATION'
     1/37X' WITH INPUT OF TOTAL TEMPERATURE, TOTAL PRESSURE AND ALPHA'/)
      GO TO 9
    4 WRITE(6,8)
    8 FORMAT(37X' RADIAL FLUID CONDITIONS BASED ON PITOT STATIC INFORMAT
     1ION'/45X' WITH INPUT OF TOTAL TEMPERATURE AND ALPHA'/)
    9 WRITE(6,10)IRUN,RPM,WDES,PAMB,TI,NS
   10 FORMAT(' RUN NUMBER 'I3,F10.1' RPM   MASS FLOW RATE='F10.4' LBM/SE
     1C'/' BAROMETRIC PRESSURE='F10.4'PSFA  INLET TEMPERATURE='F10.4' DE
     2G-F'/' DOWNSTREAM OF ROTOR NUMBER 'I2//)
      WRITE(6,11)
   11 FORMAT(' RADIUS(IN)  PT(PSFA)   P(PSFA)  TT(DEG-R)      T         V
     1        VA         VU         VMACH       W         WA         WU
     2  WMACH'/)
      WRITE(6,12)(R(I),PT(I),P(I),TT(I),T(I),V(I),VA(I),VU(I),VMACH(I),W
     1(I),WA(I),WU(I),WMACH(I),I=1,NP)
   12 FORMAT(F6.2,8X,F8.3,2X,F8.3,2X,F8.3,2X,F8.3,2X,F8.3,2X,F8.3,2X,F8.
     13,2X,F8.3,2X,F8.3,2X,F8.3,2X,F8.3,2X,F8.3)
      WRITE(6,13)
   13 FORMAT(/' RADIUS(IN) ALPHA    BETA        U'/)
      WRITE(6,14)(R(I),ALPHA(I),BETA(I),U(I),I=1,NP)
   14 FORMAT(F6.2,2X,F8.3,2X,F8.3,2X,F8.3)
      WRITE(6,15)
   15 FORMAT(1H1)
      CONTINUE
      RETURN
      END



      SUBROUTINE NONDIM(PT,P,TT,T,V,VA,VU,VMACH,W,WA,WU,WMACH,R,U,ALPHA,
     1BETA,PBAR,TI,NP,IRUN)
      DIMENSION PT(1),P(1),TT(1),T(1),V(1),VA(1),VU(1),VMACH(1),W(1),WA(
     11),WU(1),WMACH(1),R(1),U(1),ALPHA(1),BETA(1),PTR(100),PR(100),TTR(
     2100),TR(100),VR(100),VAR(100),VUR(100),WR(100),WAR(100),WUR(100),R
```

TABLE B-1 (continued)

```
     3R(100),UR(100)
      Z=R(NP)
      A=U(NP)
      B=PBAR
      C=TI+459.7
      D=B/(32.16*53.35*C)*A**2
      DO 1 I=1,NP
      PTR(I)=(PT(I)-B)/D
      PR(I)=(P(I)-B)/D
      TTR(I)=TT(I)/C
      TR(I)=T(I)/C
      VR(I)=V(I)/A
      VAR(I)=VA(I)/A
      VUR(I)=VU(I)/A
      WR(I)=W(I)/A
      WAR(I)=VAR(I)
      WUR(I)=WU(I)/A
      UR(I)=U(I)/A
      RR(I)=R(I)/Z
    1 CONTINUE
      SUM=0.
      DO 2 I=1,NP
      SUM=SUM+VAR(I)
    2 CONTINUE
      PN=NP
      PHIAV=SUM/PN
      WRITE(6,3)IRUN
    3 FORMAT(//' NON-DIMENSIONALIZED FLUID CONDITIONS FOR RUN NUMBER'I3/
     1' ALL VELOCITIES REFERRED TO PERIPHERAL TIP VELOCITY  '/' PRESSURE
     2S REFERRED TO RHO*UT**2        '/' TEMPERATURES REFERRED TO INLET T
     3EMPERATURE'//)
      WRITE(6,4)
    4 FORMAT(' R/RO  DPT/RHO*UT*2 DP/RHO*UT*2  TT/TI       T/TI       V/UT
     1    VA/UT      VU/UT       W/UT      WA/UT      WU/UT       ALPHA      BE
     2TA '//)
      WRITE(6,5)(RR(I),PTR(I),PR(I),TTR(I),TR(I),VR(I),VAR(I),VUR(I),WR(
     1I),WAR(I),WUR(I),ALPHA(I),BETA(I),I=1,NP)
    5 FORMAT(F7.4,3X,F7.4,3X,F7.4,3X,F7.4,3X,F7.4,3X,F7.4,3X,F7.4,3X,F7.4,3X,F7.
     14,3X,F7.4,3X,F7.4,3X,F7.4,3X,F7.3,3X,F7.3)
      WRITE(6,6)PHIAV
    6 FORMAT(//' AVERAGE AXIAL VELOCITY COEFFICIENT VA/UT='F7.4)
      WRITE(6,7)
    7 FORMAT(1H1)
      RETURN
      END
```

TABLE B-2 SAMPLE OF ACCURACY OF POLYNOMIAL FIT OF MEASURED DATA

COEFFICIENTS OF Y=B1+B2*X+ETC AND ERRORS

B(1)= 1.1893155D 03 ERRB= 2.256E 02 B(2)= 2.4811451D 02 ERRB= 6.383E 01 B(3)= -2.86022000 01 ERRB= 6.713E 00
B(4)= 1.3478942D 00 ERRB= 3.111E-01 B(5)= -2.3671961D-02 ERRB= 5.361E-03 B(

SIGMA= 2.9211050E-01 F LEVEL= 1.2992601F 00 SUM SQ DEV= 5.6P85738E-02

COEFFICIENTS OF Y=T1*P1+T2*P2+ETC AND ERRORS

T(1)= 2.1260333D 03 ERRT= 7.542E-02 T(2)= -4.2136928D-02 ERRT= 3.491E-02 T(3)= -1.1081578D-01 ERRT= 1.819E-02
T(4)= -2.5079506D-02 ERRT= 9.764E-03 T(5)= -2.3671961D-02 ERRT= 5.361E-03 T(

I	X(I)	F(I)	Y(I)	DELY(I)	W(I)
1	1.1000000D 01	2.1253596D 03	2.1251750D 03	-1.8460393E-01	1.0000000E 00
2	1.1500000D 01	2.1256658D 03	2.1259460D 03	2.8027272E-01	1.0000000E 00
3	1.2000000D 01	2.1262778D 03	2.1262723D 03	-5.4926053E-03	1.0000000E 00
4	1.2500000D 01	2.1262778D 03	2.1263304D 03	5.2552789E-02	1.0000000E 00
5	1.3000000D 01	2.1262778D 03	2.1262612D 03	-1.6675498E-02	1.0000000E 00
6	1.3500000D 01	2.1262778D 03	2.1261701D 03	-1.0770929E-01	1.0000000E 00
7	1.4000000D 01	2.1262778D 03	2.1261272D 03	-1.5058839E-01	1.0000000E 00
8	1.4500000D 01	2.1262778D 03	2.1261670D 03	-1.1086053E-01	1.0000000E 00
9	1.5000000D 01	2.1262778D 03	2.1262883D 03	1.0418546E-02	1.0000000E 00
10	1.5500000D 01	2.1262778D 03	2.1264545D 03	1.7668557E-01	1.0000000E 00
11	1.6000000D 01	2.1263816D 03	2.1265937D 03	2.1210891E-01	1.0000000E 00
12	1.6500000D 01	2.1264851D 03	2.1265982D 03	1.1311305E-01	1.0000000E 00
13	1.7000000D 01	2.1262778D 03	2.1263250D 03	4.7157567E-02	1.0000000E 00
14	1.7500000D 01	2.1262778D 03	2.1255954D 03	-6.8241942E-01	1.0000000E 00
15	1.8000000D 01	2.1238293D 03	2.1241954D 03	3.6604041E-01	1.0000000E 00

ORTHOGONAL POLYNOMIAL COEFF FOR K= 2

-1.4500000D 01 1.0000CCD 00

ORTHOGONAL POLYNOMIAL COEFF FOR K= 3

2.055833D 02 -2.900000D 01 1.00000CD 00

ORTHOGONAL POLYNOMIAL COEFF FOR K= 4

-2.927550D 03 6.224000D 02 -4.35000CD 01 1.000000D 00

ORTHOGONAL POLYNOMIAL COEFF FOR K= 5

4.173581D 04 -1.185168D 04 1.249679D 03 -5.800000D 01 1.0000000 00

TABLE B-3 SAMPLE OF DIMENSIONAL COMPUTER OUTPUT FOR NISRE PORTION OF PROGRAM FLOW

NAVAL POSTGRADUATE SCHOOL
MONTEREY, CALIFORNIA

RADIAL FLUID CONDITIONS BASED ON NON-ISENTROPIC RADIAL EQUILIBRIUM EQUATION
WITH INPUT OF TOTAL TEMPERATURE, TOTAL PRESSURE, ALPHA AND MASS FLOW RATE

ASSUMED BLOCKAGE FACTOR=.9600

RUN NUMBER 35 1193.0 RPM MASS FLOW RATE= 26.1730 LBM/SEC
BAROMETRIC PRESSURE= 2114.4355PSFA INLET TEMPERATURE= 77.9000 DEG-F
DOWNSTREAM OF ROTOR NUMBER 1

RADIUS(IN)	PT(PSFA)	P(PSFA)	TT(DEG-R)	T	V	VA	VU	VMACH	W	WA	WU	WMACH
10.80	2124.696	2107.762	544.295	543.052	122.178	73.400	97.672	0.107	74.871	73.400	-14.755	0.066
10.87	2124.878	2107.903	544.152	542.907	122.302	74.839	96.731	0.107	76.624	74.839	-16.443	0.067
11.12	2125.409	2108.375	543.730	542.481	122.453	78.893	93.652	0.107	81.931	78.893	-22.107	0.072
11.37	2125.793	2108.806	543.413	542.169	122.234	81.644	90.969	0.107	86.117	81.644	-27.376	0.075
11.62	2126.054	2109.203	543.185	541.951	121.712	83.371	88.673	0.107	89.393	83.371	-32.255	0.078
11.86	2126.217	2109.578	543.031	541.813	120.915	84.290	86.692	0.106	91.982	84.290	-36.822	0.081
12.11	2126.303	2109.929	542.935	541.737	119.935	84.633	84.980	0.105	94.093	84.633	-41.118	0.082
12.36	2126.332	2110.257	542.886	541.710	118.825	84.579	83.461	0.104	95.909	84.579	-45.222	0.084
12.61	2126.322	2110.576	542.871	541.719	117.605	84.259	82.045	0.103	97.583	84.259	-49.223	0.086
12.86	2126.287	2110.868	542.880	541.752	116.373	83.839	80.706	0.102	99.264	83.839	-53.145	0.087
13.11	2126.241	2111.145	542.903	541.799	115.147	83.407	79.386	0.101	101.052	83.407	-57.052	0.089
13.35	2126.194	2111.406	542.933	541.851	113.964	83.046	78.045	0.100	103.029	83.046	-60.978	0.090
13.60	2126.156	2111.655	542.963	541.902	112.853	82.819	76.660	0.099	105.248	82.819	-64.947	0.092
13.85	2126.132	2111.892	542.986	541.945	111.839	82.765	75.219	0.098	107.738	82.765	-68.973	0.094
14.10	2126.128	2112.115	543.000	541.975	110.940	82.907	73.717	0.097	110.505	82.907	-73.060	0.097
14.35	2126.145	2112.328	543.001	541.991	110.161	83.241	72.155	0.097	113.534	83.241	-77.207	0.100
14.59	2126.184	2112.530	542.988	541.989	109.506	83.753	70.547	0.096	116.792	83.753	-81.399	0.102
14.84	2126.243	2112.723	542.959	541.970	108.965	84.405	68.914	0.096	120.227	84.405	-85.617	0.105
15.09	2126.317	2112.897	542.916	541.934	108.548	85.166	67.302	0.095	123.773	85.166	-89.814	0.108
15.34	2126.400	2113.063	542.860	541.885	108.205	85.946	65.738	0.095	127.340	85.946	-93.962	0.112
15.59	2126.483	2113.218	542.796	541.826	107.908	86.667	64.288	0.095	130.824	86.667	-97.998	0.115
15.84	2126.557	2113.364	542.727	541.763	107.605	87.224	63.014	0.094	134.099	87.224	-101.856	0.118
16.08	2126.607	2113.502	542.659	541.702	107.230	87.490	61.998	0.094	137.024	87.490	-105.457	0.120
16.33	2126.620	2113.635	542.601	541.652	106.731	87.342	61.343	0.094	139.441	87.342	-108.697	0.122
16.58	2126.577	2113.764	542.559	541.623	106.020	86.616	61.139	0.093	141.178	86.616	-111.495	0.124
16.83	2126.460	2113.891	542.543	541.625	105.005	85.129	61.475	0.092	142.065	85.129	-113.734	0.125
17.08	2126.247	2114.014	542.565	541.672	103.590	82.676	62.415	0.091	141.943	82.676	-115.379	0.124
17.33	2125.914	2114.143	542.637	541.777	101.628	78.991	63.943	0.089	140.701	78.991	-116.436	0.123
17.57	2125.436	2114.277	542.771	541.955	98.970	73.791	65.955	0.087	138.333	73.791	-117.909	0.121
18.00	2124.195	2114.523	543.190	542.483	92.191	60.449	69.606	0.081	132.396	60.449	-117.790	0.116

RADIUS(IN)	ALPHA	BETA	U
10.80	53.075	-11.374	112.438
10.87	52.272	-12.392	113.175
11.12	49.889	-15.654	115.759
11.37	48.092	-18.536	118.344
11.62	46.765	-21.151	120.929
11.86	45.805	-23.598	123.514
12.11	45.117	-25.912	126.099
12.36	44.619	-28.133	128.683
12.61	44.237	-30.293	131.268
12.86	43.910	-32.371	133.853
13.11	43.585	-34.373	136.438
13.35	43.222	-36.288	139.022
13.60	42.789	-38.104	141.607
13.85	42.265	-39.807	144.192
14.10	41.642	-41.388	146.777
14.35	40.919	-42.846	149.362
14.59	40.108	-44.183	151.946
14.84	39.230	-45.409	154.531
15.09	38.318	-46.522	157.116
15.34	37.412	-47.551	159.701
15.59	36.567	-48.511	162.286
15.84	35.846	-49.425	164.870
16.08	35.323	-50.320	167.455
16.33	35.082	-51.217	170.040
16.58	35.217	-52.156	172.624
16.83	35.835	-53.186	175.209
17.08	37.050	-54.376	177.794
17.33	38.990	-55.847	180.379
17.57	41.791	-57.763	182.964
18.00	49.028	-62.834	187.396

TABLE B-4 SAMPLE OF NON-DIMENSIONAL COMPUTER OUTPUT FOR NISRE PORTION OF PROGRAM FLOW

NON-DIMENSIONALIZED FLUID CONDITIONS FOR RUN NUMBER 35
ALL VELOCITIES REFERRED TO PERIPHERAL TIP VELOCITY
PRESSURES REFERRED TO RHO*UT**2
TEMPERATURES REFERRED TO INLET TEMPERATURE

R/RO	DPT/RHO*UT**2	OP/RHO*UT**2	TT/TI	T/TI	V/UT	VA/UT	VU/UT	W/UT	WA/UT	WU/UT	ALPHA	BETA
0.6000	0.1275	-0.0829	1.0125	1.0101	0.4520	0.3917	0.5212	0.3995	0.3917	-0.0788	53.075	-11.374
0.6039	0.1297	-0.0811	1.0122	1.0099	0.4526	0.3994	0.5162	0.4089	0.3994	-0.0877	52.272	-12.382
0.6177	0.1363	-0.0753	1.0114	1.0091	0.4534	0.4210	0.4998	0.4372	0.4210	-0.1180	49.889	-15.654
0.6315	0.1411	-0.0699	1.0108	1.0085	0.4523	0.4357	0.4854	0.4595	0.4357	-0.1461	48.092	-18.536
0.6453	0.1443	-0.0650	1.0104	1.0081	0.4495	0.4473	0.4732	0.4770	0.4449	-0.1721	46.765	-21.151
0.6591	0.1463	-0.0603	1.0101	1.0078	0.4452	0.4498	0.4626	0.4908	0.4498	-0.1965	45.805	-23.508
0.6729	0.1474	-0.0560	1.0099	1.0077	0.4400	0.4516	0.4535	0.5021	0.4516	-0.2194	45.117	-25.612
0.6867	0.1478	-0.0519	1.0098	1.0076	0.4341	0.4513	0.4454	0.5118	0.4513	-0.2413	44.619	-28.133
0.7005	0.1477	-0.0479	1.0098	1.0077	0.4276	0.4496	0.4378	0.5207	0.4496	-0.2627	44.237	-30.293
0.7143	0.1472	-0.0443	1.0098	1.0077	0.4210	0.4474	0.4307	0.5297	0.4474	-0.2836	43.910	-32.371
0.7281	0.1466	-0.0409	1.0099	1.0078	0.4145	0.4451	0.4236	0.5392	0.4451	-0.3044	43.585	-34.373
0.7419	0.1461	-0.0376	1.0099	1.0079	0.4081	0.4432	0.4165	0.5498	0.4432	-0.3254	43.222	-36.288
0.7557	0.1456	-0.0345	1.0100	1.0080	0.4022	0.4419	0.4091	0.5616	0.4419	-0.3466	42.789	-38.104
0.7694	0.1453	-0.0316	1.0100	1.0081	0.3968	0.4417	0.4014	0.5749	0.4417	-0.3681	42.265	-39.807
0.7832	0.1452	-0.0288	1.0100	1.0081	0.3920	0.4424	0.3934	0.5897	0.4424	-0.3899	41.642	-41.398
0.7970	0.1455	-0.0262	1.0100	1.0082	0.3878	0.4442	0.3850	0.6058	0.4442	-0.4120	40.919	-42.846
0.8108	0.1459	-0.0237	1.0100	1.0082	0.3844	0.4469	0.3765	0.6232	0.4469	-0.4344	40.108	-44.183
0.8246	0.1467	-0.0213	1.0100	1.0081	0.3815	0.4504	0.3677	0.6416	0.4504	-0.4569	39.230	-45.409
0.8384	0.1476	-0.0191	1.0099	1.0081	0.3792	0.4545	0.3591	0.6605	0.4545	-0.4793	38.318	-46.522
0.8522	0.1486	-0.0170	1.0098	1.0080	0.3774	0.4586	0.3508	0.6795	0.4586	-0.5014	37.412	-47.551
0.8660	0.1497	-0.0151	1.0097	1.0079	0.3758	0.4625	0.3431	0.6981	0.4625	-0.5229	36.567	-48.511
0.8798	0.1506	-0.0133	1.0095	1.0077	0.3742	0.4655	0.3363	0.7155	0.4655	-0.5435	35.846	-49.425
0.8936	0.1512	-0.0116	1.0094	1.0076	0.3722	0.4669	0.3308	0.7312	0.4669	-0.5627	35.323	-50.320
0.9074	0.1514	-0.0099	1.0093	1.0075	0.3695	0.4661	0.3273	0.7441	0.4661	-0.5800	35.082	-51.217
0.9212	0.1508	-0.0083	1.0092	1.0075	0.3658	0.4622	0.3263	0.7534	0.4622	-0.5949	35.217	-52.156
0.9350	0.1494	-0.0068	1.0092	1.0075	0.3603	0.4543	0.3280	0.7581	0.4543	-0.6069	35.835	-53.186
0.9488	0.1467	-0.0052	1.0092	1.0076	0.3528	0.4412	0.3331	0.7574	0.4412	-0.6157	37.050	-54.376
0.9626	0.1426	-0.0036	1.0094	1.0078	0.3423	0.4215	0.3412	0.7508	0.4215	-0.6213	38.930	-55.847
0.9763	0.1366	-0.0020	1.0096	1.0081	0.3281	0.3938	0.3520	0.7382	0.3938	-0.6244	41.791	-57.763
1.0000	0.1212	0.0011	1.0104	1.0091	0.2920	0.3226	0.3714	0.7065	0.3226	-0.6286	49.029	-62.834

AVERAGE AXIAL VELOCITY COEFFICIENT VA/UT= 0.4389

TABLE B-5 SAMPLE OF DIMENSIONAL COMPUTER OUTPUT FOR FLOW PROBE PORTION OF PROGRAM FLOW

NAVAL POSTGRADUATE SCHOOL
MONTEREY, CALIFORNIA

RADIAL FLUID CONDITIONS BASED ON PITOT STATIC INFORMATION
WITH INPUT OF TOTAL TEMPERATURE AND ALPHA

RUN NUMBER 35 1193.0 RPM MASS FLOW RATE= 26.1730 LBM/SEC
BAROMETRIC PRESSURE= 2114.4355PSFA INLET TEMPERATURE= 77.9000 DEG-F
DOWNSTREAM OF ROTOR NUMBER 1

RADIUS(IN)	PT(PSFA)	P(PSFA)	TT(DEG-R)	T	V	VA	VU	VMACH	W	WA	WU	WMACH
11.00	2125.360	2107.776	544.143	542.849	124.679	77.735	97.439	0.109	79.638	77.785	-17.091	0.070
11.50	2125.666	2108.415	542.939	541.672	123.338	85.446	88.946	0.108	90.820	85.446	-30.780	0.080
12.00	2126.278	2109.027	543.706	541.440	123.294	85.956	88.390	0.108	93.401	85.956	-36.541	0.082
12.50	2126.278	2109.915	543.250	542.048	120.122	84.791	85.087	0.105	96.015	84.791	-45.050	0.084
13.00	2126.278	2110.695	543.133	541.990	117.195	84.657	81.041	0.103	100.575	84.657	-54.300	0.088
13.50	2126.278	2110.916	542.822	541.696	116.325	85.075	79.333	0.102	104.809	85.075	-61.214	0.092
14.00	2126.278	2111.696	542.822	541.753	113.317	84.870	75.086	0.099	110.439	84.870	-70.667	0.097
14.50	2126.278	2111.922	543.250	542.196	112.475	86.287	72.147	0.099	116.862	86.287	-78.811	0.102
15.00	2126.278	2112.143	542.783	541.747	111.556	87.062	69.749	0.098	122.667	87.062	-86.414	0.108
15.50	2126.278	2112.363	542.667	541.647	110.666	87.915	67.216	0.097	128.817	87.915	-94.153	0.113
16.00	2126.382	2112.693	542.706	541.703	109.760	89.469	63.582	0.096	136.426	89.469	-102.993	0.120
16.50	2126.485	2113.351	542.628	541.666	107.496	87.731	62.117	0.094	140.438	87.731	-109.663	0.123
17.00	2126.278	2114.257	542.550	541.670	102.815	82.220	61.732	0.090	141.575	82.220	-115.254	0.124
17.50	2126.278	2115.597	542.861	542.079	96.921	74.246	62.299	0.085	141.019	74.246	-119.892	0.124
18.00	2123.829	2115.818	543.094	542.507	83.972	54.647	63.757	0.074	135.177	54.647	-123.639	0.118

RADIUS(IN)	ALPHA	BETA	U
11.00	51.400	-12.385	114.520
11.50	46.150	-19.810	119.725
12.00	45.800	-23.031	124.931
12.50	45.100	-27.982	130.136
13.00	43.750	-32.677	135.342
13.50	43.000	-35.736	140.547
14.00	41.500	-39.782	145.753
14.50	39.900	-42.407	150.958
15.00	38.700	-44.786	156.164
15.50	37.400	-46.963	161.369
16.00	35.400	-49.020	166.575
16.50	35.300	-51.340	171.780
17.00	36.900	-54.497	176.985
17.50	40.000	-58.231	182.191
18.00	49.400	-66.155	187.396

TABLE B-6 SAMPLE OF NON-DIMENSIONAL COMPUTER OUTPUT FOR FLOW PROBE PORTION OF PROGRAM FLOW

NON-DIMENSIONALIZED FLUID CONDITIONS FOR RUN NUMBER 35
ALL VELOCITIES REFERRED TO PERIPHERAL TIP VELOCITY
PRESSURES REFERRED TO RHO*UT**2
TEMPERATURES REFERRED TO INLET TEMPERATURE

R/RO	DPT/RHO*UT**2	DP/RHO*UT**2	TT/TI	T/TI	V/UT	VA/UT	VU/UT	W/UT	WA/UT	WU/UT	ALPHA	BETA
0.6111	0.1357	-0.0827	1.0122	1.0098	0.6653	0.4151	0.5200	0.4250	0.4151	-0.0211	51.400	-12.285
0.6389	0.1395	-0.0748	1.0099	1.0076	0.6582	0.4560	0.4746	0.4846	0.4560	-0.1642	44.150	-19.810
0.6667	0.1471	-0.0672	1.0095	1.0071	0.6579	0.4587	0.4717	0.4984	0.4587	-0.1950	45.900	-23.031
0.6944	0.1471	-0.0562	1.0105	1.0083	0.6610	0.4525	0.4540	0.5124	0.4525	-0.2404	45.100	-27.992
0.7222	0.1471	-0.0465	1.0103	1.0082	0.6254	0.4518	0.4325	0.5367	0.4518	-0.2809	43.750	-32.477
0.7500	0.1471	-0.0437	1.0097	1.0076	0.6207	0.4540	0.4233	0.5593	0.4540	-0.3267	43.000	-35.736
0.7778	0.1471	-0.0340	1.0097	1.0077	0.6047	0.4529	0.4007	0.5893	0.4529	-0.3771	41.500	-39.792
0.8056	0.1471	-0.0312	1.0105	1.0085	0.6002	0.4605	0.3850	0.6236	0.4605	-0.4204	39.900	-42.407
0.8333	0.1471	-0.0285	1.0096	1.0077	0.5953	0.4646	0.3722	0.6546	0.4646	-0.4611	38.700	-44.736
0.8611	0.1471	-0.0257	1.0094	1.0075	0.5905	0.4691	0.3587	0.6874	0.4691	-0.5024	37.400	-46.963
0.8889	0.1484	-0.0216	1.0095	1.0076	0.5857	0.4774	0.3393	0.7280	0.4774	-0.5496	35.400	-49.020
0.9167	0.1497	-0.0135	1.0094	1.0076	0.5736	0.4682	0.3315	0.7494	0.4682	-0.5952	35.300	-51.340
0.9444	0.1471	-0.0022	1.0092	1.0076	0.5486	0.4387	0.3294	0.7555	0.4387	-0.6150	36.900	-54.497
0.9722	0.1471	0.0144	1.0098	1.0083	0.5172	0.3962	0.3324	0.7525	0.3962	-0.6398	40.000	-58.231
1.0000	0.1167	0.0172	1.0102	1.0091	0.4481	0.2916	0.3402	0.7213	0.2915	-0.6598	49.400	-64.156

AVERAGE AXIAL VELOCITY COEFFICIENT VA/UT= 0.4405

TABLE B-7 SAMPLE OF DIMENSIONAL COMPUTER OUTPUT FOR HOT-WIRE PORTION OF PROGRAM FLOW

NAVAL POSTGRADUATE SCHOOL
MONTEREY, CALIFORNIA

RADIAL FLUID CONDITIONS BASED ON HOT WIRE INFORMATION
WITH INPUT OF TOTAL TEMPERATURE, TOTAL PRESSURE AND ALPHA

RUN NUMBER 35 1193.0 RPM MASS FLOW RATE= 26.1730 LBM/SEC
BAROMETRIC PRESSURE= 2114.4355PSFA INLET TEMPERATURE= 77.9000 DEG-F
DOWNSTREAM OF ROTOR NUMBER 1

RADIUS(IN)	PT(PSFA)	P(PSFA)	TT(DEG-R)	T	V	VA	VU	VMACH	W	WA	WU	WMACH
11.00	2125.360	2109.697	544.143	542.994	117.474	73.290	91.808	0.103	76.728	73.290	-22.712	0.067
11.50	2125.666	2109.664	542.939	541.768	118.599	82.162	85.528	0.104	88.895	82.162	-34.108	0.078
12.00	2126.278	2110.699	542.706	541.567	116.974	81.551	83.860	0.103	91.309	81.551	-41.071	0.080
12.50	2126.278	2110.979	543.250	542.130	115.974	81.863	82.149	0.102	94.891	81.863	-47.987	0.083
13.00	2126.278	2111.204	543.133	542.030	115.100	83.144	79.593	0.101	100.104	83.144	-55.749	0.088
13.50	2126.278	2111.229	542.822	541.722	114.975	84.087	78.412	0.101	104.553	84.087	-62.135	0.092
14.00	2126.278	2111.260	542.822	541.724	114.850	86.017	76.101	0.101	110.681	86.017	-69.651	0.097
14.50	2126.278	2111.886	543.250	542.196	112.475	86.287	72.147	0.099	116.862	86.287	-78.811	0.102
15.00	2126.278	2112.535	542.783	541.779	109.851	85.731	68.683	0.096	122.485	85.731	-87.481	0.107
15.50	2126.278	2113.149	542.667	541.707	107.351	85.282	65.202	0.094	128.534	85.282	-96.167	0.113
16.00	2126.382	2113.375	542.706	541.755	106.851	87.098	61.897	0.094	136.174	87.098	-104.678	0.119
16.50	2126.485	2113.658	542.628	541.691	106.102	86.594	61.311	0.093	140.362	86.594	-110.469	0.123
17.00	2126.278	2113.570	542.550	541.622	105.602	84.448	63.405	0.093	141.534	84.448	-113.580	0.124
17.50	2126.278	2114.346	542.861	541.989	102.352	78.407	65.791	0.090	140.345	78.407	-116.400	0.123
18.00	2123.829	2117.343	543.094	542.620	75.483	49.123	57.312	0.066	139.050	49.123	-130.084	0.122

RADIUS(IN)	ALPHA	BETA	U
11.00	51.400	-17.218	114.520
11.50	46.150	-22.598	119.725
12.00	45.800	-26.731	124.931
12.50	45.100	-30.378	130.136
13.00	43.750	-33.843	135.342
13.50	43.000	-36.462	140.547
14.00	41.500	-38.998	145.753
14.50	39.900	-42.408	150.958
15.00	38.700	-45.579	156.164
15.50	37.400	-48.433	161.369
16.00	35.400	-50.238	166.575
16.50	35.300	-51.908	171.780
17.00	36.900	-53.369	176.985
17.50	40.000	-56.036	182.191
18.00	49.400	-69.313	187.396

TABLE B-8 SAMPLE OF NON-DIMENSIONAL COMPUTER OUTPUT FOR HOT-WIRE PORTION OF PROGRAM FLOW

NON-DIMENSIONALIZED FLUID CONDITIONS FOR RUN NUMBER 35
ALL VELOCITIES REFERRED TO PERIPHERAL TIP VELOCITY
PRESSURES REFERRED TO RHO*UT**2
TEMPERATURES REFERRED TO INLET TEMPERATURE

R/RO	DPT/RHO*UT**2	DP/RHO*UT**2	TT/TI	T/TI	V/UT	VA/UT	VU/UT	W/UT	WA/UT	WU/UT	ALPHA	BETA
0.6111	0.1357	-0.0589	1.0122	1.0100	0.6269	0.3911	0.4899	0.4094	0.3911	-0.1212	51.400	-17.218
0.6389	0.1395	-0.0593	1.0099	1.0078	0.6329	0.4384	0.4564	0.4749	0.4384	-0.1835	46.150	-22.598
0.6667	0.1471	-0.0464	1.0095	1.0074	0.6242	0.4352	0.4475	0.4873	0.4352	-0.2192	45.800	-26.731
0.6944	0.1471	-0.0429	1.0105	1.0084	0.6189	0.4368	0.4394	0.5064	0.4368	-0.2561	45.100	-30.378
0.7222	0.1471	-0.0401	1.0103	1.0082	0.6142	0.4437	0.4247	0.5342	0.4437	-0.2975	43.750	-33.843
0.7500	0.1471	-0.0398	1.0097	1.0077	0.6135	0.4487	0.4184	0.5579	0.4487	-0.3316	43.000	-36.462
0.7778	0.1471	-0.0394	1.0097	1.0077	0.6129	0.4590	0.4061	0.5904	0.4590	-0.3717	41.500	-38.998
0.8056	0.1471	-0.0317	1.0105	1.0085	0.6002	0.4605	0.3850	0.6236	0.4605	-0.4206	39.900	-42.408
0.8333	0.1471	-0.0236	1.0096	1.0076	0.5862	0.4575	0.3665	0.6536	0.4575	-0.4668	38.700	-45.579
0.8611	0.1471	-0.0160	1.0094	1.0076	0.5729	0.4551	0.3479	0.6859	0.4551	-0.5132	37.400	-48.433
0.8889	0.1484	-0.0132	1.0095	1.0077	0.5702	0.4648	0.3303	0.7267	0.4648	-0.5586	35.400	-50.238
0.9167	0.1497	-0.0097	1.0094	1.0076	0.5662	0.4621	0.3272	0.7490	0.4621	-0.5895	35.300	-51.908
0.9444	0.1471	-0.0108	1.0092	1.0075	0.5635	0.4506	0.3383	0.7553	0.4506	-0.6041	36.900	-53.369
0.9722	0.1471	-0.0011	1.0098	1.0082	0.5462	0.4184	0.3511	0.7489	0.4184	-0.6211	40.000	-56.034
1.0000	0.1167	0.0361	1.0102	1.0093	0.4028	0.2621	0.3058	0.7420	0.2621	-0.6942	49.400	-49.313

AVERAGE AXIAL VELOCITY COEFFICIENT VA/UT= 0.4323

INITIAL DISTRIBUTION LIST

		No. Copies
1.	Defense Documentation Center Cameron Station Alexandria, Virginia 22314	20
2.	Library Naval Postgraduate School Monterey, California 93940	2
3.	Commander, Naval Air Systems Command Navy Department Washington, D. C. 20360	1
4.	Mr. I. Silver Propulsion Administrator (Code 330) Research and Technology Naval Air Systems Command Navy Department Washington, D. C. 20360	1
5.	Dr. F. I. Tanczos Technical Director (Code 033) Research and Technology Naval Air Systems Command Navy Department Washington, D. C. 20360	1
6.	Commander, Naval Ship Systems Command Navy Department Washington, D. C. 20360	1
7.	Capt. A. Bodnaruk, USN Naval Ship Systems Command (Code 6140) Navy Department Washington, D. C. 20360	1
8.	Superintendent Naval Academy Annapolis, Maryland 21402	1
9.	Chairman Department of Aerospace Engineering Naval Academy Annapolis, Maryland 21402	1
10.	Chairman, Department of Aeronautics Naval Postgraduate School Monterey, California 93940	2

		No. Copies
11.	Professor A. E. Fuhs Department of Aeronautics Naval Postgraduate School Monterey, California 93940	1
12.	Professor M. H. Vavra Department of Aeronautics Naval Postgraduate School Monterey, California 93940	3
13.	Office of Naval Research (Power Branch) Attn: Mr. J. K. Patton, Jr. Navy Department Washington, D. C. 20360	1
14.	Dr. E. S. Lamar (Code 03C) Chief Scientist Research and Technology Naval Air Systems Command Washington, D. C. 20360	1
15.	Commander, Naval Ordnance Systems Command Navy Department Washington, D. C. 20360	1
16.	Mr. G. L. Desmond Aerodynamics and Structures Admin. (Code 320) Research and Technology Naval Air Systems Command Navy Department Washington, D. C. 20360	1
17.	Professor Duncan Rannie California Institute of Technology Pasadena, California 91109	1
18.	LCDR S. F. Gallo, USN Commander Carrier Division TWENTY F.P.O. New York, N. Y. 09501	3
19.	Professor R. D. Zucker Department of Aeronautics Naval Postgraduate School Monterey, California 93940	1

DOCUMENT CONTROL DATA - R & D

Security classification of title, body of abstract and indexing annotation must be entered when the overall report is classified)

1. ORIGINATING ACTIVITY *(Corporate author)*
Naval Postgraduate School
Monterey, California 93940

2a. REPORT SECURITY CLASSIFICATION
Unclassified

2b. GROUP

3. REPORT TITLE
Comparison of Measured and Calculated Flow Properties After the Rotating Cascades of a Three-Stage Axial-Flow Compressor

4. DESCRIPTIVE NOTES *(Type of report and inclusive dates)*
None

5. AUTHOR(S) *(First name, middle initial, last name)*
Salvatore Frank Gallo

6. REPORT DATE	7a. TOTAL NO. OF PAGES	7b. NO. OF REFS
June 1968	135	7

8a. CONTRACT OR GRANT NO.

b. PROJECT NO.

c.

d. Distribution unlimited

9a. ORIGINATOR'S REPORT NUMBER(S)

9b. OTHER REPORT NO(S) *(Any other numbers that may be assigned this report)*

10. DISTRIBUTION STATEMENT
This document is subject to special export controls and each transmittal to foreign governments or foreign nationals may be made only with prior approval to the Naval Postgraduate School.

11. SUPPLEMENTARY NOTES

12. SPONSORING MILITARY ACTIVITY
Naval Postgraduate School
Monterey, California 93940

13. ABSTRACT

This work was undertaken to check the feasibility of obtaining the velocity profiles downstream of the rotors of turbomachines by measuring only the radial distributions of total temperature, total pressure, and absolute flow angle and using these data to calculate the flow velocities by the non-isentropic radial equilibrium equation such that the measured flow rate is matched. Curvature effects are ignored in this analysis.

The velocities calculated by this method are compared with those obtained by measurements with flow probes and hot-wire anemometers.

The tests were conducted on a 3-stage axial flow compressor of the Turbo-Propulsion Laboratory at the Naval Postgraduate School. Measurements were made over the entire operating range of the compressor at a fixed rotor speed of about 1200 rpm.

14 KEY WORDS	LINK A		LINK B		LINK C	
	ROLE	WT	ROLE	WT	ROLE	WT
Compressor						
Axial Flow						
Radial Equilibrium						
Hot-Wire Anemometry						